General Disclaimer

One or more of the Following Statements may affect this Document

- This document has been reproduced from the best copy furnished by the organizational source. It is being released in the interest of making available as much information as possible.

- This document may contain data, which exceeds the sheet parameters. It was furnished in this condition by the organizational source and is the best copy available.

- This document may contain tone-on-tone or color graphs, charts and/or pictures, which have been reproduced in black and white.

- This document is paginated as submitted by the original source.

- Portions of this document are not fully legible due to the historical nature of some of the material. However, it is the best reproduction available from the original submission.

EXOTECH
INCORPORATED

N/I

SEVERE PLANETARY ENVIRONMENTS AND THEIR IMPLICATIONS ON TECHNOLOGY FOR FUTURE SPACECRAFT MISSIONS

Prepared for

Headquarters

National Aeronautics and Space Administration

Under Contract NASw-1744

August 1969

EXOTECH INCORPORATED
Systems Research Division
525 School Street, S.W.
Washington, D.C. 20024

Abstract

Existing and evolving models of planetary environments, and of planetary missions currently receiving NASA consideration are reviewed. Current and developing applicable technology is evaluated in terms of providing systems to operate successfully within the hostile planetary environments. On-going research intended to close indicated technology gaps is summarized, and recommendations are made for further efforts needed to develop hardware for advanced planetary exploration.

TABLE OF CONTENTS

1.0 INTRODUCTION

The planets and free space of the Solar System are characterized by wide ranges of values for the environmental factors of temperature, electromagnetic and particulate radiation, gravity, and where atmospheres exist, chemical constituents, pressure, and unique meteorological phenomena. The space engineer must cope with these factors in producing spacecraft which will operate within their influence. Some aspects of these environments are known to be within his technical experience or capability, others must be considered severe in that the existing state-of-the-art is challenged in achieving exploration goals. It is this latter area which is of concern in this study.

This monograph contains reviews of

1. Planetary and space environments
2. Proposed planetary missions
3. On-going technological research directly applicable to advanced space missions

In the review of planetary environments emphasis is placed on the most recently available information which bears upon the environmental parameters of interest. Unfortunately, quantitative knowledge of the other planets of our Solar System, although rapidly advancing, is far from complete, and in some cases, extensive reliance on rather abstruse theory is needed to resolve observations into satisfactory models. Of necessity, however, we must consider the best available knowledge or theories as the constraints against which we evaluate the feasibility of particular missions against the limitations of existing technology. Data and uncertainty limits are expressed in uniform and commonly used units throughout this report.

In the mission review we have examined the profiles and features of several of the planetary missions being considered in the next fifteen years. Scientific objectives, hardware requirements, and schedule constraints as presently conceived for these missions are described, and certain recent design proposals are mentioned. Approved planetary missions (Mariner '71,

Viking '73) are only lightly treated since the research and technological activities supporting these programs are well underway. Missions, although unapproved, which have been afforded serious study and planning, are treated in more detail to emphasize their supporting research and technology (SRT) requirements.

Current research and development activities intended to provide equipment suitable for operation within the influence of planetary environments are discussed. Although this review concentrates on NASA activities, applicable efforts of other organizations are included. A chart summarizing these activities, their objectives, sponsors, and principal investigators is presented in Appendix A.

Recommendations and conclusions to assist in the formulation of future SRT programs have been developed based upon our analysis of the technological implications of severe planetary environmental parameters.

2.0 PLANETARY ENVIRONMENTS

A confident understanding of the characteristics of the environments to which future planetary spacecraft will be exposed is essential to an effective supporting research and technology (SRT) program. Although there are serious gaps in our knowledge of specific planetary environments, sufficient information does exist which, when reviewed in the light of future missions, provides a suitable basis for establishing and pursuing needed technological development.

In this section, the generally accepted theories pertaining to the environmental aspects of the planets and interplanetary regions of the Solar System are reviewed with particular emphasis upon those properties which will adversely affect spacecraft performance. Characteristics which are known not to present serious constraints are not emphasized; those aspects which represent severe constraints are analyzed in more detail.

2.1 MERCURY

Mercury's small size (4842 km diameter) and proximity to the sun make the innermost planet a difficult object for observation, and consequently, for a body so close to earth, relatively little is known about it. The mean solar distance is 0.387 AU but with an eccentricity of 0.206 (exceeded only by Pluto's), the distance varies from 0.308 to 0.467 AU.

Surface markings have been observed and mapped although the markings are of low contrast and discernable only when seeing conditions are particularly good. On the basis of comparison of certain markings at various times, Mercury was long considered to have a synchronous period of rotation (88 days); radar soundings, however, have provided more recent evidence that the period of rotation is 59 ± 7 days. This value is supported by estimates based upon other observations of visual markings and, furthermore, a rotation period of 2/3 of the synchronous period, or 58.6 days, is considered a stable condition.

Resemblance of Mercury to our own moon is evident in several physical characteristics, including size. Albedo in the visible spectrum is 0.056 vs. 0.067 for the moon, and polarization characteristics are somewhat alike.

This points to similarities in surface microstructure, if not in actual composition.

Low albedo and high solar intensity result in high surface temperatures on the sunlit side. (See figures 2-1 and 2-2.) Since the solar

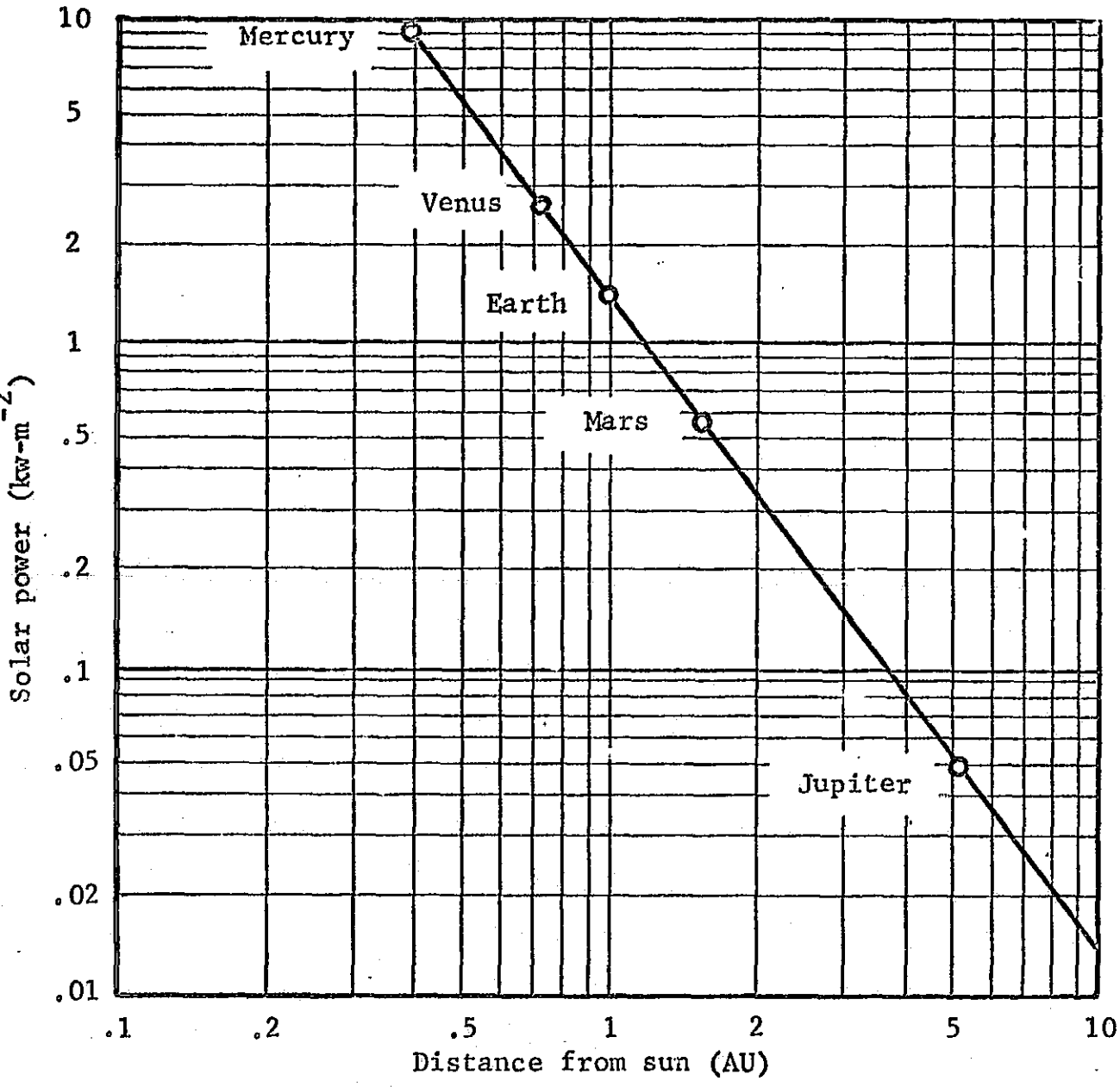

Figure 2.1 Solar power as a function of heliocentric distance

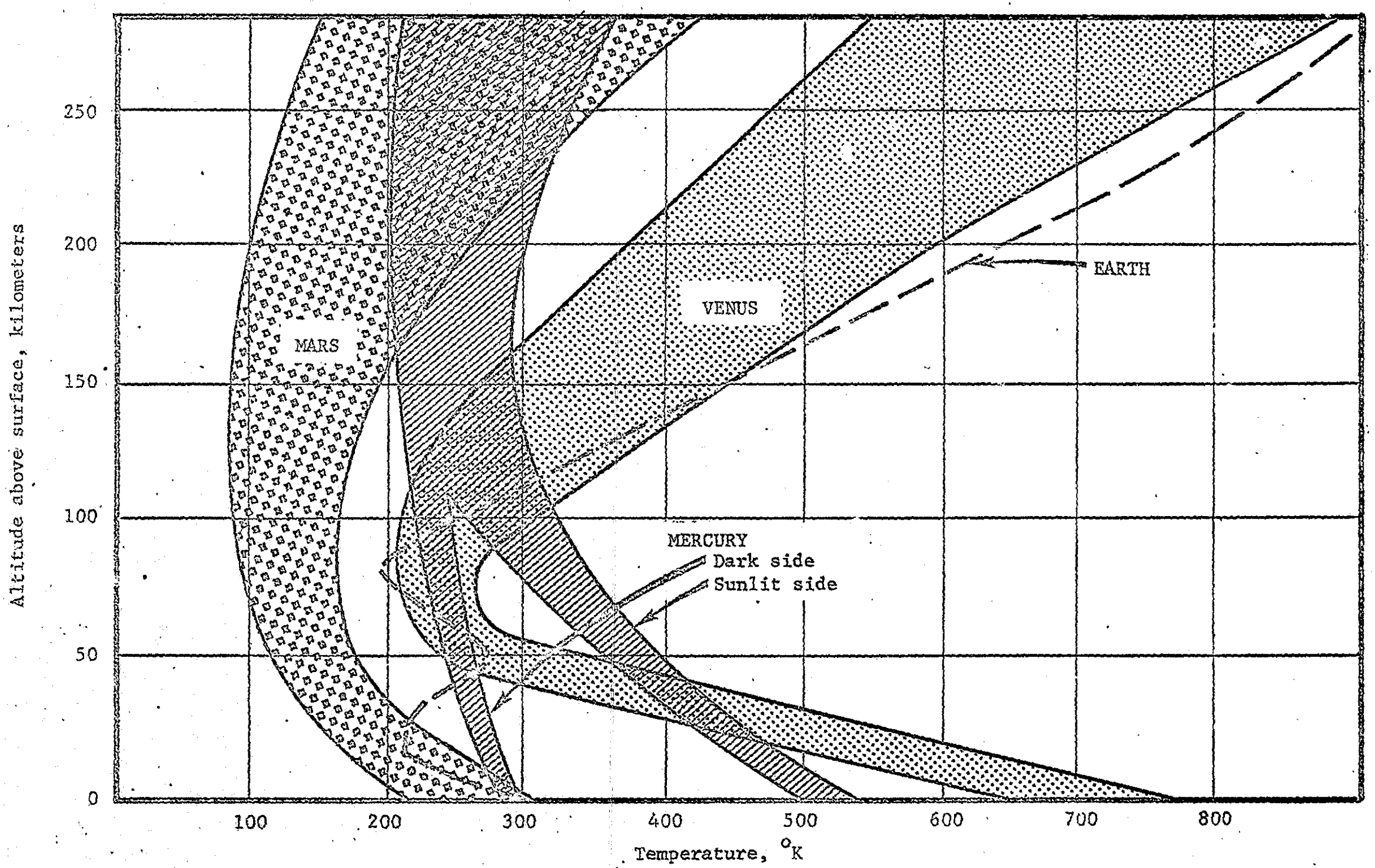

Figure 2.2 Atmospheric temperature vs altitude. Comparison of Inner Planets.

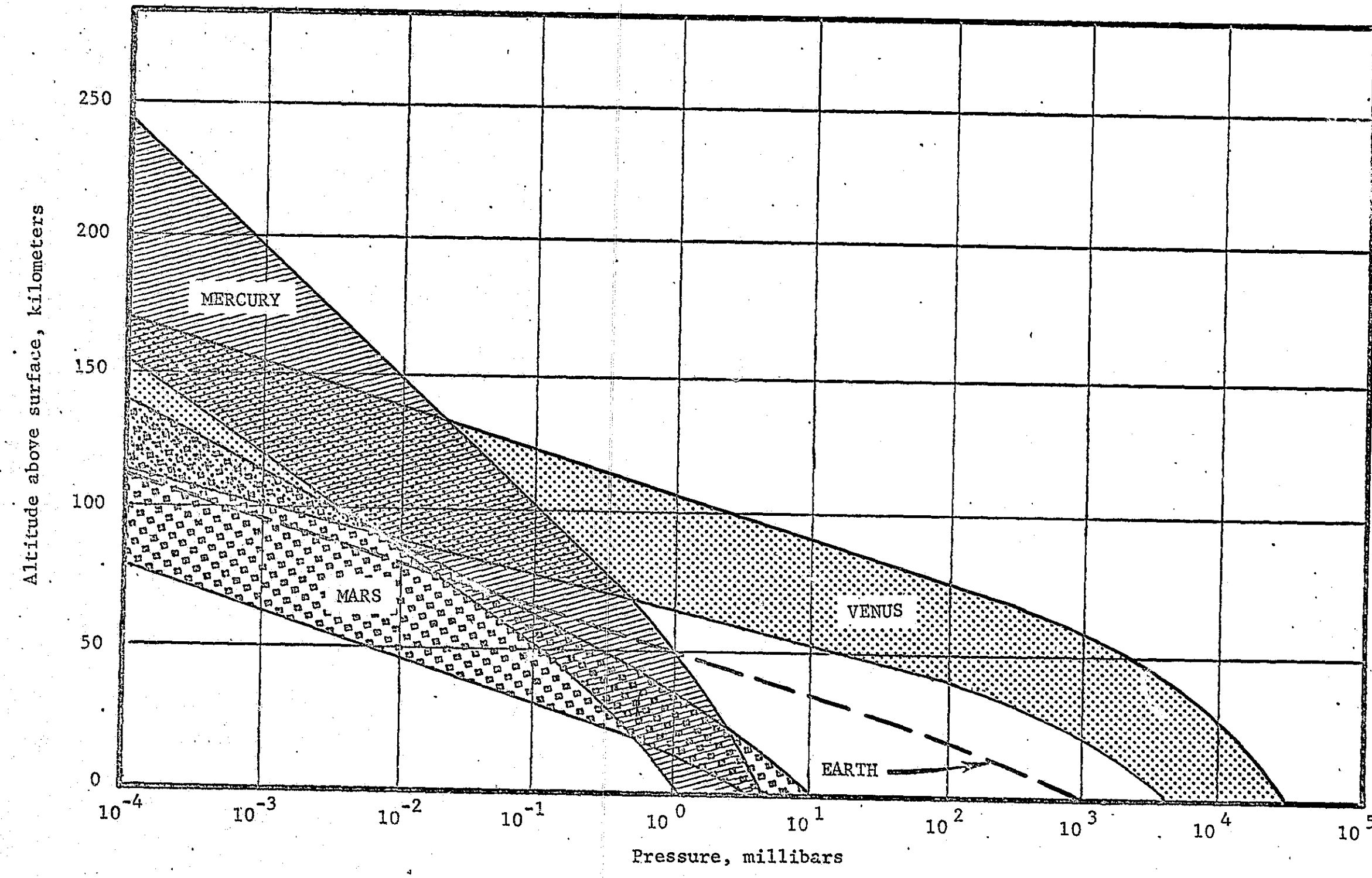

Figure 2.3 Atmospheric pressure vs altitude. Comparison of Inner Planets.

distance varies by a factor of 1.5 illumination varies by a factor of 2.3. A mean equilibrium temperature, based only upon solar energy and measured albedo at the subsolar point, is 505°K. Reasonable agreement with this prediction has been obtained by several methods using various parts of the spectrum (ref. 80).

Mercury's environmental parameters of concern to the spacecraft designer are the high level of solar illumination, the high surface temperature, the thin atmosphere (surface pressure about 5 mb) and the thermal transients associated with eclipse. (See figures 2-1, 2-2 and 2-3.) The extremes experienced in surface temperatures (73°K to 673°K) will constrain the selection of components and materials for landers. The thin atmosphere will necessitate significant retro-propulsion in landing operations which could cause extensive exhaust product contamination of the atmosphere and surface.

2.2 VENUS

With a remarkably high albedo of 0.81, Venus receives less solar energy in direct radiation at its surface than does the Earth, even though the incident solar intensity is twice that incident on Earth, as shown in Figure 2.1. The spectrum of radio noise indicates a most probable source temperature of 923 K-973 K. Thermal analysis convincingly shows that the radiation source is the bottom of the atmosphere (ref. 80). The Soviet Venera 4 experiment in 1967 released a temperature reporting probe which substantially confirmed this temperature range.

The high brightness temperature observed is popularly resolved in terms of the "greenhouse" effect. Radiation in the visible and infrared which does pass through the atmosphere is absorbed and reradiated in the far infrared, to which the atmosphere is more opaque. This differential in opacity requires a low altitude temperature buildup to about 700°K in order to maintain thermal equilibrium. (See figure 2-4.) The planet's long rotational period (230 days), high thermal conductivity, and inertia of its atmosphere, suggests that surface temperature gradients should be smooth, and variations relatively modest. Vigorous vertical circulatory patterns are probable at higher altitudes, and a pronounced surface component directed

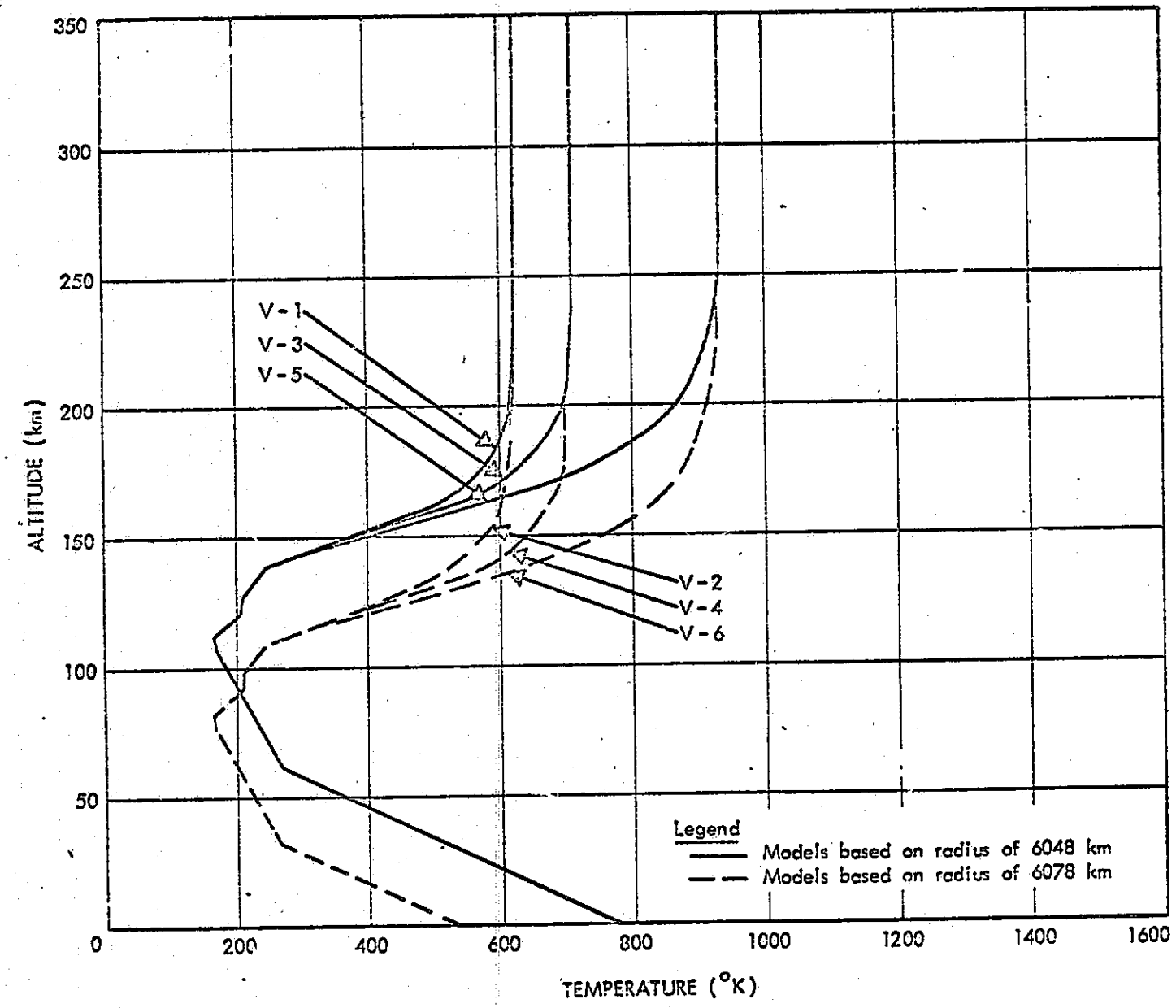

FIGURE 2.4 Atmospheric temperature of Venus
NASA SP-8011
1968

from the subsolar to the anti solar points is theorized (ref. 10).

The Soviet Venera 4 experiment launched in November, 1965, represents to date the only direct observations of the atmospheric properties of Venus. Pressure, density, and temperature sensors carried on a probe measured and returned continuous values of these parameters for periods of 50, 70, and 94 minutes, respectively, during a parachute descent through the Venusian atmosphere (ref. 66). Impact point was close to the equator on the night side. Some months later, the Mariner II flyby experiment provided additional data on the atmospheric density as the vehicle was eclipsed by the planet.

An unresolved discrepancy concerning the Venusian radius and, hence, influencing predictions of surface temperature arose when data from the Soviet probe was compared against measurement using other techniques. Heretofore, the planetary radius determinations considered most accurate had been performed by radar soundings. Target reflections have been shown by signal time spread to emanate from a relatively small area of the Venusian globe. Signal transit time and Doppler shift provide a fairly accurate measure of the range and range rate between the Earth station and the nearest point of Venus's surface. Pure celestial mechanics are then employed to determine the station position relative to the center of mass of the Earth-Moon system and that of Venus at the instant of the sounding. The sought for radius is then determined subject, among other things, to uncertainties in the astronomical unit and to accurate inclusion of gravitational perturbation of the other planets. However, (and somewhat surprisingly) the ephemeris uncertainties contribute less to the error range than do uncertainties in the radar observations.

Radar experiments conducted by Lincoln Laboratories and JPL provide independent values of 6050 ± 0.5 km and 6053.7 ± 2.2 km, respectively, for the radius of Venus. Mariner II passed within 35,000 km of Venus and provided indirect determinations of pressure and density profiles from S band radio signal distortions. The occultation of the signal in conjunction with orbital and model atmospheric parameters provided a confirmation of the surface radius value obtained from the radar experiments.

At the moment of a pressure-controlled parachute deployment, the Soviet landing module relayed a single radio altimeter reading which incicated an altitude of 26 kilometers. From that point atmospheric parameters were telemetered continuously until failure, and the profiles against the altitude were indirectly constructed from the descent characteristics of the parachute. The fact that telemetry abruptly ceased at approximately the time required to fall 25 km supports the altimeter reading. However, when integrated into the radar and Mariner II data, it would appear that the resulting radius would be approximately 25 km too large (see Figure 2.5). Error limits in planetary ephemeris, vehicle trajectory, radar ranging, and occultation modeling are not considered sufficient to explain the discrepancy. Furthermore, extrapolation of temperature measurements to the "lower" surface results in either excessive surface temperatures or thermal models inconsistent with radiometric data. That Venera 4 impacted on a local high altitude surface feature is conceivable, but not likely considering the rather smooth target that Venus presents to radar signals.

If one accepts the values of Venus radius based on terrestrial radar soundings and the Mariner experiment, it is possible to conclude that the Soviet probe may have misreported its original altitude, and that the probe may have encountered failure at an actual altitude of about 35 km. It is interesting to note that the two experiments are not independently considered in this analysis. A part of tha altitude and temperature discrepancies result from the assumption of a 100% CO_2 atmosphere for the interpretation of the Mariner occultation experiment. This model was suggested, in turn, by atmospheric data returned by Venera 4. A better temperature agreement between probe and radiometric observation follows from the assumption of a smaller CO_2 concentration in the Venus atmosphere.

Figures 2.4, 2.5, and 2.6 from NASA Design Criteria Monograph, Models of Venus Atmosphere (1968), summarize data for atmospheric pressure and temperature. Estimates of the chemical composition of the Venusian atmosphere are presented in Table 2-1.

Magnetometers aboard Mariner II indicated a magnetic field less than one-tenth that of Earth. This parameter was refined by the Soviet Venera 4

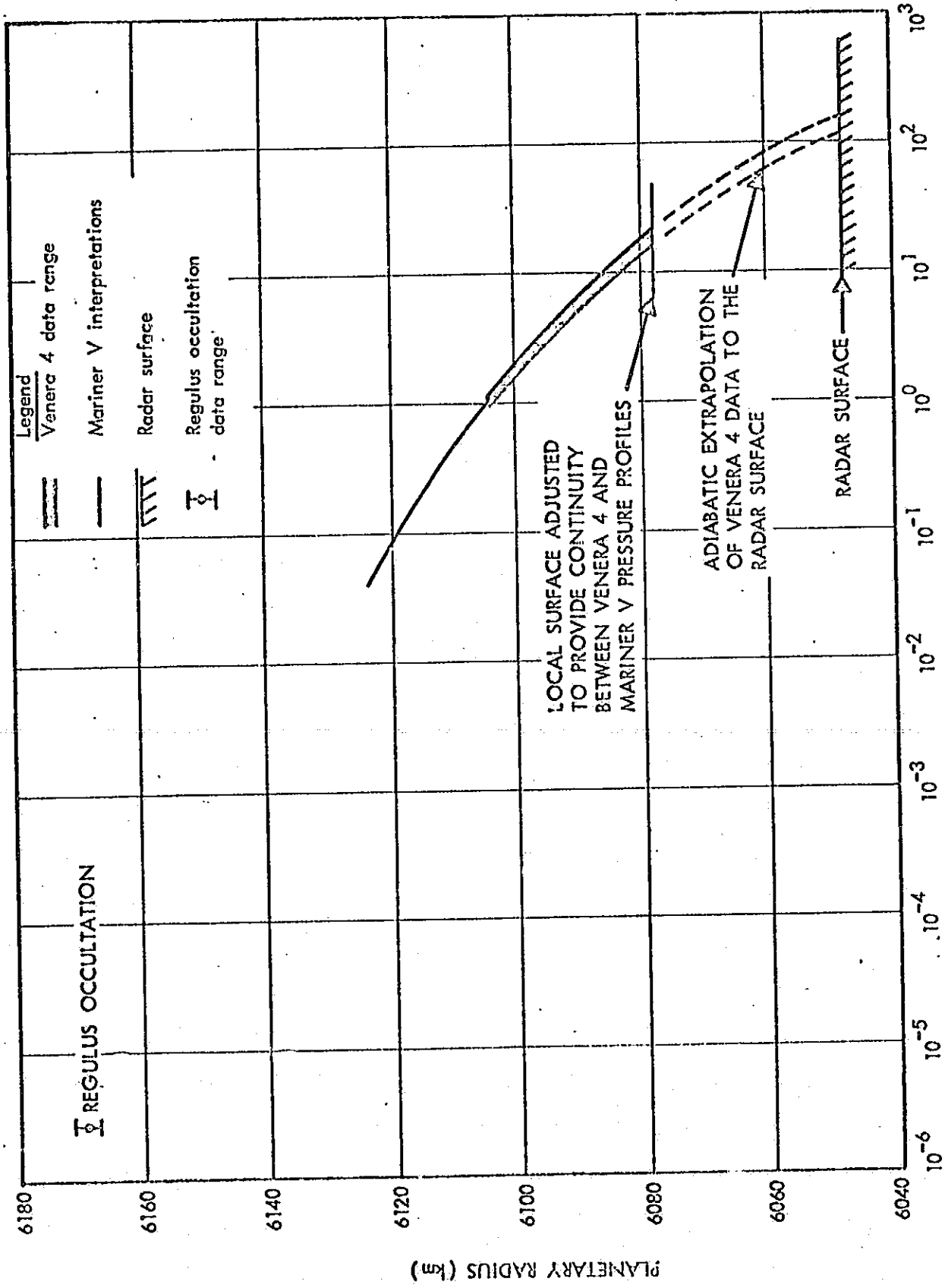

FIGURE 2.5: Atmospheric Pressure of Venus
NASA SP-8011
1968

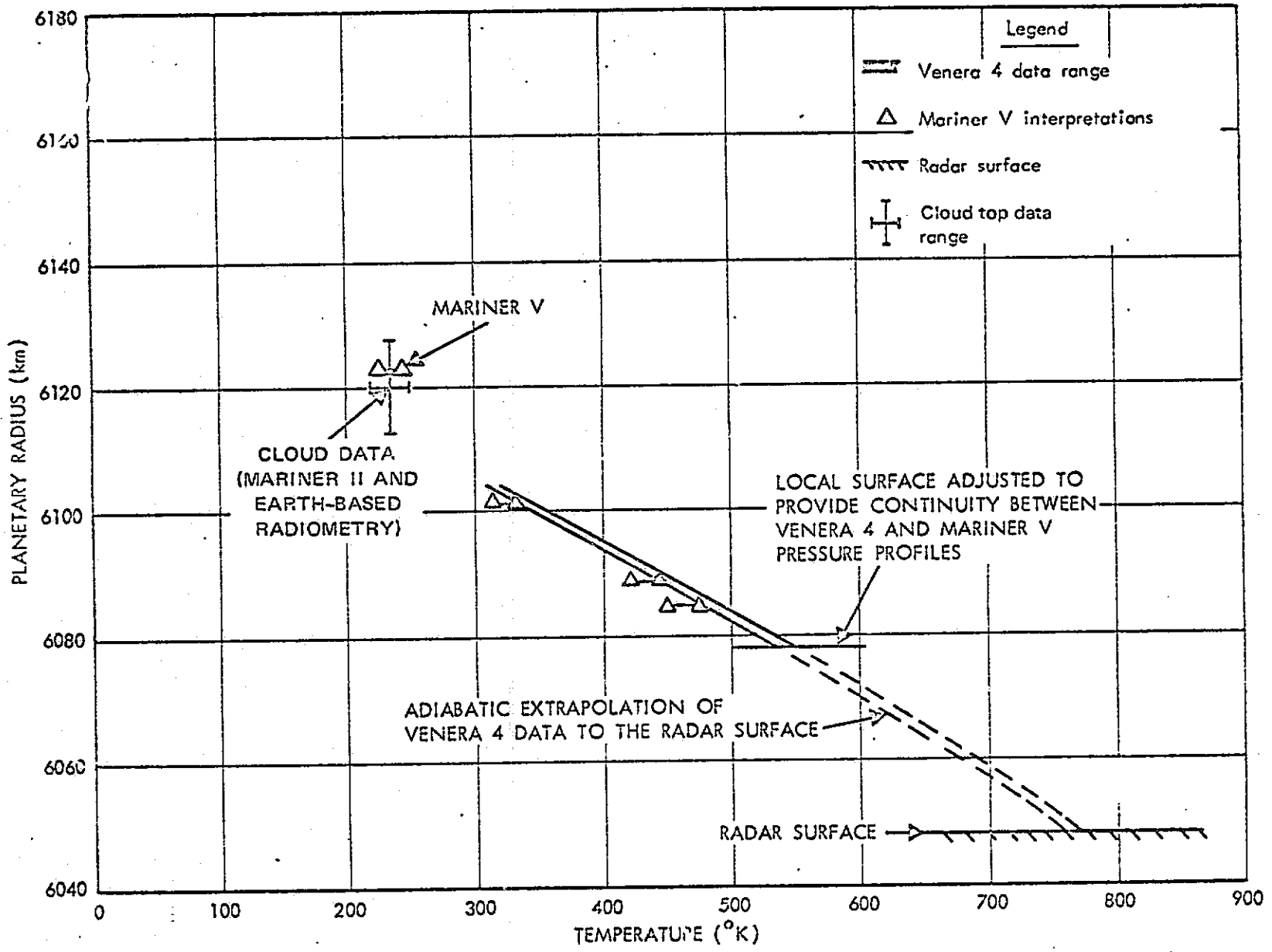

FIGURE 2.6: Lower Atmospheric Temperature of Venus
NASA SP-8011
1968

TABLE 2-1

COMPOSITION OF THE VENUS ATMOSPHERE

Component	Estimated Percent by Volume	Source
CO_2	90 ± 10	Vinogradov
N_2	<7	"
NH_3	$<5X10^{-6}$	Benedict
N_2O	$<5X10^{-5}$	"
CO	$\simeq 4.5X10^{-3}$	"
H_2O	$>5X10^{-2}$ and $<7X10^{-1}$	Vinogradov
O_2	$\simeq 3X10^{-3}$	Hunten
HCl	$\simeq 10^{-4}$	Benedict
HF	$\simeq 10^{-6}$	"
He	$\simeq 10^{-2}$	McElroy
CH_4	$<7X10^{-5}$	Kuiper
COS	$<5X10^{-5}$	"

Summarized from Proceedings of Second Arizona Conference on Planetary Atmospheres, Tucson, March 11-13, 1968, in Journal of Atmospheric Sciences, Vol. 25, No. 4, July 1968.

in 1967 to a value of less than three ten-thousandths that of Earth. No evidence for Van Allen like belts surrounding Venus has been demonstrated (ref. 89).

The indicated temperature and thermal conductivity of the lower atmosphere will limit to a matter of minutes the lifetime of impact-survivable probes constructed of conventional components, even with imaginative methods of insulation. Venus exploration, then, emerges as a major impetus for advances in high temperature technology.

Buoyant stations such as discussed in the next chapter appear to be the most attractive method of prolonged investigation of Venus. The relatively high atmospheric density allows satisfactory payload support with modest balloon displacement. This, plus an apparently smooth temperature profile are two of the aspects of the atmospheric environment which can be considered favorable to Venus exploration because they provide a zone in which environmental conditions may be found that will not quickly degrade or destroy the payload.

The apparently unbroken cloud cover of Venus will require extensive analysis if knowledge is to develop concerning the meteorological system of this planet. At present, there is no spatial information concerning the clouds, either vertically or horizontally. We assume, but cannot be certain, that the aerosol particles are an atmospheric condensate. They could be a simple homogeneous substance, or a mixture whose parameters are subject to rapid temporal or spatial change. Difficulties stemming from lack of knowledge of what to expect in designing cloud instrumentation are compounded by the fact that any approach requires assumptions based upon terrestrial experience in the interpretation of the results.

It has been conjectured that a combination of high temperatures, water vapor and carbon dioxide may combine to produce an atmosphere possessing corrosive properties. While not ruling out this possibility, we take the position that extensive concern is not warranted at this time for the following reasons:

1. In the total Venus environment, the probability is small that corrosion would be a limiting factor as compared to temperature and pressure. Corrosion protection is practically an automatic result of any reasonable protection from temperature and pressure.

2. Failure induced by corrosion is likely only on missions requiring long or repeated exposure to a corrosive environment. Early missions requiring long esposure to the atmosphere will most likely be conducted at altitudes where temperature and pressure stresses are easily met.

2.3 MARS

The Martian environment is by far the most favorable of the planets for approach, entry and analysis. Mars is presently considered the only extraterrestrial body in the Solar System which affords a reasonable opportunity for the support of life forms as we know them.

The most conspicuous Martian fearures visible from the earth are the white polar caps which alternately grow and shrink with the seasons. The caps have been extensively studied and tables are available for the prediction to the cyclic behavior (ref. 38). The north polar cap is larger and has a winter extension of over ten million square kilometers. As the caps advance they are partially obscured by a haze, but on retreat their outline is sharp. The development is characterized both upon advance and retreat by fragmentation into the same patterns each year, indicating differential rates along topographical features. The polar caps are believed to be water, probably in the form of small crystals such as hoarfrost, and in a layer that is certainly very thin. The retreat of the cap in late spring is very rapid in comparison to the melting rate of the earth's snow cover, although the two planets have axial inclinations which are nearly the same. During retreat, the edge of the cap is lined by a dark band, which is susuggestive of damp soil from melting ice. There are doubts, however,

that this is a correct explanation; meteorlogical conditions tend to favor sublimation, and calculations by some authors cite insufficient polar ice volume to account for the band effect in this way (ref. 70, 80).

Light and dark surface features are generally associated with low and high elevation terrain, respectively. Contrasting areas have been observed to change in shape, however, as dust storms pass over them. Sagen et al (ref. 97) relate these changes to large scale migration of surface dust particles. Assuming a relatively uniform surface composition (chiefly of pulverized ferric oxides and absorbed water) he shows that particles with radii of less than about 100 microns can be carried by even modest winds over distances comparable with the gross planetary markings. Deposits of the very fine particles are lightest in color due to a relatively greater amount of unidirectional reflection in the surface albedo. Larger grain sizes tend to scatter light, producing multiple path reflection, and appear darker. Local albedoes decrease or increase, respectively, as fine dust is lifted or deposited.

Knowledge of Martian surface conditions was greatly increased by the TV experiment carried on Mariner IV which made a fly-by encounter of the planet on July 15, 1965. About one percent of the surface was photographed and recovery of useful data was possible in most of the pictures (ref. 7). Images were obtained in both green and red light for a simple analysis of the soil and atmosphere spectral characteristics. Valuable inputs of relief scale were made available, an important parameter when interpreting visual data.

The most striking result of the Mariner IV experiment was the discovery of craters, apparent in every frame which had suitable contrast and resolution. Size and distribution of the craters are described in figure 2.7. Gross similarities to Earth's Moon are obvious in all of the usable images transmitted. In spite of the similarities between the landscapes of the Moon and Mars, the surface of Mars is not expected to display the small craters found in great numbers on the moon. The Martian atmosphere would cause meteors of masses of several hundred kilograms to burn up; additionally, soil erosion due to wind would further smooth the landscape.

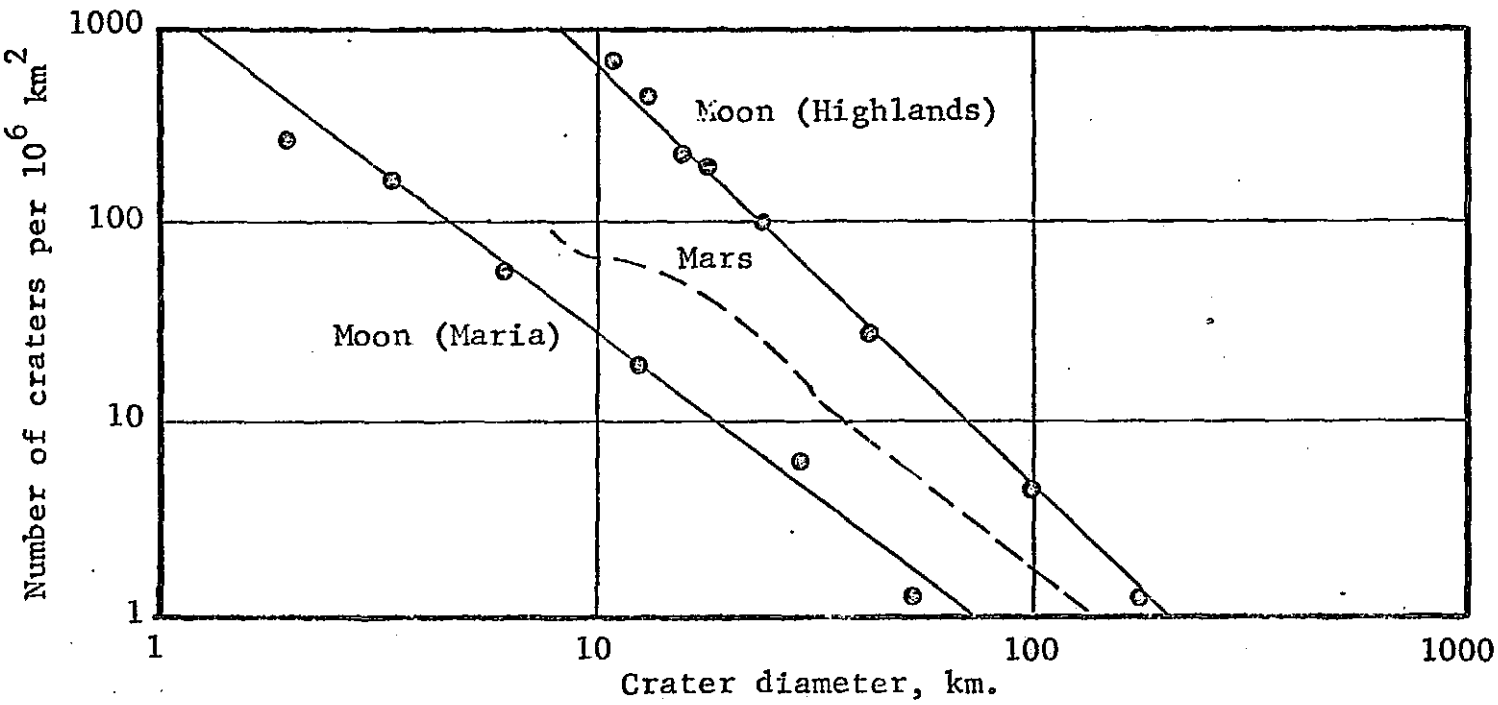

Figure 2.7: Comparison of Martian and Lunar crater populations as a function of crater diameter.

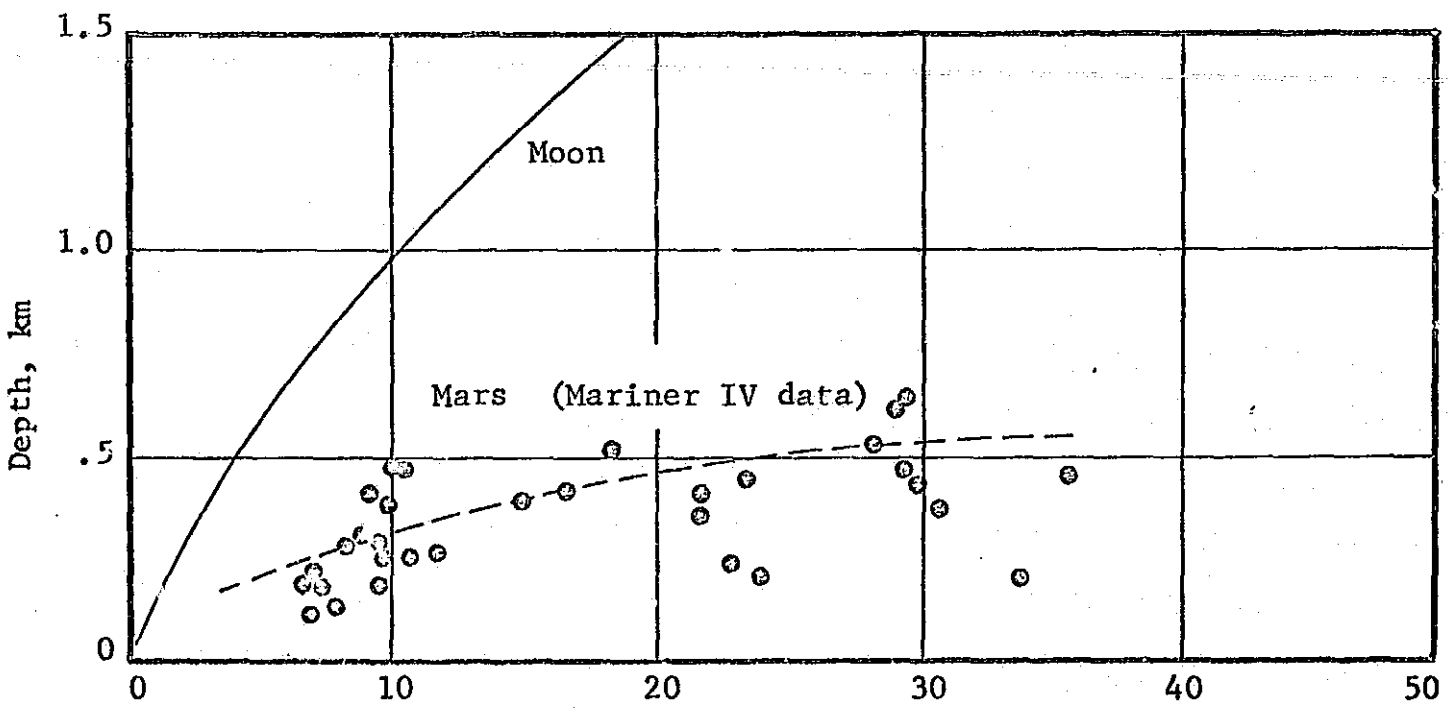

Figure 2.8: Martian crater depth as a function of diameter.

Ref: Mariner-Mars 1964 Final Project Report
NASA SP-139

The Mariner photographs suggest that the craters' edges are less rugged than those of the moon, and that their average depth appears to be only about one fourth as great, for a given diameter. (See figure 2.8) These characteristics of Martian craters are in consonance with the concept of high rates of soil erosion due to atmospheric circulation. Winds in the lower atmosphere tend to break up, eddy, and stagnate on the lee side of high terrain features. Airborne particles are preferentially deposited at these points. Thus, the floor of craters, and to a lesser extent, any relatively low features which are to the lee in prevailing winds, are subject to appreciable settling and packing mechanisms other than gravitational force, and couls not be expected to provide adequate support for some classes of rovers and landers. (See figure 2.9) One can expect low velocity, steady winds and gradients due to general atmospheric circulation (ref. 9); dust devils* and yellow clouds can also be expected. Langley Research Center has estimated a probability of 2×10^{-2} that a dust devil will sweep over Viking during its 90-day lifetime on the surface (ref. 79).

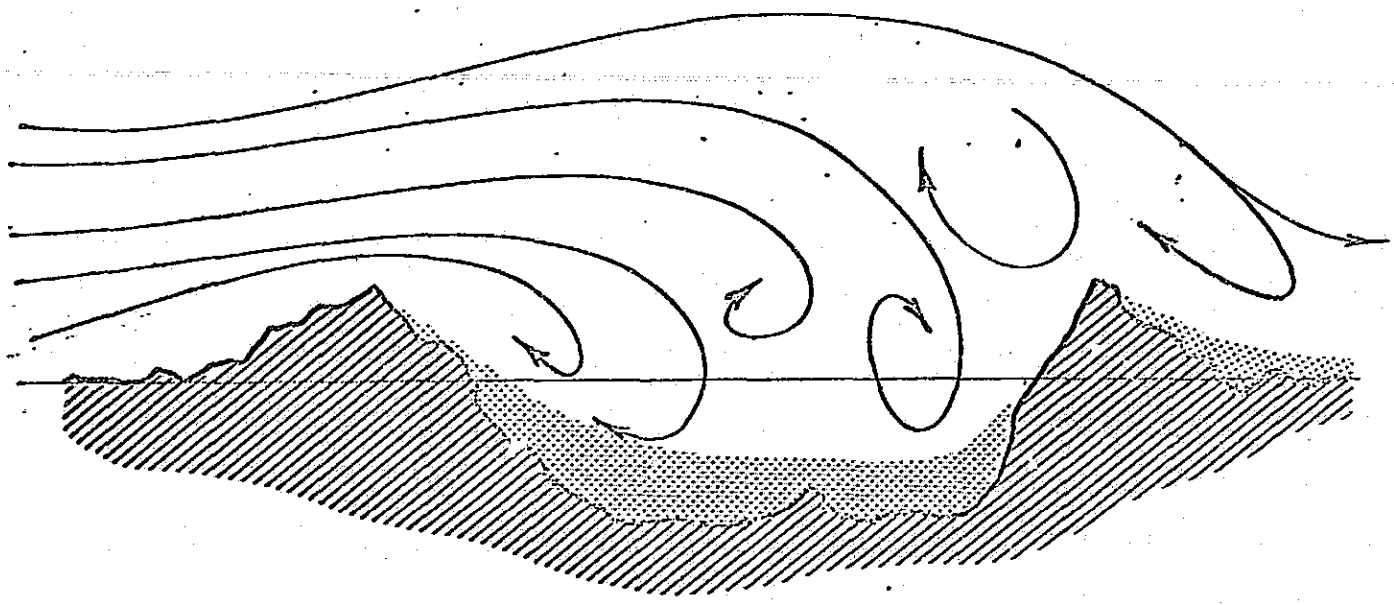

Figure 2.9 Martian craters may be filled with deep, loosely packed dust. Airborne soil particles settle out of stagnant air masses to the lee of high elevation areas.

*Dust devils are cyclone-like storms with vortex areas estimated to be 8-10 km and duration of about 4 hours.

Yellow clouds usually form as small areas and grow larger with time, sometimes obscuring the entire visible disk. The size of the clouds resolvable from Earth ranges from near 100 km^2 (or near the solution limit) to approximately 10^6 km^2. Yellow clouds usually disappear within 24 to 48 hours but occasionally last as long as 30 days, as in 1956. The particles composing the clouds are thought to have sizes of about 20 to several hundred microns; particles as small as 3μ might form the rare planet-wide obscurations that last a month or more.

Dust storms may result in localized deposit or abrasion mechanisms which could seriously degrade the performance of a soft-landed payload. Accumulation of dust in recesses could block the view of optical or other sensors; mechanical joints could be fouled by grit; thermal balances could be upset by accumulation of soil on equipment surfaces, or by sand blasting of thermal coatings.

Estimation of local, small scale surface characteristics invariably involves the question of the entent to which the characteristic Martian color can be attributed either to distortion by the atmosphere or to actual absorption by the crust. Extensive spectral shaping by the atmospheric constituents, or by airborne particles is generally accepted. Kiess, Karrar and Keiss, (ref. 65) have presented a model in which the unstable brownish features and white polar areas are explained as concentrations of NO_2 and N_2O_4, respectively, whose mutual equilibrium is continually disturbed by winds. Many others, however, reject such interpretations in favor of soil dust storms and atmospheric precipitates (possibly H_2O) in crystalline form. If atmospheric scattering is accepted as the dominant mechanism for the Martian hue, then an upper limit is available for the size of the particles suspended in the atmosphere. Particle opacity would be the primary effect upon transversing light for bodies exceeding approximately one micron, and attenuation by particles larger than this would be essentially neutral.

Major advances in atmospheric definition were made in 1965 from interpretations of the Mariner IV occultation experiment and also of earth-based spectroscopic observations during a favorable opposition in that year. The

extent of improvement is clearly reflected, for example, in the fact that surface pressure models in publications appearing prior to 1965 still ranged over nearly two orders of magnitude. Martian surface pressure now is bounded with confidence between five and fifteen millibars.

When the Mariner IV vehicle passed behind Mars, communication signals exhibited a Doppler-like phase shift due to refraction by the planet's atmosphere. Accurate measurement of the shift provided the degree of change of the effective radio path length just as the spacecraft was being eclipsed. Appropriate corrections were applied to the data for such effects as trajectory errors, oscillator drift, and changes in range rate and earth atmospheric refraction due to earth rotation. The resultant measure of the refractivity furnished independent constraints in construction of an atmospheric model for Mars, and in addition, a measure of the planet's radius was made available by noting the duration of the occulted signal. (See figure 2.10 and 2.11)

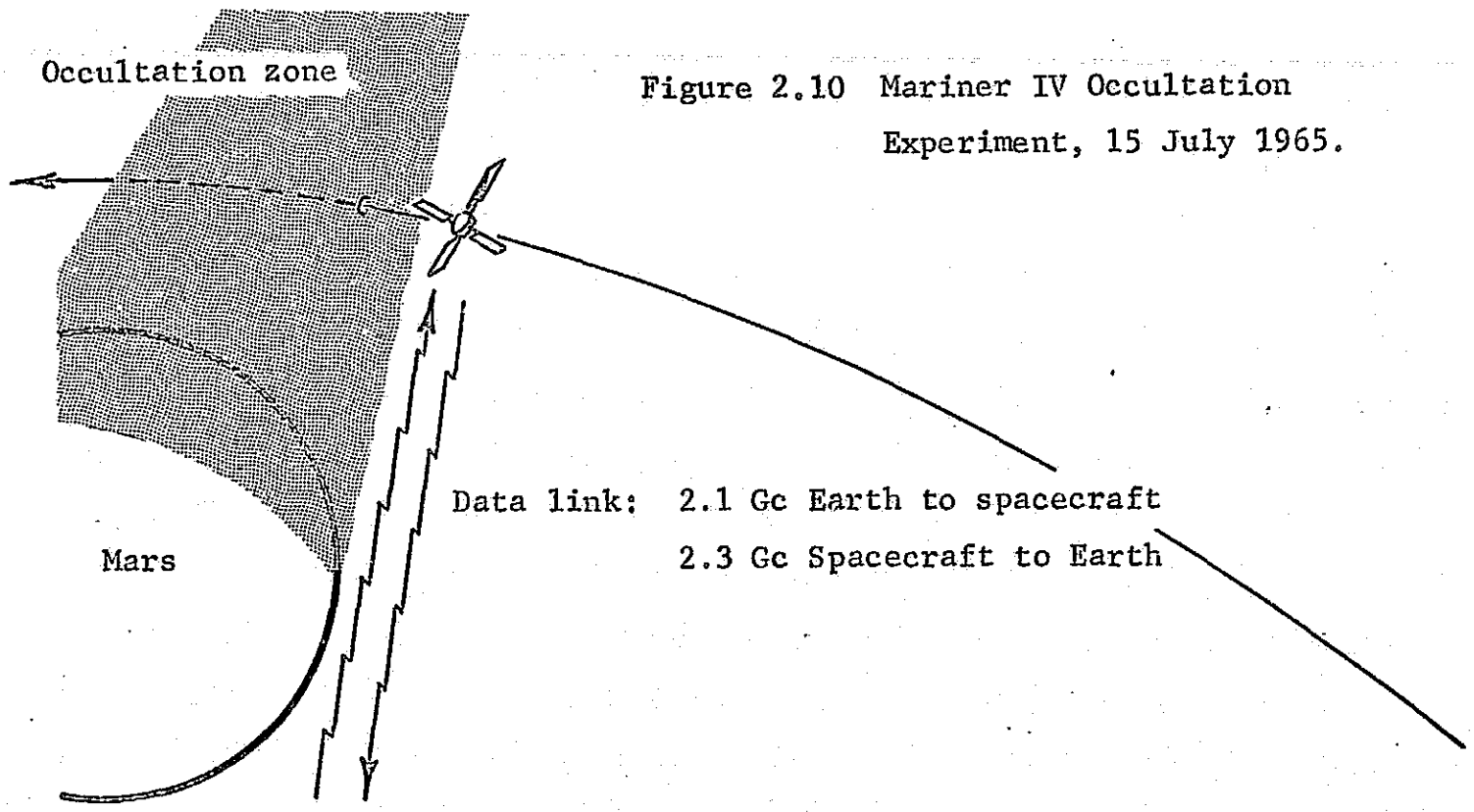

Figure 2.10 Mariner IV Occultation Experiment, 15 July 1965.

Immersion of Mariner IV into the occultation zone occurred at 1300 hours local time over an area approximately 50°S latitude which was experiencing late winter, and emerged at 2300 hours local time over 60°N latitude. Data indicated that at the surface, the summer night is considerably (60°K) warmer than the winter day. This is a familiar terrestrial phenomenon, although the temperature extremes are greater on Mars. A negative refraction region was not noted during emersion, indicating an absence of an ionizing layer in the upper atmosphere on the nighttime side. A relatively large pressure difference was found between immersion and profiles which could be possibly explained by local surface elevation features, but it was noted that emersion data contained uncertainties because phase lock of the data link was not established until 7½ seconds after occultation ended.

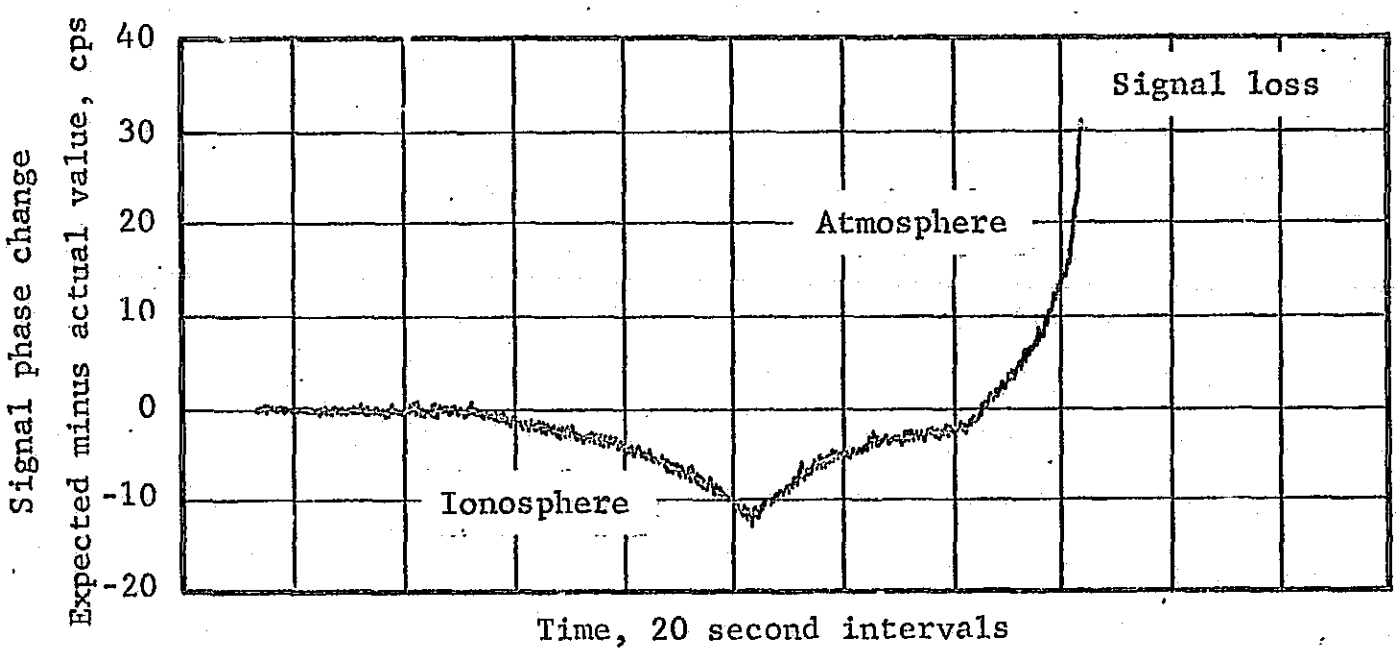

Figure 2.11 Radio signal phase change prior to immersion into occultation zone of Mariner IV experiment.

Before atmospheric refractivity can be translated into density, temperature, and other characteristics, the composition of the atmosphere must be

assumed. Fortunately, the gaseous constituents derived from spectrographic methods are now bounded sufficiently to provide quite accurate results. Two models, one pure CO_2, and the other a mixture of 80% CO_2 and 20% N_2 were used (ref. 44) to derive a temperature profile of the lower atmosphere from the occultation data (figure 2.12). Since the effect of other gases (either known or suspected) is negligible, these models were considered to adequately bracket real conditions. In the calculations of pressure, for example, the differences between the two composition models change the results by less than one percent. The Mariner experiment indicated that the atmosphere is less dense than had been expected, which will increase deceleration problems associated with probe or landing vehicle entries. Density of the upper atmosphere falls off rapidly, however, indicating the feasibility of low altitude orbits.

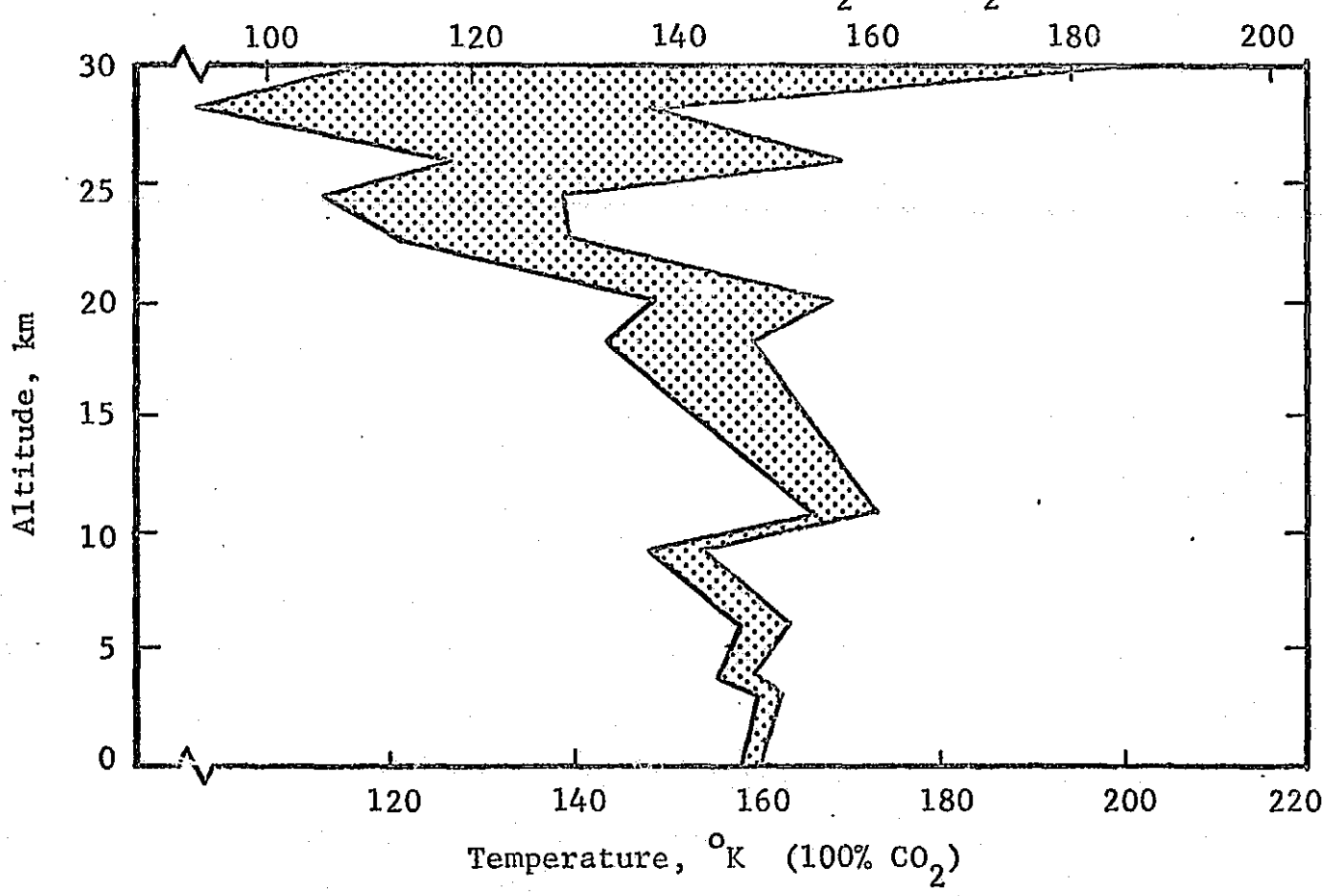

Figure 2.12 Temperature profile of Martian atmosphere derived from Mariner IV occultation experiment

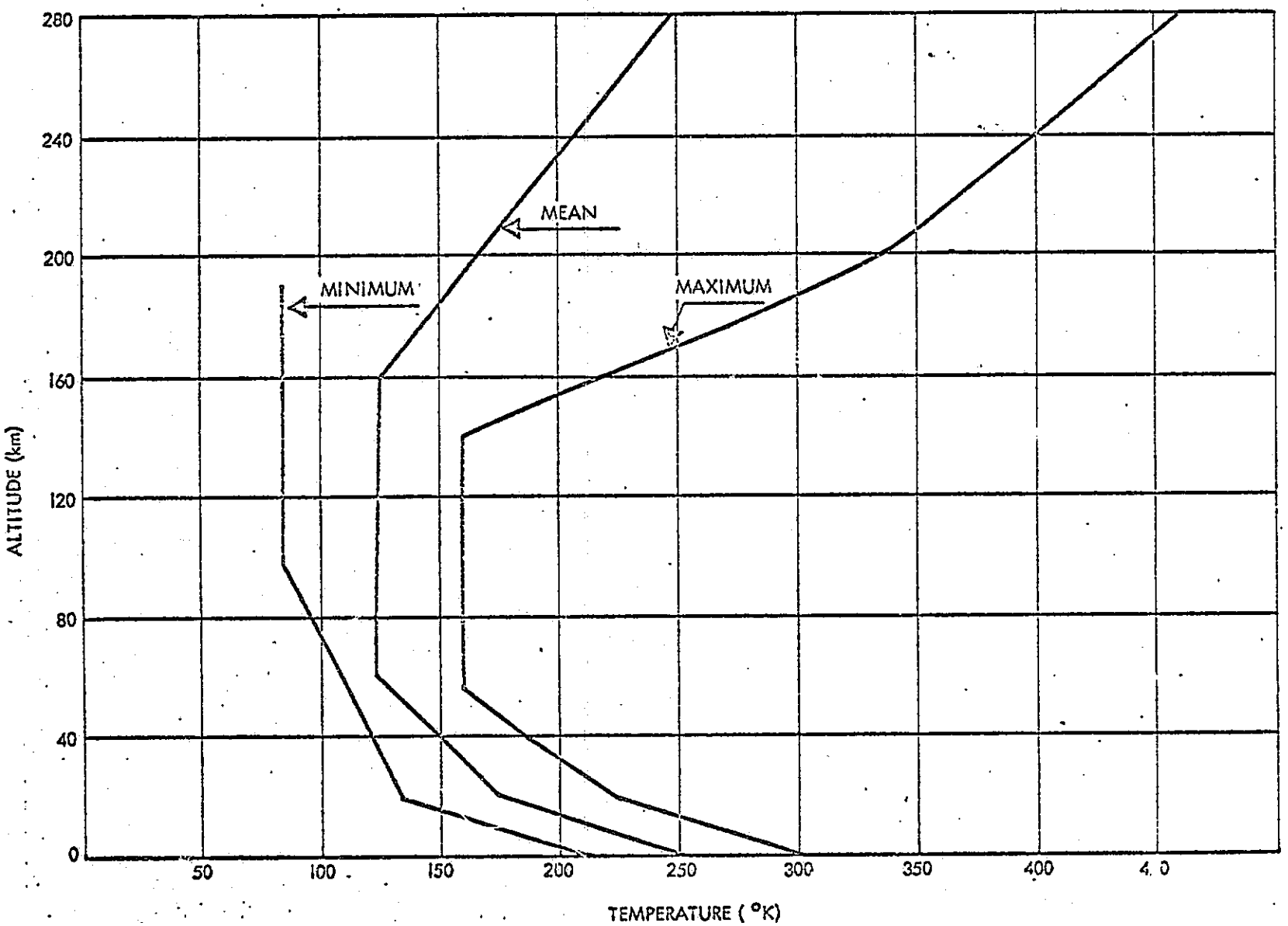

Figure 2.13 Atmospheric temperature profile of Mars. NASA SP-8010 [illegible]

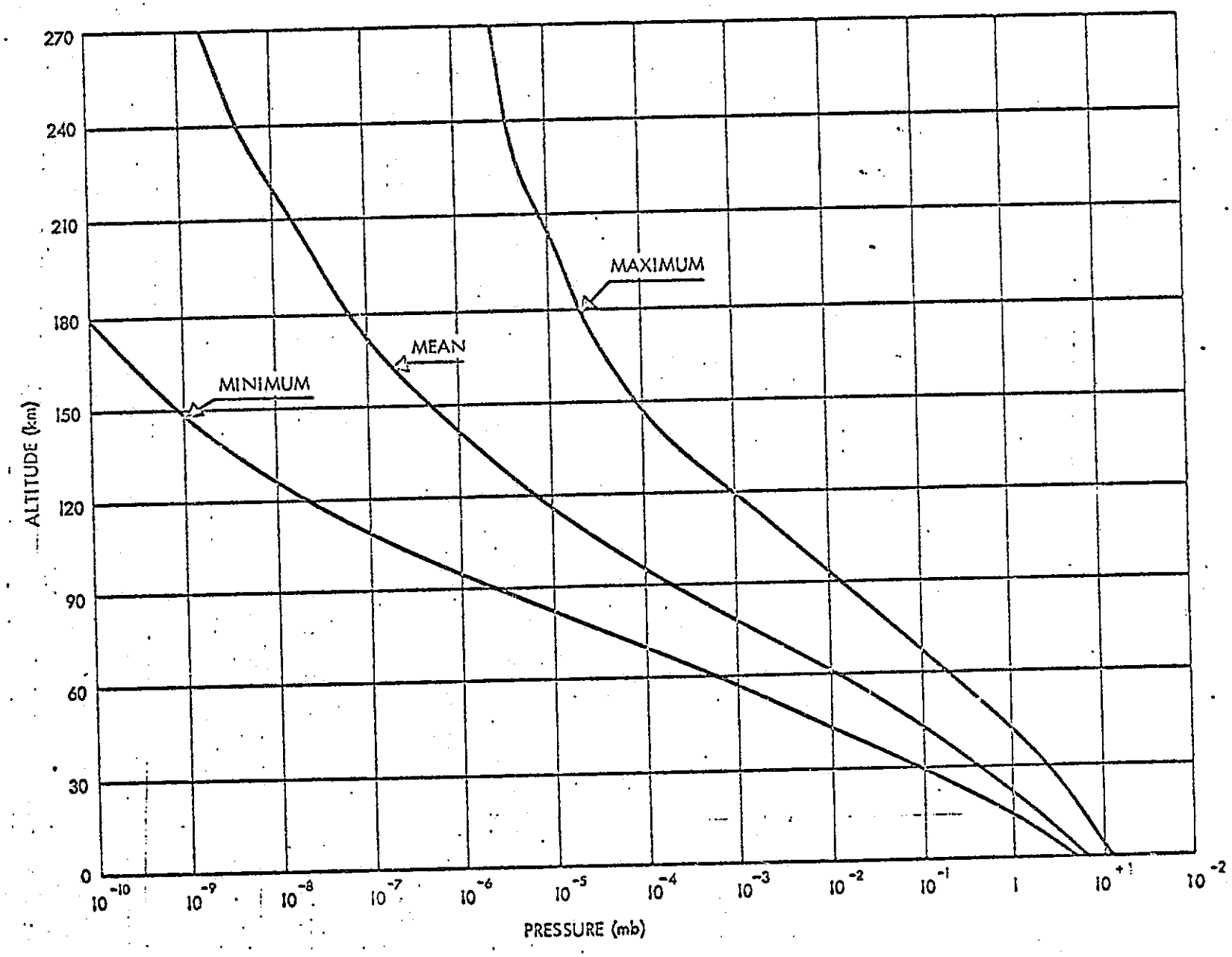

Figure 2.14 Atmospheric pressure profile of Mars. NASA SP-8010 1968

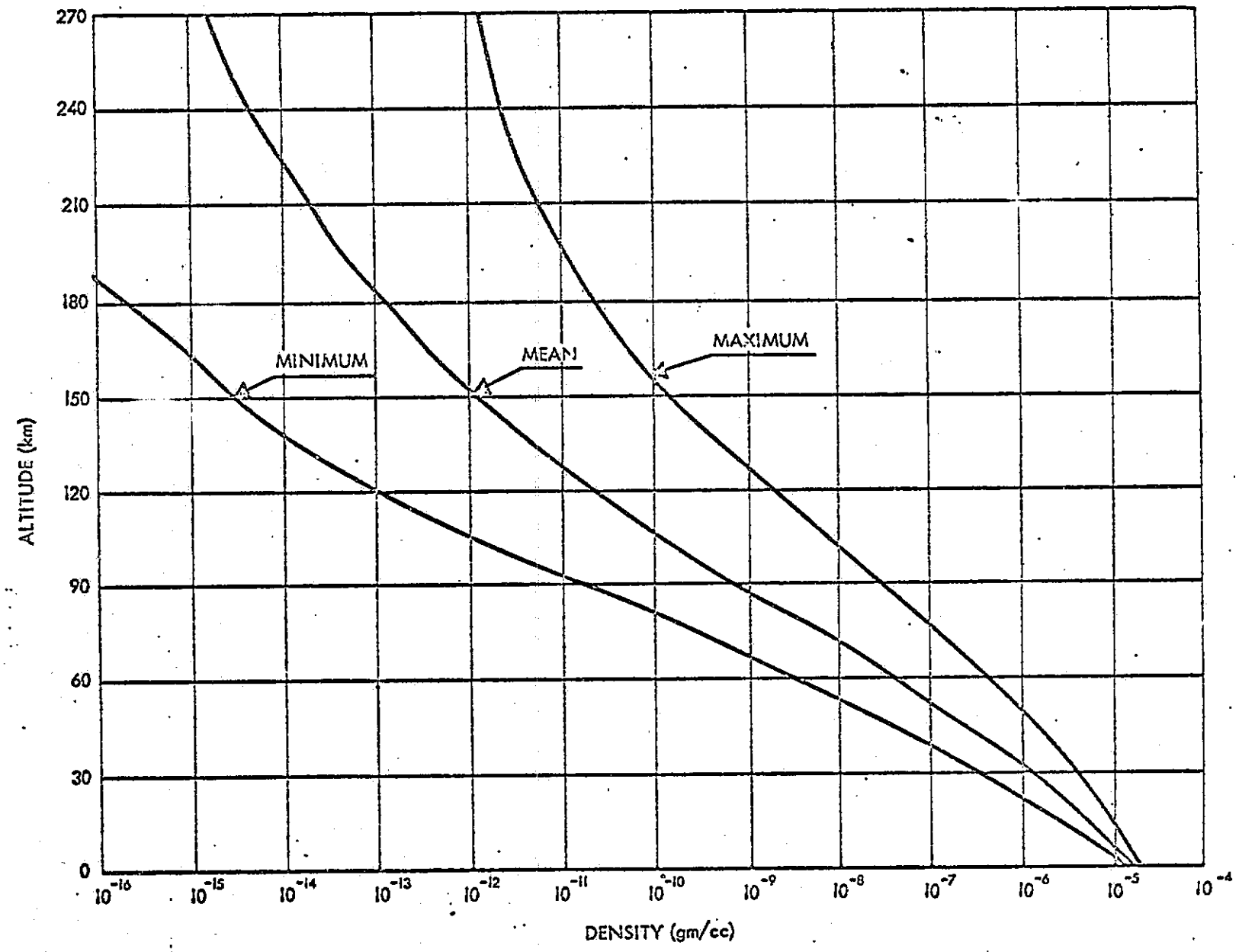

Figure 2.15 Atmospheric density profile of Mars. NASA SP-8010 1968

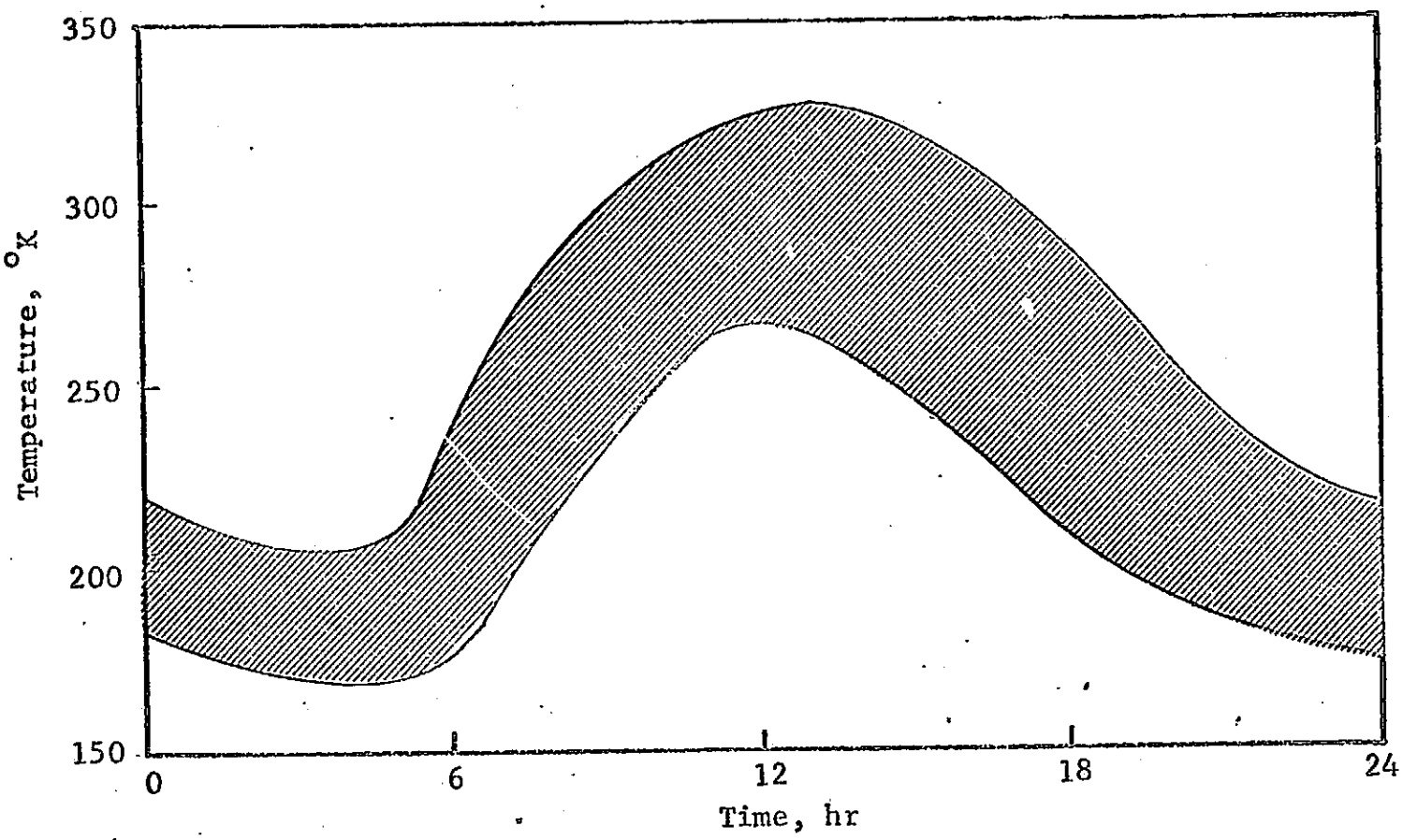

Figure 2.16 Daily temperature variation of surface of planet Mars at the equator. Relatively large uncertainty limits reflect the variation due to seasonal effect. Ref. Viking Project Mars Engineering Report M73-106-0, 1969

Fairly accurate characterization of atmospheric parameters is available from occultation studies, particularly when the atmosphere is thin, as is the case with Mars. Determination of density profiles is essential to the proper design of probes or landing vehicles. The occultation experiment is particularly attractive because it requires relatively little additional equipment to perform. A comprehensive mapping of atmospheric parameters under a wide variety of diurnal and seasonal conditions is possible from occultation observations of an orbiting vehicle, especially when the orbital plane is highly inclined.

The pressure range present near the Martian surface may promote arcing and corona effects in regions of high potential gradients such as will be present on antenna arrays, and could seriously degrade communication effectiveness. Likelihood of corona is increased by the conjectured presence of argon in the atmosphere, which would lower the ionization potential. Argon has not been confirmed as a constituent, however, because the earth's atmosphere is opaque to the spectral regions required for the test.

Figures 2.13, 2.14, and 2.15, exerpted from a recently published NASA space design criteria monograph, summarizes the atmospheric parameters of most significance to the space designer. These graphs are derived from computer calculated models based largely upon the results of the Mariner IV experiment discussed above, and upon the assumption of an 80% CO_2 and 20% N_2 atmospheric mixture.

Temperature of the lower atmosphere is strongly dependent upon latitude, season, and time of day. (See figure 2.16.) Although diurnal temperature variations will be large because of the thinness and transparency of the atmosphere, meteorological conditions will be highly repetitious and predictable, and will justify extrapolation on relatively few data points.

2.4 JUPITER

Jupiter differs markedly in several respects from the planets previously discussed. Enormous size and mass, low density, and high rotational velocity serve immediately to differentiate it from the inner four planets. Other environmental factors intensify the contrasts. Because of apparently high concentrations of the light solar elements, primary impetus for modern investigation is the promise of new insights into the origin of the Solar System.

Direct visual observation of Jupiter's surface (if it possesses one in the sense of a solid-gaseous interface) is prevented by a permanent, highly reflective layer of dense clouds. The clouds, however, exhibit rather distinct bands of various hues and intensities along latitudinal lines. Adjacent bands show differential velocities of the order of several hundred km per hour, which must result in wind shear disturbances of phenomenal magnitudes. Extreme atmospheric turbulence is confirmed by rapidly changing

cloud patterns. The disk of Jupiter has been partitioned with the aid of long term observations of the cloud bands into the areas illustrated. in figure 2.17. Over time periods ranging from hours to years, the markings are observed to change. Hence,the illustration below is highly stylized since at any particular time one or more bands are likely to be indistinct or lacking altogether. Certain reported fluctuations of the bands, particularly in coloration, have periods

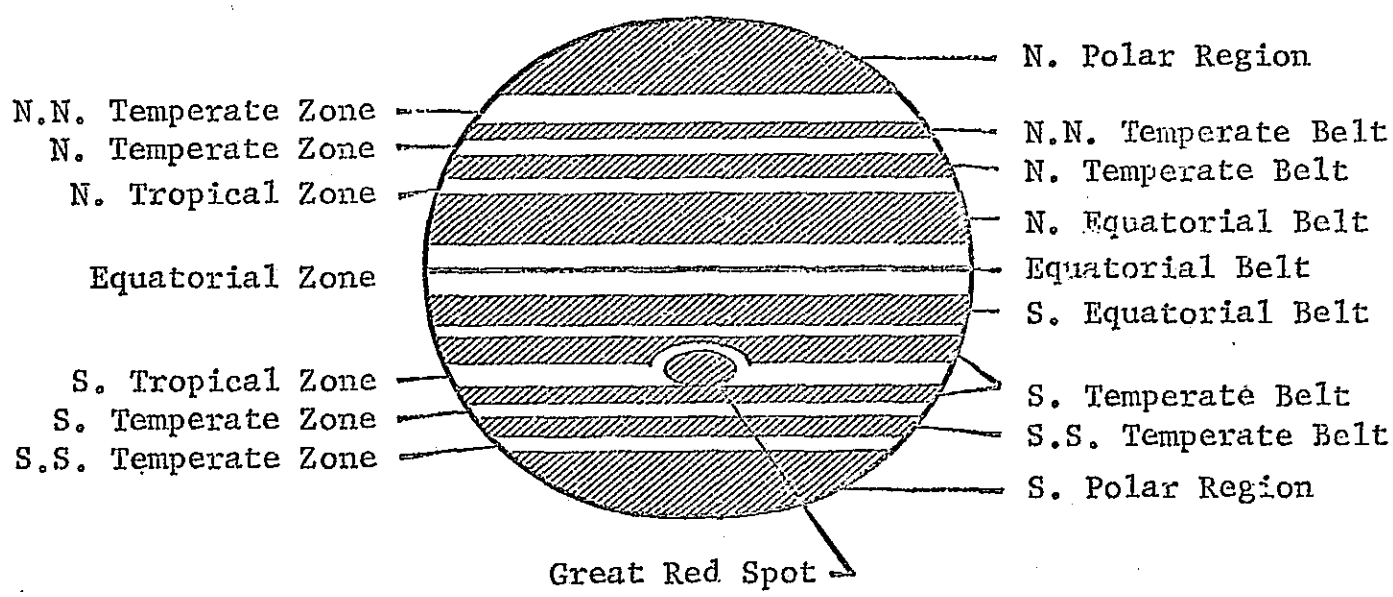

Figure 2.17 Nomenclature used in discussions of Jupiter surface markings.

slightly over twelve years -- the planet's period of solar revolution. This strongly suggests a seasonal variation, in spite of a nearly circular orbit and a very slight (3.09^{o}) inclination of the equatorial to the orbital planes. Only one visible Jovian feature, the so-called Great Red Spot, exhibits any degree of stability. First receiving mention in 1831, this anomaly has been under continuous study for almost a century. At first, it was suggested that the spot was an indication of a high elevation area on the solid surface. However, subsequent observations soon revealed extensive longitudinal drifting relative to an established rotational period for the Spot's mean latitude. Usually associated with the Great Red Spot is the South Tropical Disturbance, apparently a long lasting anomaly in the atmospheric circulation. No universally acceptable theory exists for either the Spot or the Disturbance.

Jupiter's rotational rate is not exceeded by that of any other major planet of the Solar System. With no solid surface displayed, however, the rate evades assignment of a single exact value, and must be qualified not

Table 2-2 Rotation periods of Jupiter based on visual observation (ref. 78)

Situation and/or name of current	Approx latitude, deg	Change of longitude in 30 days		Rotation period		
		λ_1, deg	λ_2, deg	hr	min	sec
N Polar Current	+90 to +47	-------	+1	9	55	42
NNN Temperate Belt (NNN Temperate Current).	+43	-------	−15	9	55	20
NN Temperate Belt and Zone (NN Temperate Current A).	+40 to +36	-------	+1	9	55	42
S edge of NN Temperate Belt (NN Temperate Current B).	+35	-------	−78	9	53	55
N edge of N Temperate Belt and S Part of N Temperate Zone (N Temperate Current A).	+33 to +29	-------	+18	9	56	5
Middle of N Temperate Belt (N Temperate Current B).	+27	-------	−105	9	53	17
S edge of N Temperate Belt (N Temperate Current C).	+23	−62	------	9	49	7
N Tropical Zone and N part of N Equatorial Belt (N Tropical Current).	+22 to +14	-------	−9	9	55	29
Middle of N Equatorial Belt 1898–1900	(?)	-------	−6	9	55	32
Middle of N Equatorial Belt 1927–1948	+13	-------	−67	9	54	9
S edge of N Equatorial Belt and N part of Equatorial Zone (Great Equatorial Current: Northern Branch).	+10 to +3	−4	------	9	50	[b]24
Middle of Equatorial Zone (Great Equatorial Current: Central Branch).	+3 to −3	−4	------	9	50	[b]24

only by the latitude, but by the method of observation (ref. 78). The three methods which have been employed are: (1) Visual observations of enduring anomalies in the cloud deck. Table 2-2 indicates the mean rotational rate of each zone based upon long term observations using this method. (2) Comparison of periodic radiation patterns in the microwave region. A rather stable period of 9h 55m 28s has been established by this method. (3) Doppler analysis of spectral line shifts in radiation from near the limbs. This method is rarely used because its uncertainty range is the highest of the three.

Rapid axial rotation produces a pronounced flattening at the poles. An independent measure of the oblateness is obtained from observations of the precession of the inclined orbital planes of the inner satellites, a result of tidal forces of the equatorial bulge. The comparisons between this "dynamic" and the optically determined oblateness, together with their respective error limits, provide important constraints in forming a theoretical surface and interior model of Jupiter. The various Jovian interior models are essentially presentations of plausible ranges of solid, liquid, and vapor distributions which satisfy gravitational, oblateness, and thermal constraints, based upon theories of the extent to which Jupiter's core is thermally active. A representative interior model is shown in Figure 2.18.

At Jupiter, the intensity of direct solar radiation is only a few percent of that incident on Earth. (See figure 2.1) The heavy cloud layers help to stabilize the temperature of the lower atmosphere, and further reduce the effect of diurnal solar transients on the atmospheric wind patterns. The well defined circulatory patterns are, therefore, an expected result and provides boundary conditions for an internal planetary model if it is accepted that internal heat sources play a dominant role in the thermal dynamics of the planet. Unfortunately, there has been little apparent success in attempting to incorporate the observed atmospheric conditions into a comprehensive thermal model. The major impediment to the study of atmospheric circulation is the lack of a visible solid surface to use as a coordinate system in determining the velocities of the cloud layers. Since the atmosphere moves to conserve its angular momentum, a precise determination of the rotational period of the surface would permit accurate estimates

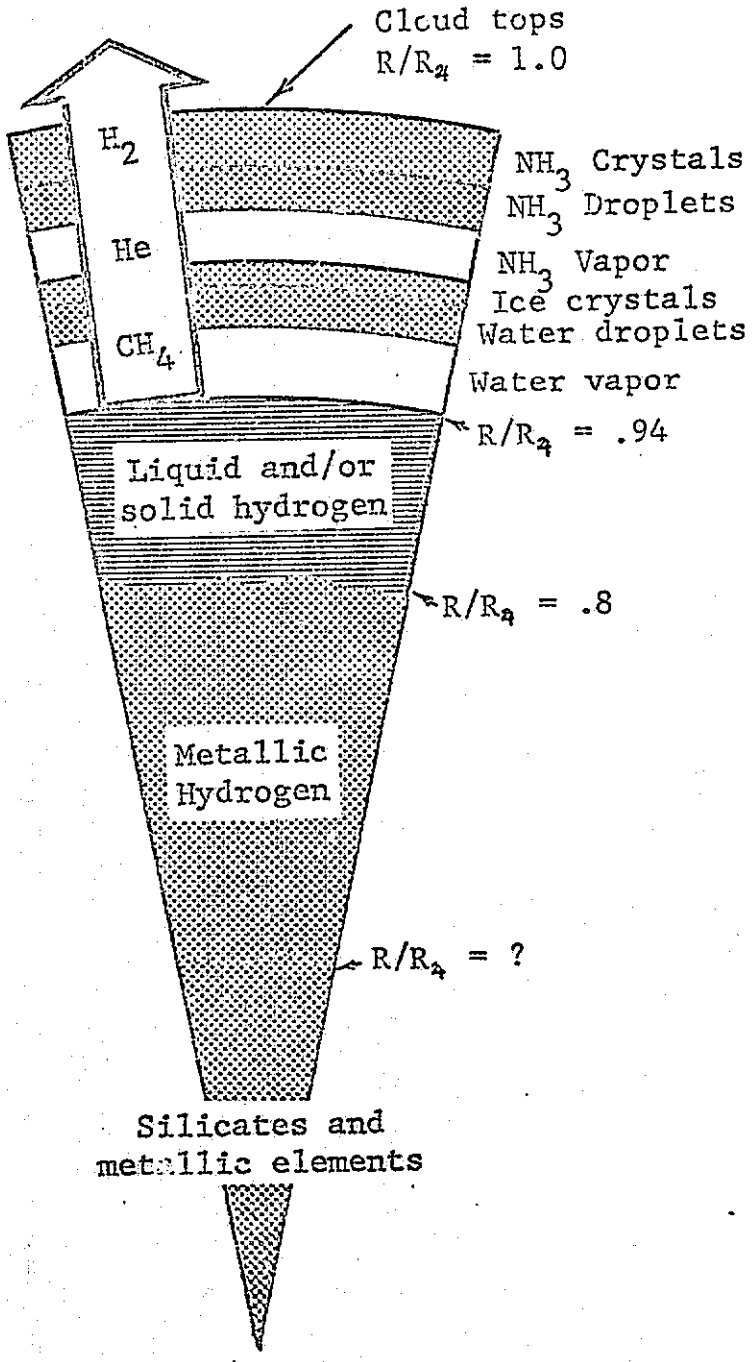

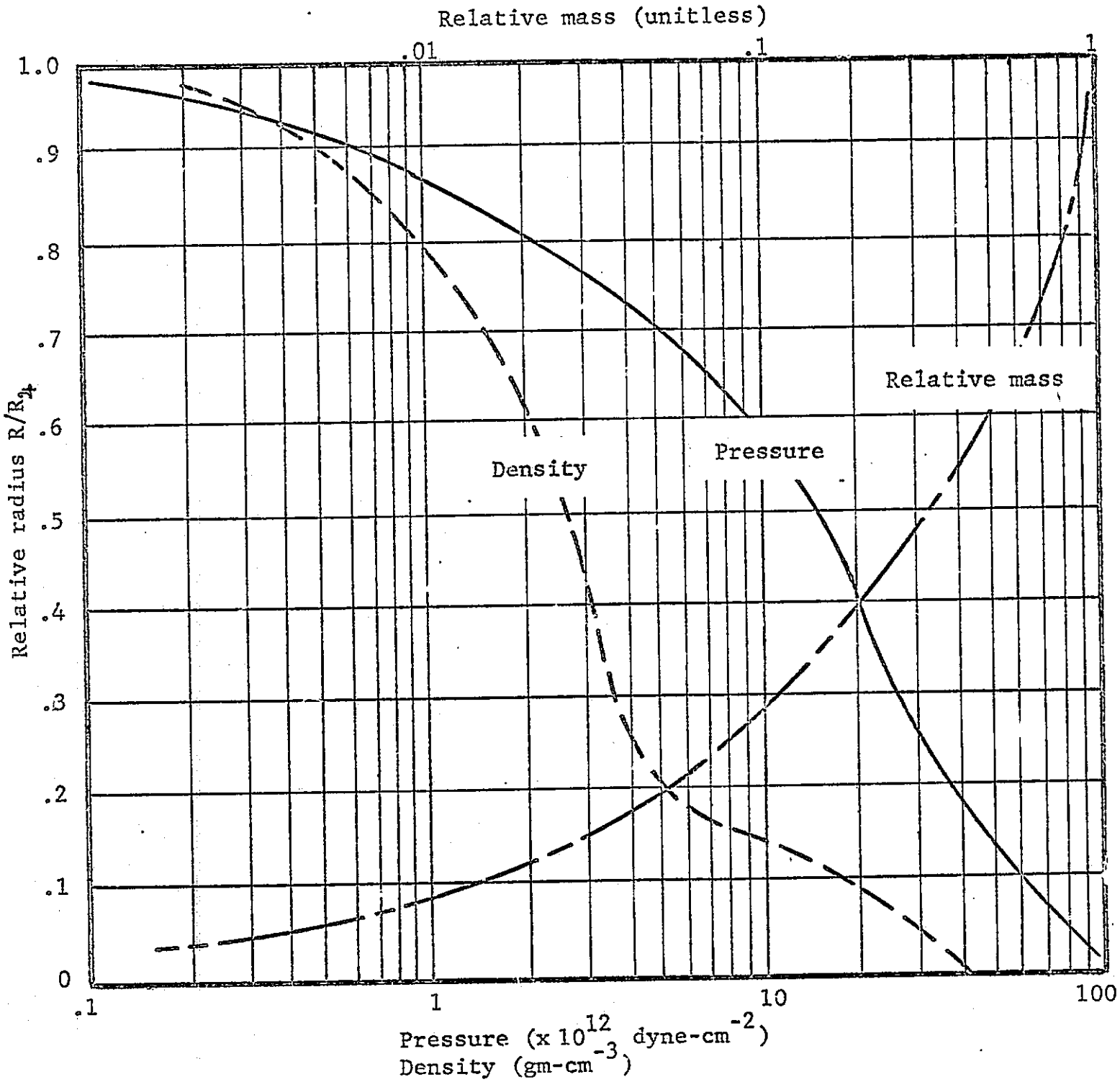

Figure 2.18 Internal parameters of a Jovian interior model. NASA SP-3031

of mass displacements involved and important additional information would then be available for characterizing the dynamics of the planet.

The only molecules positively associated with Jupiter are hydrogen (H_2), methane (CH_4), and ammonia (NH_3), but it is apparent from spectrographic analysis that significant amounts of other gases are also present.

Cruikshank and Binder (ref. 32) have recently submitted estimates for minor components of Jupiter's atmosphere, based on absorption curves in the 0.93 - 1.63 micron region. A background mixture of 55.6 m-atm CH_4 and 0.211 m-atm NH_3 at a total pressure of 1.4 atmospheres was selected as most suitable for an overall curve fit in their experiments, but it should be noted that these gases are minor constituents when compared with the several kilometer-atmospheres of hydrogen known to be present on this planet. The spectral resolution in this investigation allowed for significant improvements over previously compiled results. Table 2-3 lists compounds that are, due to spectrometric evidence, suspected to be present in the Jovian atmosphere.

A mean brightness temperature measured in the 8 - 13 micron range with thermocouple techniques yields 130°K with relatively good agreement between several investigators. Other techniques used for temperature analysis, including rotational analysis of H_2 and CH_4 lines, saturation analysis of NH_3 clouds, and microwave observations in the 8 mm to 3 cm range all lead to temperatures between 130°K and 200°K. The fact that these measurements all exceed the theoretical equilibrium temperature of 108 ± 1°K indicates that internal sources may play a dominant role in the thermal picture of Jupiter.

The wide variety of opinions and speculative nature of theories relating to regions beneath the cloud layer point to the inappropriateness at this time of attempting an engineering-oriented model of the atmosphere. Much more important to the question of probe type missions to Jupiter is the high approach velocity resulting from the gravitational attraction of the planet. Entry problems are compounded by the abundance of hydrogen in the atmosphere. Abrasion resulting from high specific energy exchanges between these light molecules and a penetrating probe could not be successfully

TABLE 2-3 Minor Constituents of the Jovian Atmosphere Based on Spectroscopic Evidence

Molecule	Wave Length μ	Maximum limit of Amount Above Jupiter Cloud Layer, m-atm.	Laboratory Pressure, atm.
CH_4	1.44	10-20	1.4
	1.10	100	1.4
	1.23	100	1.4
NH_3	1.51	0.2	1.4
	1.53	0.2	1.4
	1.08	5	1.4
C_2H_2	1.538	0.04	0.9
C_2H_4	0.872	2	0.9
C_2H_6	0.904	2.5	0.9
HD	0.74	500	0.9
CH_3D	0.994	20	0.9
CH_3NH_2	1.52	0.02	1.0
SiH_4	0.974	20	-
HCN	1.53	0.05	0.9
H_2S	1.58	0.25	1.4
CO_2	1.6	1	0.5

From Cruikshank, Dale P. in Astrophysics and Space Science, 3:347-356, March 1969.

challenged by heat shield techniques suitable for the inner planets. Communication problems would be severe, also, since an orbiting vehicle acting as a relay station would be in sight of a probe for only a short time period. Direct communication to Earth from a probe appears highly unfeasible at over 4 AU.

Jupiter exhibits a wide range of electromagnetic radiation which cannot be attributed solely to thermal or solar origin. Many of the details of this phenomenon are still open to speculation, but the presence of intensive magnetic and Van Allen-like particle fields associated with this planet is unquestioned. Three separate regions of the spectrum usually receive individual treatment in studies of Jovian radio emission.

a) 1-3 centimeters

Radiation in the 1 cm region is accepted as being of thermal origin and caused by motions of the atmospheric molecules because agreement with the infrared brightness temperature is satisfactory. The 3 cm region exhibits stronger radiation than that attributable to the infrared, but it is possible that its origin is below the cloud layer.

b) 3-7 centimeters

Decimeter radiation is believed to be caused by electrons spiraling about and oscillating along magnetic lines in a manner similar to those in the Earth's Van Allen belts. Available estimates for the magnitude of the particle flux surrounding the planet vary widely, but an electron flux of approximately 1000 times that associated with the Earth is currently used in mission analysis (ref. 103). (See figure 2.19.)

c) 7-70 meters

The emission in the decameter region is characterized by sporadic bursts. No theory presently exists for this behavior, but a turbulent or "patchy" plasma distribution has received acceptance. Jupiter's innermost satellite, Io, has a remarkable effect upon the nature of the emission, with maximum radiation received at regular intervals correlatable with the satellite's phase angles. Ghedhill (ref. 50) offers an explanation of this phenomenon in terms of an inclined, disk-shaped compressed region which the satellite penetrates twice during each orbit. A co-rotating magnetosphere

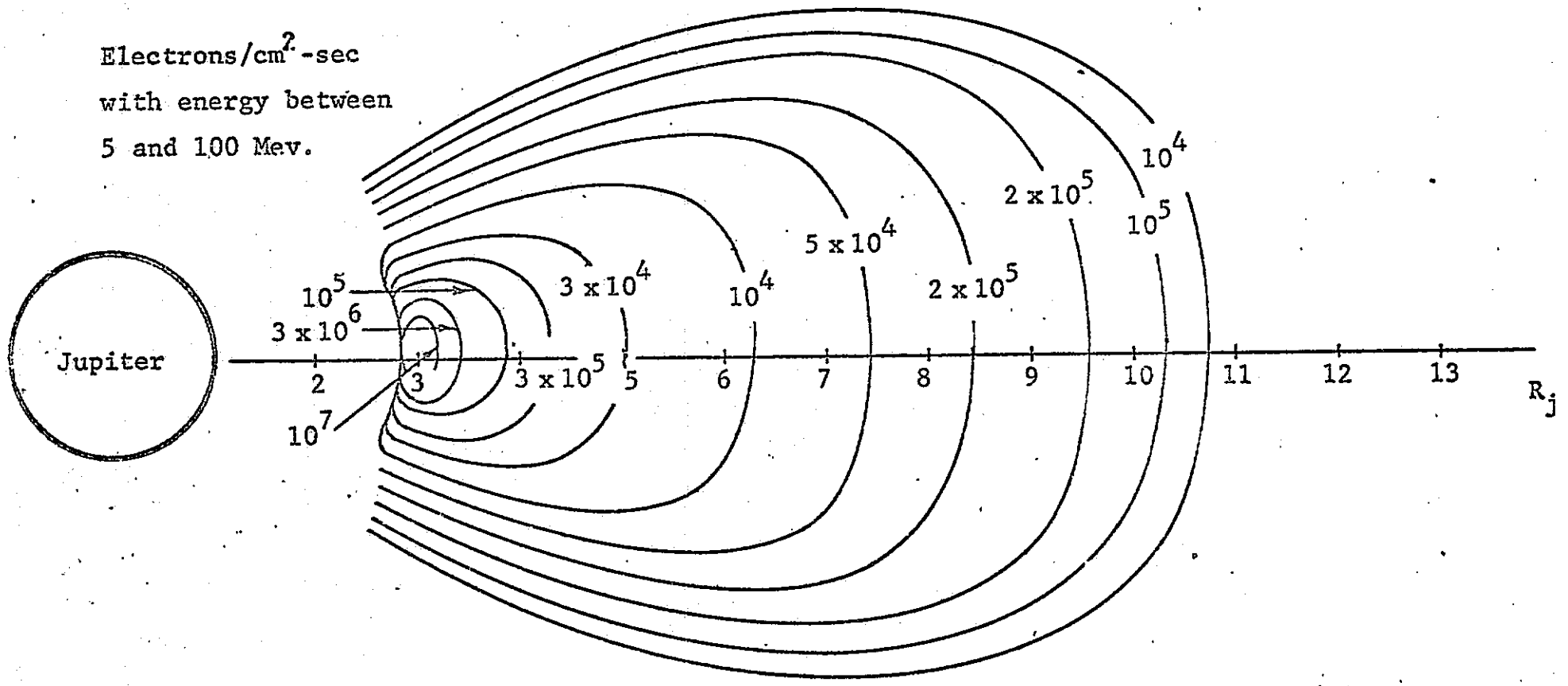

Figure 2.19 Representative model of the Jovian trapped radiation zones (Ref. 103)

TABLE 2-4 Selected constants of satellite system of Jupiter

Name and number of satellite	Distance to Jupiter		Period of sidereal revolution, days	Diameter, km	Relative mass $M_J = 1$	Density, gram/cm^3
	Relative $R_J = 1$	Semimajor Axis km				
V (Almalthea)	2.539	181 260	0.49818	160(?)	----	?
I (Io)	5.905	421 560	1.76914	3800	$(3.8\pm0.3)\times10^{-5}$	2.5
II (Europa)	9.396	670 780	3.55118	3100	$(2.4\pm.05)\times10^{-5}$	3.0
III (Ganymede)	14.99	1 070 140	7.15455	5600	$(8.2\pm0.1)\times10^{-5}$	1.7
IV (Callisto)	26.36	1 881 800	16.68902	5200	$(5.1\pm0.4)\times10^{-5}$	1.3
VI (Hestia)	160.7	11 472 000	250.6	130(?)	?	?
VII (Hera)	164.4	11 736 000	260.1	30(?)	?	?
X (Demeter)	164	11 708 000	260	50(?)	?	?
XII (Andrastea)	290	20 703 000	617	15(?)	?	?
XI (Pan)	313	22 345 000	692	15(?)	?	?
VIII (Poseidon)	326	23 273 000	735	40(?)	?	?
IX (Hades)	332	23 701 000	758	40(?)	?	?

From Reference 78

is necessary for the plasma concentration. Decimeter radiation also has been associated with longitudinal coordinates on the planet's surface, but a clear correlation has not been established.

Emission in the region between decimeter and decameter wavelengths is not well understood because of technical limitations of receivers and the background of galactic noise. Wavelengths longer than the decameter region are subject to attenuation and reflection by the Earth's ionosphere, normally restricting studies to wavelengths of less than 15 meters.

Jupiter has twelve known satellites which are divided into two major groups according to their proximity to the planet. Table 2-4 lists some of the physical constants of the system. Four out of five inner satellites are comparable in size to our moon, with the largest, Ganymede, being only slightly smaller than Mars. The innermost satellite, J-V, revolves at a record 26.53 km/sec only 181,200 km above the planet's cloud layer, and its orbit is strongly perturbed by the planet's equatorial bulge. The outer system is comprised of bodies of insignificant masses under the graviational influence of the Sun as strongly as that of the planet. Hence, their orbits are not even approximately elliptical.

Although the largest satellites might be expected to retain tenuous atmospheres, no direct evidence has yet been found. A temporary increase in the apparent magnitude of Io upon emerging from Jupiter's shadow has been attributed to a covering of frost due to the temperature drop associated with the eclipse. (Ref. 78.) Of the satellites large enough to display surface markings, locked synchronous rotation is evident.

2.5 INTERPLANETARY REGIONS

The planets do not move in empty space, but are accompanied in their circuits around the sun by countless millions of lesser particles of neutral matter. This material is known by such names as asteroids, meteoroids, cometary debris, and cosmic dust, and range in size from gaseous molecular aggregates to bodies measured in hundreds of kilometers. All of these objects move in orbits under the gravitational forces of the sun and planets. The smallest are additionally influenced significantly by the

sunlight which irradiates them. Collisions with space debris can result in damage to, or total failure of spacecraft because of the high relative velocities involved. Therefore, an evaluation of collision probabilities for a given mission profile is necessary for proper vehicle design.

A significant proportion of the smallest size particles in the Solar System are believed to have cometary origins. According to the popular "dirty iceberg" theory, the volatile nucleus of the comet disintegrates during approach to the sun, and produces an associated swarm of meteoroids as imbedded gravel-like particles are freed. The swarm eventually loses definition by perturbations, and spreads out along the original comet trajectory. Meteoroid swarms are responsible for annual meteor showers observed at orbital intersection points and represent particle density distributions several orders of magnitude above background. Aside from these relatively few recently developed (astronomically speaking) and well-defined meteoroid swarms, the spatial distribution of cometary material debris has apparently become quite uniform.

The major portion of the Solar System's debris lies between the orbits of Mars and Jupiter, and with few exceptions, moves in posigrade orbits of low eccentricity and inclination. Ceres, the largest of these asteroids (diameter: 770 km), has been suggested as a target for advanced missions, but is not included in our assessment. Several thousand members of the asteroid belt have been observed optically and orbital elements for 1726 have been published. Periodic variations in their observed brightness indicate irregular shapes and support the hypothesis that these bodies resulted from an explosion or collision of a planet. While it is not possible to detect from earth asteroids smaller than about 1 km in diameter, their existence is not doubted. Continual collisions between asteroids are believed to be occurring which gives rise to the popular expression of "grinding itself to bits." Several estimates of the population of the asteroid belt have been submitted in recent years due to a need for a quantitative model on which to base engineering designs for vehicles intended to penetrate the belt. The models are usually extrapolations of the mass population distribution of the known asteroids, according to certain

theoretical considerations. Inputs to such models include:

1. Gegenschein or Zodiacal light
2. Crater distributions on Mars and the Moon
3. Near Earth micrometeoroid populations determined from satellites and meteors burning in the atmosphere
4. Empirical rock crushing experiments by various methods

Collisions with high speed atoms ejected from the sun (solar wind) combine with radiation pressure to sweep the solar system of the smallest particles. The solar influence tends to place a lower limit on the size of interplanetary debris at a given heliocentric distance and this factor is usually reflected in meteoroid population models generated for the purpose of spacecraft design criteria. Were there no micrometeoroid regenerating mechanisms, solar pressure would have eventually cleared the solar space environment of particles up to perhaps several hundred microns in diameter.

In general, mass distributions are assumed to follow the form

$$N \sim m^{-\alpha}$$

where N is the number per unit volume of particles having masses greater than or equal to m. The choice of α is highly significant as can be seen in figure 2.20. Kessler (ref. 8) points out that values of α as low as .67 would effectively eliminate the hazard to spacecraft, whereas values approaching 1, suggested by terrestrial rock crushing experiments, predict a meteoroid flux several orders of magnitude above that near earth. He has developed a model (figure 2.21) for the central portion of the belt using $\alpha = .84$. Devine (ref. 39), in developing a similar model chose a nominal value of .75. Particles of greatest concern lie in the range of approximately 10^{-2} to 10^{-5} grams. Smaller particles are not inherently damaging, whereas shielding against meteoroids greater than 10^{-2} grams becomes prohibitively expensive in payload. Trainor (ref. 103) suggests a bumper shield for the Outer Planetary Explorer spacecraft capable of stopping bodies of masses up to 10^{-3} grams.

The meteoroid impact hazard to spacecraft is very difficult to assess because of the great uncertainties which persist regarding the particle

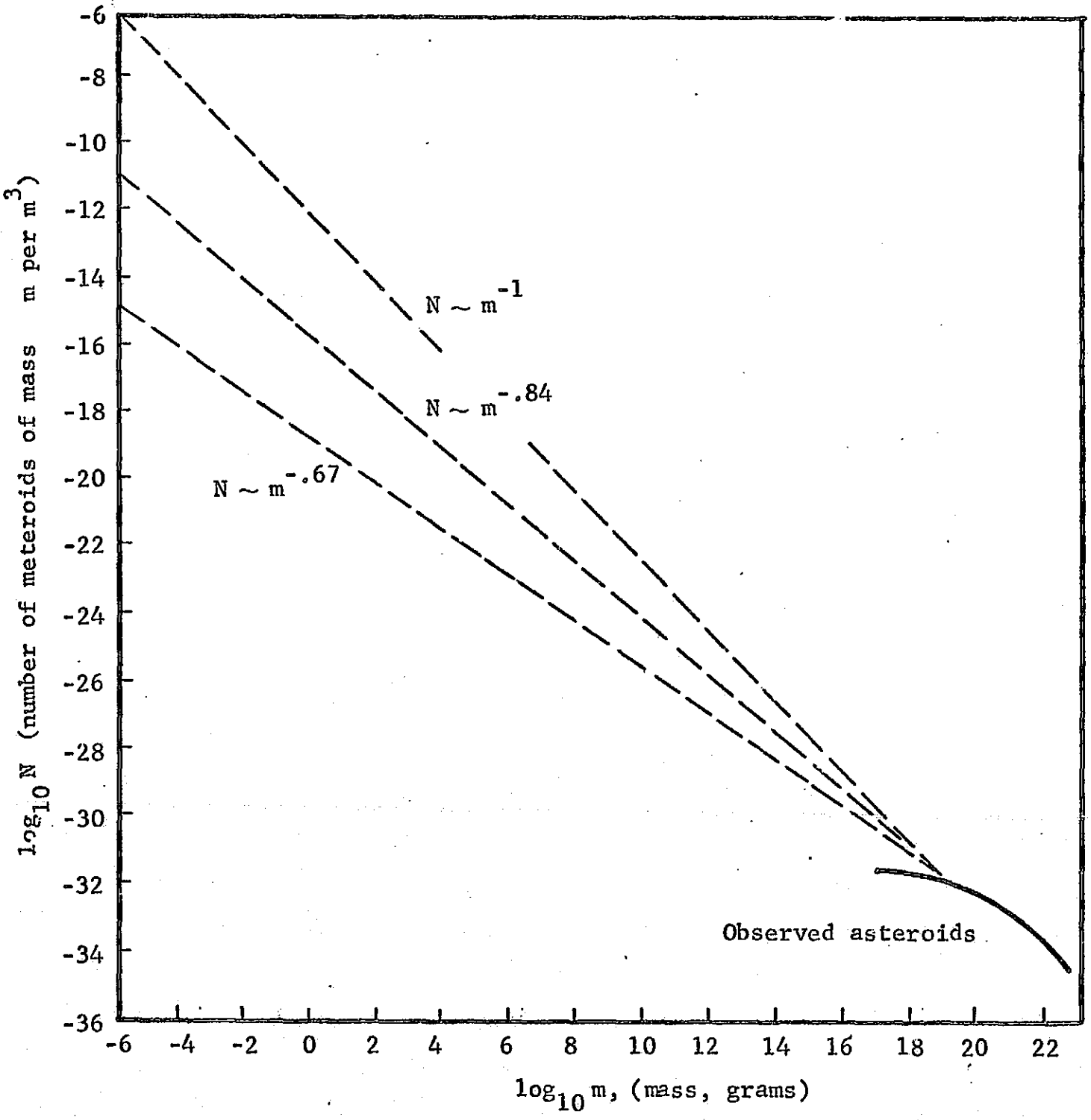

Figure 2.20 Asteroidal debris models based upon extrapolation from observed asteroids. (Ref. 8)

flux originating from both cometary and asteroidal sources. Present models of the meteoroid environment represent extrapolations of rather limited data requiring one or more assumptions concerning the particle's origin, density velocity, etc. A decade of space flight experience in the cometary debris

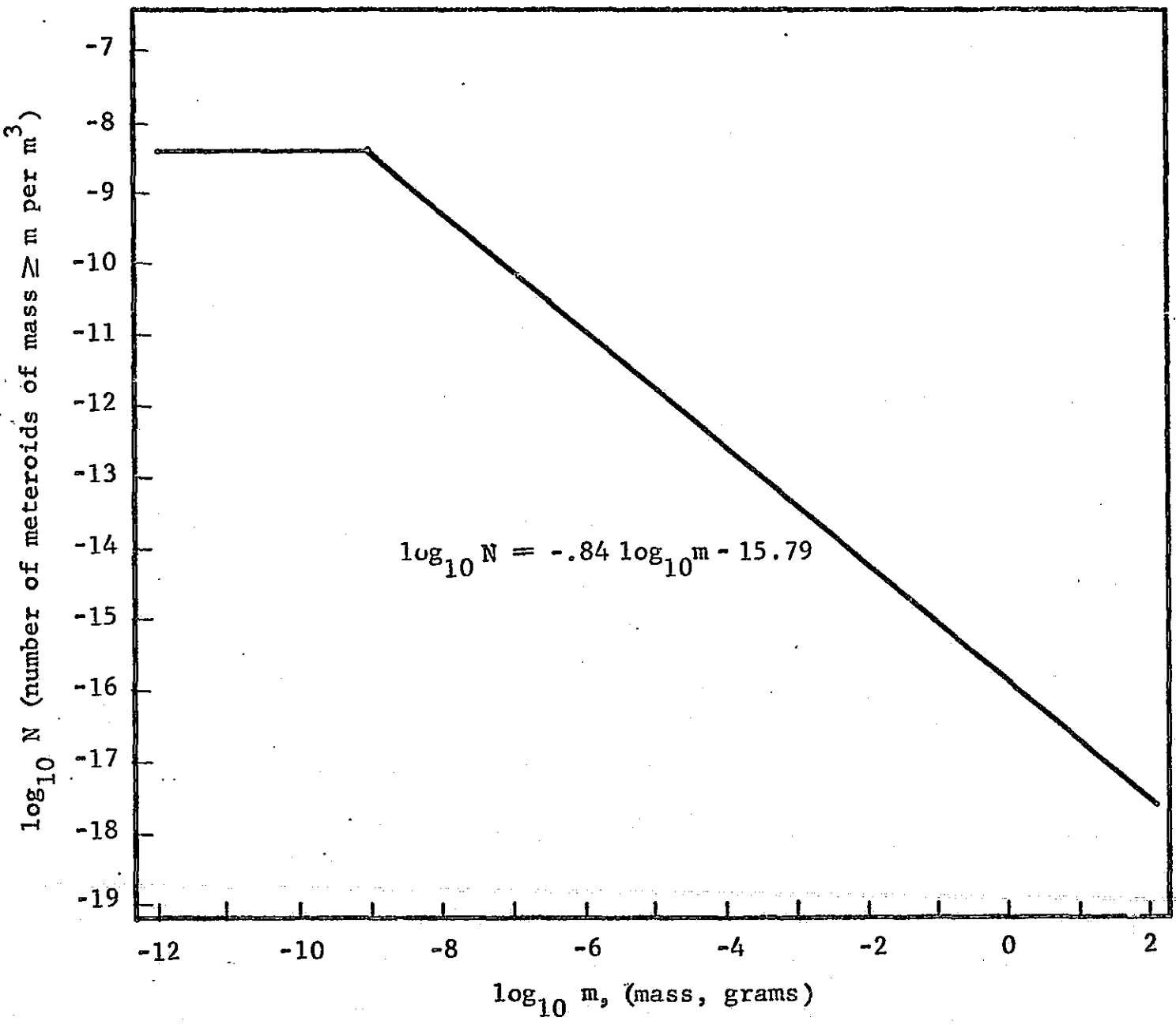

Figure 2.21 Asteroid mass distribution at 2.5 AU. (Ref. 8)

environment near 1 AU has involved many spacecraft functioning for several years without sensible impact damage, with the result that concern has diminished for catastrophic or severely damaging impacts in the near earth region. Although there is similarity between the integrated fluxes of cometary debris and the upper limit asteroidal debris models, it does not follow that the spacecraft impact damage risk in the asteroidal belt is similar to that near Earth. The implications of most recent models of interplanetary debris concerning the hazards of spacecraft damage include: 1) acceptance of a moderate risk of damage, 2) substantial shielding of

the spacecraft or 3) avoidance of the asteroid belt. These implications must be considered realistic until such time as new data becomes available which reduces the model uncertainty by eliminating the upper limit model. Such data will probably be obtained only by in situ detection of asteroidal debris by missions to or through the asteroidal belt.

2.6 OUTER PLANETS

Data pertinent to the mechanical and physical characteristics of the planets beyond Jupiter are tabulated in Table 2-5.

The surfaces of these planets, if they possess sizeable solid cores, are completely hidden from observation by dense, cloudy atmospheres. The sunlight by which we observe them is reflected by only a shallow layer of the gaseous envelopes and gives us very little information concerning the lower layers of the atmospheres or of the surfaces which they overlay. The only gases revealed by the spectroscope in the atmospheres of these planets are ammonia and methane, both noxious and inimical to life. These gases are compounds of nitrogen and carbon, respectively, with hydrogen atoms. Other gases that are present in the Earth's atmosphere, such as nitrogen, oxygen, and water are expected to be present in the atmospheres of the outer planets, but because of the low temperatures that prevail they are probably in the liquid or solid state.

Saturn

Spectroscopically, Saturn appears similar to Jupiter although our knowledge is more limited because of its greater distance from Earth. The methane bands appear as very strong features and hydrogen has also been observed. A rotational temperature of $90^{o}K$ has been derived from the hydrogen spectra.

The rings of Saturn, lying in Saturn's equatorial plane, extend from about 12,500 to 76,000 km above Saturn's surface. A gap between the outermost ring and the inner rings, called the Cassini Gap, is about 4000 km wide. It has been suggested that Saturn swing-by missions travel through this gap to avoid possible damaging encounters with particulate matter within the rings.

Name	Mercury	Venus	Earth	Mars	Jupiter	Saturn	Uranus	Neptune	Pluto
Symbol	☿	♀	⊕	♂	♃	♄	♅	♆	♇
Mean Distance from Sun Millions of km Astronomical Unit, A.U.	 57.9 0.387	 108.1 0.723	 149.5 1.000	 227.8 1.524	 777.8 5.203	 1426.1 9.539	2869.1 19.191	4495.6 30.071	5898.9 39.457
Diameter (Earth=1)	0.38	0.967	1.000	0.523	10.97	9.03	3.72	3.38	0.45
Mean Diameter, km	4,842.1	12,322.0	12,742.46	6,664.3	139,785	115,064	47,402	43,070	5,734
Surface Gravity (Earth = 1)	0.38	0.87	1.00	0.39	2.65	1.17	1.05	1.23	<.5?
Velocity of escape km/sec	4.3	10.4	11.2	5.1	61.0	36.7	22.4	25.6	<5.3
Oblateness	0	0	1/(298.38)	1/192	1/15	1/(9.5)	1/14	1/40	?
Mass (Earth = 1)	0.0543	0.8136	1.0000	0.1069	318.35	95.3	14.58	17.26	<0.1?
Mean Density ($H_2O = 1$)	5.46	4.96	5.52	4.12	1.33	0.71	1.56	2.47	<5.5?
Known Moons	0	0	1	2	12	9	5	2	0
Inclination of Equator to Orbit Plane	<7°	?	23°30′	24°	3°	26°45′	98°	29°	?
Eccentricity of Orbit	0.206	0.007	0.017	0.093	0.048	0.056	0.047	0.008	0.249
Mean Orbit Velocity km/sec	47.85	35.01	29.76	24.11	13.05	9.64	6.78	5.47	4.84

TABLE 2-5 Physical constants of the planets

Uranus and Neptune

Uranus and Neptune both have more than ten times the mass of Earth, but are less than half as dense. Intense methane bands have been observed in the spectra of Uranus and Neptune, completely altering the continuous spectra from the yellow to the infrared and perhaps concealing weaker bands of other molecules. No ammonia has been observed in the spectra of either planet, if it exists, it is undoubtedly frozen as would be carbon dioxide and water.

Pluto

Little is known of Pluto other than its orbital characteristics and its mass. Its density is as yet undetermined. No atmosphere has yet been observed. Most readily observable chemical species would freeze out if the temperature is near the assumed value of $50^{o}K$.

3.0 PLANETARY MISSIONS

There is little need for extensive research in the development of hardware capable of operation in, for example, high temperature environments unless some future mission must perform in such an environment. Furthermore, the schedules planned for future missions which may encounter severe environments can effectively guide the timing of supporting research. This section, therefore, reviews future missions which have been studied and proposed for funding. It identifies the planetary environments to which the hardware will be exposed, and reviews schedules for these missions so that associated SRT can be planned.

Our mission listing is not complete nor does it consider all configuration alternatives. It is sufficient, however, for the present purpose, i.e. to permit the identification of the pertinent spacecraft technology deficiencies for furthur discussion in chapter 4.

3.1 GENERAL CHARACTERISTICS

Planetary flights can be conveniently classified in increasing complexity according to required trajectory maneuvers at planetary encounter.

The simplest mission profile is the direct impact trajectory. Examples include the recent series of Ranger flights to the Moon. High reliability is possible in this mode because ballistic accuracy needed to effect impact is significantly reduced by the planet's gravitational field. Relatively few scientific objectives, however, can be conveniently achieved by impact of a single vehicle due to limited geographical coverage and experimental duration.

A second profile class is represented by the fly-by mission in which most of the scientific objectives are achieved during the few hours of closest planetary approach. Reliability problems caused by severe environmental factors are minimal but so are the opportunities to observe temporal phenomena and to verify and correlate data. The Mariner program has acheived to date four highly successful Mars and Venus fly-by missions. Many of the outer planet missions discussed in this section employ this mode.

Orbiting missions, achieved by retro-braking against the heliocentric trajectory and gravitational capture by the planet, can provide spatial and temporal observations of planetary phenomona.

The most demanding mission profile provides for a soft landing of a probe or the entire spacecraft and extended experiments to study the atmosphere and the surface of the planet. This mission type is of particular interest since it is required to operate for extended periods in atmospheric environments which often represent the most serious threats to the successful performance of the hardware.

Some missions consist of combinations of these four classes of profiles. For example, a soft lander is combined with an orbiter for Viking '73.

To explore the outer planets, the gravitational field of an intermediate planet, (usually Jupiter) is used to accelerate the spacecraft to its final destination. Gravity assist becomes particularly attractive to shorten the total flight time because the long duration of such missions will result in serious reliability implications. This is treated in more detail in a later section.

The schedule of planetary exploration is largely determined by the launch windows or time periods available in which the missions are considered feasible. Outside these windows, energy requirements for target encounter exceed the launch vehicle capability, or the mission duration becomes unreasonably long. Launch windows may be lengthened by sacrificing payload, but the trade-off here is economic justification for the mission. Launch windows for planetary missions rarely exceed several score days in length, and opportunities for missions to encounter more than one planet occur infrequently. (See table 3-2.) An unusual opportunity in 1977 to encounter several of the outer planets with a single vehicle has been widely studied (ref. 63, 82).

Some of the more widely studied missions which provide examples of hardware-environment interactions in the planetary program are summarized below.

TABLE 3-1

PROPOSED SCHEDULE OF PLANETARY MISSIONS

MISSION	TARGETS	TYPE	EARLIEST PROPOSED LAUNCH DATE
Mariner	Mars	ORB	1971
Viking	Mars	ORB & LAND	1973
Pioneer F/G	Jupiter	FB	1972
Mariner	Mercury-Venus	SB & (PRB)	1973
Planetary Explorer	Venus	ORB	1973
FB/Out of Ecliptic	Jupiter	FB & (PRB)	1974
Planetary Explorer	Mars	ORB	1975
Multi-Probe	Venus	ORB & PRB	1975
Mariner	Venus	ORB	1975
Asteroid Belt Survey	Asteroid Belt	(ORB)	1975
Buoyant Probe	Venus	ORB & PRB	1976
Mariner Comet	D'Arrest	FB	1976
Jupiter Orbiter	Jupiter	ORB	1976
Jupiter-Saturn-Pluto	Jupiter-Saturn-Pluto	SB & PRB	1977
High Data	Mars	ORB	1977
Rover	Mars	ROV	1977
Saturn Orbiter	Saturn	ORB & PRB	1978
Rough Lander	Venus	ORB & PRB	1978
Jupiter-Uranus-Neptune	Jupiter-Uranus-Neptune	SB & (PRB)	1979
Mariner Asteroid	Eros	FB	1981
Jupiter Probe	Jupiter	FB & PRB	1980
Solar Electr.	Mercury	ORB	1982
Soft Lander	Venus	LAND	1983
Jupiter Moon	Io	LAND	1985
Mariner Comet	Kopff	RENDEZ	1983
Mariner Comet	Halley	FB	1985

Legend:

ORB = orbiter

LAND = soft lander

FB = fly-by

PRB = probe

(PRB) = probe as alternative configuration

SB = swing-by

RENDEZ = rendezvous

(ORB) = orbits the sun within the asteroid belt

ROV = rover

MULTIPLE OUTER PLANET LAUNCH OPPORTUNITIES

TARGET(S)	LAUNCH YEAR						NEXT OPPORTUNITY
	1976	1977	1978	1979	1980-81	1981-82	
JUPITER SWINGBY MISSIONS:							
SATURN	X	X	X	X			1996
URANUS			X	X	X	X	1992
NEPTUNE			X	X	X	X	1991
PLUTO	X	X	X	X			1989
MULTIPLE PLANET SWINGBY MISSIONS:							
JUPITER-URANUS-NEPTUNE			X	X	X	X	1992(?)
JUPITER-SATURN-PLUTO	X	X	X	X			2076
SATURN-URANUS-NEPTUNE				X	X	X	1982
GRAND TOUR	X	X	X	X	X		2155

TABLE 3.2

3.2 PROPOSED MISSIONS

(1) Mars Mariner '71 This on-going program in the Mariner series conducted by JPL will explore atmospheric and surface properties of Mars by means of an orbiting spacecraft. Two flights are currently planned for the 1971 opportunity. Planet surface topography, planetary fields, astronomical data and atmospheric properties such as pressure, temperature, density, and chemical constitutents will be measured. Instrumentation includes magnetometers, trapped radiation detectors, IR and UV spectrometers, and photo imagery. A transit time of 210 days is estimated and an operational life in orbit of one half the planet's year is desired. An elliptical orbit with apoapsis of 30,000 km and periapsis of 1800 km will eliminate the need for consideration of the adverse effects of the Mars atmosphere. Environmental factors of principal concern to the spacecraft designers are mission lifetime and thermal transients associated with Martian orbit.

Planetary quarantine requirements will require that the probability is below a specified level of accidentally delivering a potentially contaminating organism to the surface or to growth-supporting atmosphere. In this case the spacecraft will not be required to be exposed to heat sterilization prior to launch, although surfaces may be chemically decontaminated as an added precaution.

(2) Mercury-Venus '73 The year 1973 and 1975 provide opportunities to use the gravitation field of Venus to assist in missions to study Mercury. Mariner-type spacecraft will be instrumented to measure this planets' atmospheric properties, surface properties, orbital characteristics, and Venus's cloud characteristics.

Scientific payloads would closely resemble Mars Mariner '71 and will include photo imaging of both planets. It may also be possible to launch a non-survivable atmospheric probe during the Venus swing-by.

Flight times of 108 days to Venus and 183 days to Mercury have been projected. Environmental constraints will be essentially determined by the interplanetary space between Venus and Mercury. To withstand the higher level of solar intensity, gallium arsenide solar arrays will be employed. The Mariner mylar-teflon thermal blanket will be replaced by polyimide (H-film). Use of silver zinc batteries is planned.

(3) Venus Multiprobe '75 Simultaneous, wide geographical coverage of Venus by means of a number of probes has been recommended as a comprehensive approach for further study of the atmosphere of this planet. The probes would be carried aboard a single Mariner class spacecraft launched by an Atlas Centaur vehicle and released into the atmosphere in the polar, temperate, and equatorial zones on the sunlit and dark sides of the globe. A direct impact of the primary vehicle or bus is seen as the most feasible trajectory for reasons of reliability and payload economy.

One alternative configuration includes the deployment of three types of probes. Ten days prior to encounter, three so-called small probes are released with appropriate velocity increments to cause insertion into the atmosphere at the sub-solar, anti-solar, and south polar points, respectively. Ninety minutes before impact, additional larger probes are released, and experiments aboard the bus vehicle initiated and continued until destruction of the bus by atmospheric friction. Two of these latter probes may carry balloons designed to remain suspended indefinitely at an atmospheric level of 50 millibars.

Descent time of the three small probes will be approximately two hours. A nominal surface environment of 738°K and 109 atmospheres has been chosen for design purposes. Thermal protection may be achieved by a system of concentric beryllium spheres. The space between two of the spheres will be evacuated, and a change-of-phase material (possibly sodium sulfate dekahydrate) will immediately surround and maintain a constant local ambient temperature for the centrally located instrumentation. Reflective coatings on all surfaces will further enhance the insulation effectiveness. Thermal and pressure protection in the large probes is to be achieved in a similar fashion.

(4) Venus Buoyant Probe This space exploration mission may consist of an orbiting spacecraft or direct impact vehicle with one or several probes designed for suspension in Venus's atmosphere in the 50 to 150 kilometer region. At this altitude environmental constraints will not be severe and measurements of atmospheric and perhaps even surface properties can be carried out. Such a mission could probably not be undertaken prior to 1976. Environmental considerations

include pressure, temperature, contaminating atmospheric constituents, sterilization requirements, and orbital lifetime.

(5) Venus Mariner and Mars High Data Rate Mariner The primary objective of these missions is high resolution mapping of the planet surfaces (Mars optically Venus by radar). Other scientific goals include studies of atmospheric properties, planetary fields and astronomical data. Orbiter spacecraft of the Mariner design will be used. Possible instrumentation includes: Magnetometer, IR and UV Spectometer, Microwave Spectometer, Solar Plasma Probe, Cosmic Dust Detector, Particle Flux Detector, Ion Chamber, and TV Imager.

Spacecraft will include both passive (coatings and blankets) and active (louvers) thermal control. Surface finishes and materials will be selected to provide specified absorbance and emittance.

The Mars mission may include a high data rate communication system to facilitate photo imagery. Proposed launch opportunities are 1975 and 1977.

Environmental stresses can be assumed similar to Venus Multiprobe Orbiter and the Mars Mariner '71.

(6) Jupiter Flyby An early flyby of Jupiter has been suggested to refine our current questionable knowledge of the properties of this planet to aid in the operation of late 1970 decade missions, particularly outer planet swing-bys. Such a flight is possible as early as 1974. A precursor of the later outer planet swing-by spacecraft will be pulled by the gravitational field of Jupiter in a trajectory approximating that for multiple outer planet swing-bys. Of particular interest would be gravitational field characteristics, trapped radiation, atmospheric properties which could be measured remotely, surface characteristics (by occultation, etc.).

Environmental aspects of concern in system design and equipment selection include radiation, interplanetary debris, low temperatures, and the possibility of magnetic fields.

(7) Comet Exploration Missions to D'Arrest, Kopff and Halley have been suggested to further explore theories relating to the nature of comets and their

relationship to the origin of our Solar System. As a comet approaches the sun significant amounts of dust and gas are released as the nucleus is heated by solar radiation. Comets exhibit a wide range in their trajectories, some moving about the sun in orbits indistinguishable from inner planets, other following highly eccentric paths inclined at large angles to the earth's orbit plane.

The pertinent orbital characteristics of the three proposed target comets are shown below:

	#	P	T	q	Q	i
D'Arrest	10	6.70	1976	1.38	5.73	18.1
Kopff	8	6.32	1983	1.52	5.32	4.7
Halley	29	76.03	1985	0.59	35.31	162.2

where:

# = Number of observed returns to perihelion
P = Period in years
T = Date of perihelion passage of interest
q = Perihelion distance AU
Q = Aphelion distance AU
i = Inclination of orbit to ecliptic (in degrees)

A spacecraft of the Mariner class is proposed to fly-by and rendezvous with these comets to measure dust and constituency of their tails and to elucidate some processes of comet disintegration. Encounters would be arranged close to perihelion, thus minimizing required flight time. Flight profiles can be selected which minimize interplanetary environmental effects on spacecraft hardware and systems. Of principal environmental concern to the spacecraft designer will be characteristics of the comet trajectory such as dust and vapor.

(8) Asteroid Fly-By A Mariner class spacecraft has been proposed for a fly-by of the asteroid Eros, a well known asteroid used to improve solar parallax during its close approaches to earth. With a solar period of 1.76 years it approaches within 14 million miles of earth every 44 years. Its pertinent characteristics include:

Perihelion	1.13 AU
Aphelion	1.78 AU
Orbital inclination	10.8°

The Eros fly-by is planned for 1980 and should not encounter any environments more severe than those encountered by Martian fly-by.

(9) Soft Landers Soft landers are proposed for Mars (Viking '73), Venus (1983), and Io, a moon of Jupiter (1982), and a roving vehicle to be landed on Mars in 1977. With the exception of Viking '73, an on-going, approved program, the mission objectives and spacecraft designs have not been detailed. The environmental aspects, other than Io, can, however, be reasonably well defined for all missions.

The Mars missions will encounter low atmospheric pressure and density, fairly low surface temperatures, high winds, sand and dust, negligible magnetosphere, corrosive atmosphere and rough topography. The Venus lander must be designed to withstand high pressures, high temperatures, a possibly corrosive atmosphere and an unknown topography. These factors have been discussed more fully in Chapter 2 and are related to equipment state of technology in Chapter 4.

Io, the second closest-in of the many moons of Jupiter, has been suggested as a station for more detailed observations of the properties of Jupiter. Io sweeps through the intense trapped radiation belt and any planned landers must be designed to operate within this environment.

(10) Planetary Explorer '72-'75 The Planetary Explorer series is proposed to place several (currently planned 3 Venus, and 2 Mars) small scientific measurement platforms into orbit about both Mars and Venus. Durations of the orbit phases of the missions are designed to exceed one-half of each planet's year to observe and map time seasonal variations in environment. An opportunity will also be afforded for observing the interactions of the planetary and solar environments over a large heliocentric angle. The program is currently in a conceptional stage; spacecraft and subsystems are receiving preliminary design, and mission requirements and profiles are being analyzed.

Between twenty-five and fifty pounds of payload and up to twenty-five watts of power will be made available for scientific experiments. The first group of the experimental objectives involves measurements of fields and

particles and includes: Magnetic Fields; Solar Wind Plasma, Energetic Particles and Cosmic Rays; Exospheric Composition; Planetary Electromagnetic Emission; Atmospheric Distortion by Occultation; and Micro Meteorites. The occultation experiment will provide extensive mapping of the diurnal and seasonal variations of the planet's atmospheric parameters. Also, an analysis of radio transmissions when the planet is near superior conjunction will add to the knowledge of the inner solar corona. Although the prime purpose of Planetary Explorer is to survey the environments of the target planets, the spacecraft will also be able to provide measurements of the earth's magnetosphere in each of the two directions.

Mission profile Explorer insertion is designed to produce an eliptical orbit with a nominal perigee of 1000 km, which can be trimmed. Final selection of orbital elements will be coordinated with experimental requirements when the selection is made. Mission profile plans include the possibility lowering of the perigee near the end of the mission, to sample the upper atmosphere and to test for bow shock. This dip-in would be achieved in a series of 10 to 100 km steps until the 200 to 500 km altitude range is reached. Launch dates studied for Planetary Explorer are summarized below:

Mission	Year	Launch Date	Departure (Km^2/Sec^2)	Flight Time (Days)
Mars	1973	July 20	16	180
	1975	September 8	20	200
Venus	1972	March 19	13	108
	1973	November 3	14	110
	1975	June 1	7	140

Since the mission profiles of this series do not include atmospheric entry except for the dip-in option, the more severe planetary environmental aspects are avoided. Spacecraft surface temperatures of $393^{o}K$ en route and $338^{o}K$ in orbit have been estimated. Magnetic and particle fields at both planets have been shown (refs. 7 & 89) by Mariner flights to warrant no special engineering concern. A combination of albedo and solar radiation could be viewed as the

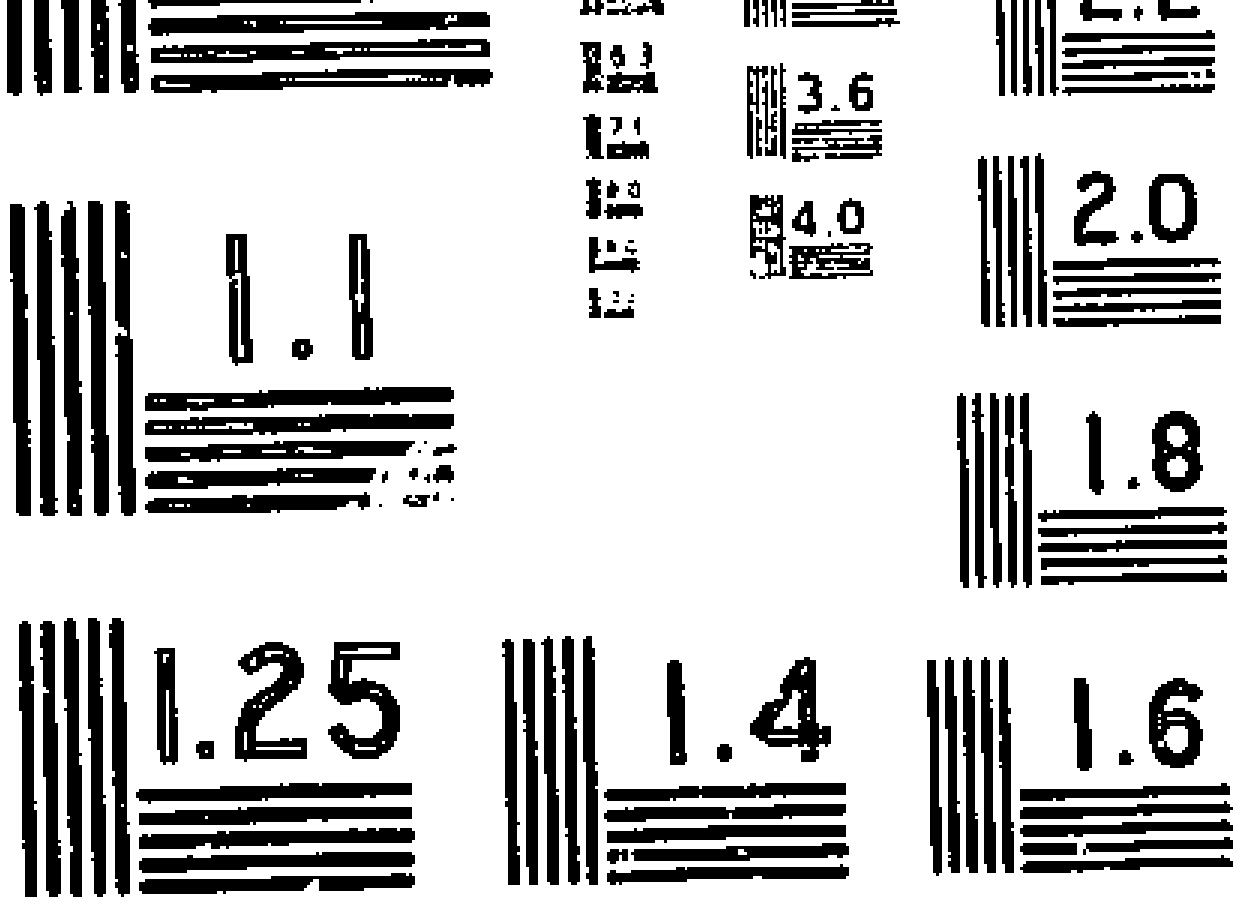

major environment-related concern of the Planetary Explorer program. Duality of missions necessitates some compromise in thermal design. Solar panel temperature limits are exceeded for Venus, for example, if maximum power is generated at 0.72 AU, making it necessary to limit available power during Venus approach and orbit. Thermal constraints are being studied for trajectory altitude correction, and for the burn of the retro-motor.

(11) Pioneer F and G Fly-by missions of Jupiter are planned for 1972 and 1973. The goals of these flights are to investigate:

- The interplanetary magnetic and electric fields and interplanetary particles of solar and galactic origins.
- The particulate matter in and beyond the asteroid belt.
- The particle and electromagnetic environment of Jupiter.
- The chemical and physical properties of the Jovian atmosphere.
- The thermal balance, composition, internal structure and evolutionary history of Jupiter and its satellites.

Much of this information will be of significant value in the planning and designing in future outer planet missions.

The experiment complement for Pioneer F and G includes:

Plasma probe
Micrometeoroid sensors
Cosmic ray detectors
Radio propagation receivers
Magnetometers
Electric field detectors
X-ray detector
Photo imagery
IR and UV radiometry

Transit time is 637 days to closest approach. The asteroid belt is encountered between 180 and 250 days. A periapsis of about 1½ times the assumed Jovian radius is planned.

Pioneer includes a thermal control system employing an insulated equipment compartment with adjustable louvers. A compartment temperature of 273°K to 303°K is planned. External mounted experiments will experience a temperature range from 173°K to 343°K. An RTG power system will probably be employed because of the low illumination intensity at Jupiter ranges. A two year total system reliability value of 0.714 has been postulated.

Environment factors of concern include asteroidal traverse, trapped radiation, temperature extremes, long life requirements, and spacecraft background RTG radiation, electromagnetic field and effluents.

(12) Other Outer Planet Missions Five other outer planet mission opportunities are listed in Table 3.2. These are:

Jupiter Orbiter
Jupiter Probe
Saturn Orbiter
Jupiter-Saturn-Pluto Tour
Jupiter-Uranus-Neptune Tour

The scientific objectives of these missions are essentially the same; viz., to obtain additional information regarding our Solar System and its origins.

Possible science experiments for outer planet missions include:

Magnetometers
AC magnetic field detectors
DC magnetic field detectors
Plasma probes
Thermal plasma detectors
Electron density detectors
Radio astronomy receivers
IR radiometers
IR spectrometers
UV spectrometers
Photo imagery
Cosmic radiation detectors
Micrometeoroid detectors
Solar x-ray detectors

Candidate spacecraft for these missions include the Outer Planetary Explorer (OPE) and the Thermoelectric Outer Planetary Spacecraft (TOPS). A radical departure from previous spacecraft designs, the proposed TOPS and OPE configurations have been influenced most strongly by two unique constraints:

1. Unprecedented communication distances and,
2. Low solar energy available during the greater part of the mission.

Extreme distances in the missions require that an unusual degree of attention be given to the communications system. The most important single feature of this system, and the one which dictates much of the overall physical design of the spacecraft, is the high gain antenna. A gain of 33.7 db, combined with a transmitter power of ten watts is required for feasible communication rates of 830 bits per second at Jupiter encounter, and one bit per second beyond 30 AU.

The use of radioisotope thermoelectric generators (RTG's) mounted on extendable booms to provide thermal and radiation isolation represents the only presently feasible solution for primary power beyond the orbit of Jupiter. Particle and gamma environments resulting from the nuclear activity of the power supplies are definitely of engineering concern.

The proposed Jupiter Orbiter and the Jupiter Probe missions will include non-survivable probes which will descend to the surface of the planet. For maximum useful life, these probes should be designed to withstand radiation, RTG background, asteroidal fluxes, and large asteroids in addition to the long transit time to the planet (almost 2 years).

The Saturn Orbiter mission (1978), which also includes a descent probe, will encounter the rings of Saturn. Protection from dust, particulate matter, and corrosive gases should be a design consideration. In addition, long transit time, travel through the asteroid belt, trapped radiation fields and RTG background will impose design constraints. The three-planet combination swing-bys, Jupiter-Saturn-Pluto in 1977, and Jupiter-Uranus-Neptune in 1979, represent two of several possible outer planet opportunities.

For orbiter missions a gravity assist mode should not be used because the high approach velocity in gravity-assisted missions actually reduces the allowable payload. Ballistic thrusting is recommended for highly eccentric orbiters; nuclear electric vehicles for circular near-planet orbits.

In any case, long transit time is of significant concern in the design of outer planet spacecraft. The problems in designing systems capable of many years of reliable operation in a space environment only slightly exceed in difficulty our inability to confidently establish whether that goal has been reached.

Other environmental-related problems which these missions will face include:

Asteroidal fluxes and materials
Trapped radiation
Saturn's rings (for Jupiter-Saturn-Pluto)
Spacecraft-originated interference (such as RTG background, electromagnetic background, and gaseous or charged particle discharges).

4.0 TECHNOLOGY IMPLICATIONS

4.1 GENERAL DESIGN APPROACH

Planetary mission hardware must survive, for the duration of its specified lifetime, environments which are often unusual and often severe. In the preliminary mission phases, therefore, it is necessary to

1. identify deleterious interactions between environmental vectors and equipment of current design,
2. determine the extent of equipment hardening which is feasible within current technology, and
3. identify present limitations in order to effectively direct future Supporting Research and Technology (SRT) programs.

The discussion in this section is organized by environmental parameter. Relative to each parameter, the capabilities and limitations of the current state-of-art are reviewed. Where deficiencies are evident, suggestions for certain SRT efforts are offered.

The outer envelope of the spacecraft provides the first line of defense against the environment, and extensive environmental modification within the spacecraft is often possible and desirable. Each subsystem, then, is subjected to its own local environment which is defined by (1) the position within the vehicle, (2) the environment exterior to the vehicle, and in most cases, (3) the duration of the vehicle's exposure to the external environment. This local environment concept is exploited where possible in spacecraft design, since circumvention is usually the cheapest and most direct method of dealing with environment problems. For all but the outer structure and external experimental sensors, the question in most cases is not how to provide components to meet environmental specifications, but rather how to build the spacecraft so that each component sees an environment sufficiently mild so that its reliability

is maintained up to the end of the mission.

There are three strategies which can be employed to provide protection from severe environmental effects. One is to harden the component so that degradation is reduced to an acceptable limit. An example can be seen in the improvement in radiation resistance of solar cells over the past ten years. By proper selection of polarity, increasing resistivity, and employing other design parameter changes, the useful lifetime of solar power systems for use in the Van Allen belts has been extended almost tenfold.

A second strategy is to enclose the sensitive component in an environment more suitable to proper functioning. For example, mechanical relays have been found to fail by cold welding after some time in space. By sealing them in a case containing air, the problem was solved.

Finally, as a third alternative, it should be recognized that a substitute component is sometimes available. Rather than attempting shielding or hardening of a sensitive component, it may be advantageous to replace it with a less sensitive one which accomplishes the same objective. The designer must be aware of his alternatives, although this is sometimes difficult in view of the rapid development of the state-of-art.

This section considers the status of space technology with regard to its ability to provide solutions to the following environmental hazards:

- extreme temperatures
- radiation
- varying illumination levels
- meteroid effects
- corrosion
- sterilization
- long mission durations

The wide variability in protective options available to the designer and the preliminary status of the future mission programs results in a degree of uncertainty in the output of this review. More detailed analysis is suggested in order to establish firm specifications for individual SRT programs.

4.2 TEMPERATURE EXTREMES

Environmental temperature extremes can be counteracted by spacecraft thermal control systems which maintain the payload at a non-malevolent temperature range (such as 283°K to 303°K. This approach requires a selection of materials for external surfaces and often an active thermal system which adds or subtracts heat so that heat transfer to the external environment will be at the required rate for maintaining an optimum temperature. Spacecraft temperature in a thermally passive spacecraft will follow a change in external environment at a rate that can be controlled by thermal separation or coupling insulation materials. Active steps often taken include the use of resistance heating, Peltier cooling devices, refrigeration and louvers which change the surface properties. A change in environment, such as eclipse by a planet, entrance into a planetary environment, or long-term motion away from the sun, complicates the problem of thermal design.

The components of a spacecraft most susceptible to extreme temperature effects are liquids or semiliquids such as lubricants and battery electrolytes, organic materials, and solid state devices.

Liquids tend to vaporize or freeze, losing their desirable properties, organic materials decompose at high temperatures and become brittle at low temperatures, and solid state devices experience changes in electric properties at both temperature extremes. Some of these effects are discussed in more detail in the following paragraphs.

(1) Batteries. Both extreme cold and extreme heat are deleterious to battery performance. At low temperatures, there is increased polarization and decreased conductivity of the electrolyte. Several projects are underway (see Appendix A) sponsored by JPL, LRC and GSFC to improve battery performance over wider temperature ranges. Technical feasibility of heat sterilizable NiCd cells has been demonstrated*; cells capable of operation at Mercury and

---

*Texas Institute progress reports under Contract #NAS 7-100.

Venus surface temperatures are neither available, nor is current research directed toward these objectives.

Some activity is underway, however, for the development of a high temperature battery. Ammonia electrolyte batteries have been investigated for operation at temperatures of 200°K but have not as yet been used in spacecraft. Some high temperature fused salt electrolyte batteries are also under investigation.

(2) Organic Materials. At low temperatures, 263°K and below, lubricants such as petroleum distillates and greases are generally ineffective. For such applications these have been largely replaced by solid materials such as molybdenum disulfide, graphite, and teflon (polytetrafluoroethylene) and composites of these materials, e.g. teflon reinforced with glass fibers and containing molybdenum disulfide. Investigations have been made into the use of niobium diselenide in efforts to develop a low friction material of higher conductivity for low pressure applications, however, the wear rate of the material is high. It has however proved useful in motor brush material uses.

Problems also exist at high temperatures. Many plastics lose their desirable properties at 373°K. Tensile strength decreases with increasing temperature, electrical resistivity for most polymers decreases exponentially with increasing temperature, requiring careful selection of organic dielectrics for high temperature applications. At nominally high temperatures, most common plastics outgas, and this is highly enhanced at low pressures.

Figure 4.1 illustrates the thermal stability curves of a typical polyimide and teflon at 673°K.

As a result of tests conducted at JPL, several plastics have been suggested for high temperature and pressure tolerance. The test conditions were six hours at 563°K and a CO_2 pressure of 18.5 atmospheres. This test may be regarded as simulating a brief stay in the Venusian atmosphere, although not near the surface. The plastics suffering no severe damage were:

GP 77, a silicon resin coating,

Viton 77-545, a fluorelastomer gasket material,

Teflon TFE, a fluoroplast,

Fiberglas 91 LD, phenolic/glass laminate, and

Kapton 100, a polyimide film.

The results suggest these materials as candidates for missions to Venus and Mercury.

JPL, under work unit 186-58-13-02, is sponsoring work to establish a listing of polymeric materials suitable for use in future lander/probe missions.

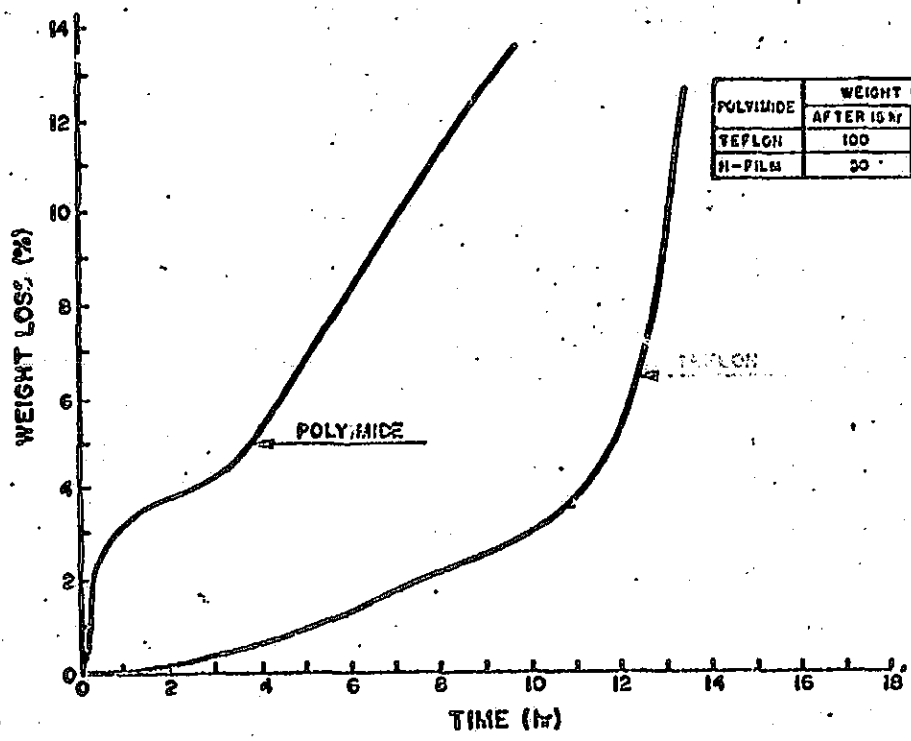

POLYIMIDE	WEIGHT LOSS (%)	
	AFTER 10 hr	AFTER 36 hr
TEFLON	100	—
H-FILM	30	100

FIGURE 4.1 Thermal Stability Comparison at 673°K

(3) Solid State Electronics. The temperature at which a semiconductor such as a transistor or diode operates, depends on the power dissipation during operation, the temperature of the environment, and thermal coupling of the device to the environment. Typically, silicon semiconductors are rated for case temperatures in the range of 323-373°K. When there is considerable

power dissipation within the unit the semiconductor must be more closely coupled to the environment by use of a heat sink.

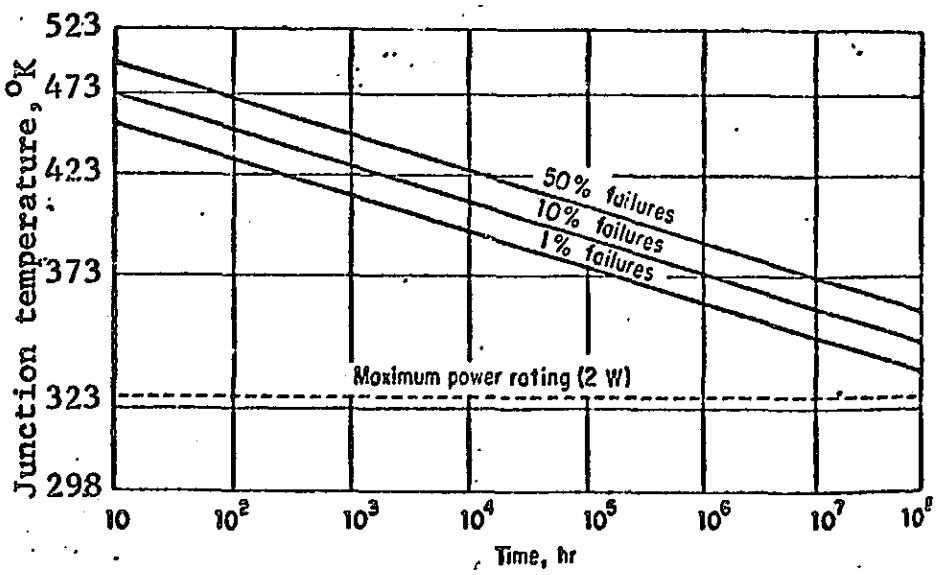

Figure 4.2 Life Expectancy of p-i-n diode under forward bias, versus temperature

In theory, it appears practicable to design silicon semiconductor devices for operating in environments near 473°K. The factors which limit operation at higher junction temperatures are the surface properties of silicon and the differential expansion at the contacts. These factors cause sudden failure and a penalty in life expectancy of the component is incurred. This mainly is the result of the deterioration of junction properties, caused by heat-accelerated diffusion of atoms across the junction. A typical example of this effect is shown in Figure 4.2. The higher the temperature, the shorter the life expectancy. For well-built semiconductor devices there is no abrupt temperature limit.

Some high temperature missions can, however, utilize silicon components through judicious design. For a Venus probe several hours of operation on the surface could be devised through a proper thermal design. One approach could take advantage of the cold upper atmospheric temperature. The probe therefore would initially be cold, and would come into equilibrium with the environment at a rate determined by the heat conductivity of its shell. With insulation, this rate could conceivably be slowed so that the insulated electronics would function for hours.

For more long-lived Venusian probes, and for missions where the high temperature problem is even more severe, silicon components do not have the operation capability of other semiconductors that are available. Gallium arsenide (GaAs), gallium phosphide (GaP) and gallium arsenide phosphide (GaAsP) have wider energy gaps than silicon, have been formed into diodes and transistors, and are better materials for high temperature applications. Silicon carbide (SiC) has an even wider energy gap and therefore has great promise. Because of the significant potential of the high temperature, radiation-resistent material, a special report on progress in SiC technology is presented in Appendix B.

Many research activities are directed toward the evolution of semiconductor devices capable of high temperature operation, e.g., by ERC, Texas Instruments, Air Force Cambridge Research Labs, Westinghouse, General Electric, RCS, N.V. Phillips, Lockheed, Norton and Carborundum. Some of these projects are included in the summary of Appendix A.

Low temperature is also a detrimental factor for electronic semiconductors. The gain of typical junction transistors decreases as temperature is reduced, generally vanishing near 100°K. Gain reduction at low temperature results primarily from decreased conductance of silicon. Sandia Corporation and others are investigating gallium doping techniques to produce units capable of operation at temperatures below 200°K.

4.3 RADIATION

Particulate radiation is part of the space environment. There is a continual background of cosmic rays; there are predominantly high energy protons with alpha particles and nuclei of heavier elements also present. In addition, there are sporadic solar proton flares; these are of high energy, emitted from the sun during sunspot activity, and represent a significant radiation hazard in free space. Near some planets (Earth and Jupiter at least) there are belts in which electrons and photons have become magnetically trapped and accelerated to high energies. Finally it may be necessary to consider radiation to a spacecraft from an onboard nuclear power device or propulsion system.

Solar flare proton showers typically last a few days and contain protons of energies up to 100MeV. Although there is considerable variance of the number and intensity of flares during solar cycles, recent flares have resulted in proton fluences of up to 10^{10} per cm^2 per year at 1 AU. Because of diffusion interactions with the solar magnetic field, the proton fluxes do not appear to decrease as fast as the inverse of the square of distance from the sun, especially for the lower proton energies. The permanent effects of radiation exposure are cumulative. Missions to the outer planets will require study of radiation exposure effects because of the long accumulation times involved. Missions to Mars will most likely be short enough to avoid serious permanent effects, but the lack of a protective magnetic field indicates that the exposure will continue for a lander on the surface. Missions to Mercury and Venus will receive exposures to higher levels of solar radiation. Proton radiation exposure is a factor to be considered for essentially all planetary missions. This problem can generally be circumvented by proper design.

For Jovian orbiters and probes, the high energy electrons of the trapped radiation belt will require special attention. Damage caused by electrons is generally indistinguishable from that caused by protons; the two may be considered to be cumulative for each of the categories discussed below. The principal distinction is in the ease of shielding. It is far simpler to provide shielding on the order of a few grams per square centimeter to stop the proton damage than it is to provide the 10-20 gms/cm^2 necessary to stop electron damage. Thus, shielding is an adequate stratagem for free space, but not as useful for missions near Jupiter.

The effects of radiation on spacecraft materials are discussed in the following paragraphs:

(1) Solid State Electronics. The effect of particulate radiation on semiconductors can be significant. This radiation strikes the ordered lattice of a crystal and can dislodge individual atoms. The resulting vacancy at a lattice site - and the atom at some interstitial position - leads to the bulk radiation damage in semiconductor devices. The damage increases with increased radiation exposure. In addition to this damage, there is also a surface effect on transistors which is poorly understood, but is believed

to be due to charge deposition in the surface layer of the device under the influence of radiation. A significant property of surface radiation damage is that it saturates. That is, after a certain amount of radiation exposure (on the order of several megarads) the surface radiation damage reaches an upper limit.

Many of the vacancy-interstitial pairs formed by recoil from the electron scattering collisions immediately recombine at room temperature with the aid of thermal vibrations. Temperature obviously plays a critical role in this annealing. The significant recombination centers are created at the lattice site, from which the atom was ejected, diffusing in the lattice until it forms a stable configuration with an impurity atom. The configuration can be dissociated generally by increasing the temperature. As a result, the number of centers can be decreased by a suitable thermal annealing of the irradiated materials.

Unfortunately, major recombination centers produced in p-type silicon have annealing energies in the 473 - 623°K range whereas the base material of pnp transistors may be annealed at lower temperatures. Offsetting this advantage of n-type silicon is the fact that the initial damage for a given dose to n-type silicon is greater than to p-type silicon, apparently due to a greater minority-carrier capture cross section. Generally, p-type silicon is preferred when selecting for radiation resistance; hence, npn transistors, n on p solar cells, etc.

A principal figure of merit for transistors affected by radiation damage is the common emitter dc current gain. For a junction transistor, this gain is related to the minority carrier lifetime in the base of the transistor. Specifically, a radiation-induced decrease in lifetime of minority carriers in the bulk material of the transistor base results in a decrease in the gain.

The base transit time is often simply related to construction parameters, so that different transistor design will have different radiation resistances. The mean base transit time depends not only on the transistor type, by serial number, but also on the operating value of the collector current and on the manufacturer's current technique of fabrication. For example, tests of 2N1613 transistors produced by three different manufacturers have significantly

different transit times. Moreover, identical units from a single manufacturer can differ. The result of these differences is a wide variance in the radiation damage sensitivities of the units.

Most transistors which are presently available, show some effects of radiation on reverse current leakage and current gain at doses in the range of 0.1 to 1 megarad. These effects are very complex but are associated with radiation effects on the surface oxide layer which is generally used to passivate the transistor surface. At doses above one megarad, permanent damage to the gain usually is dominated by degradation of minority carrier lifetime in the base region. Similar effects are observed in metal-oxide devices, and this type of design is generally unsuitable for use in radiation environments.

Unfortunately, a prediction of transistor performance after irradiation cannot be based on transistor type alone. Rather, the initial gain, the base transit time, the composition, surface features, resistivity of the base material, and other pertinent parameters determine the final performance.

Early transistors with etched surfaces (e.g., mesa and alloy constructions) were not surface-protected and their characteristics were found to depend on surface contamination. Under irradiation, mesa transistors exhibited surface effects which were associated with gas ionization in the transistor can while the device had voltage applied. This effect could be essentially eliminated by evacuating the can and maintaining the required cleanliness and evacuating transistors have not been widely adopted by the industry. Instead, the use of dielectric insulating coatings has been widely adopted (e.g. planar, surmetic and annular transistors). These insulating coatings are usually thermally grown oxides. These passivating layers may still not prevent effects of the environment on and beyond the coating.

The complicated effects of radiation on transistors are believed to be due primarily to electrical charge deposition within such dielectric coatings. Therefore one can predict that radiation surface effects on transistors might be reduced or eliminated by

- Eliminating the surface insulating layer,
- Maintaining very clean silicon surfaces, and
- Evacuating the can.

Whether this approach could be practically implemented by the semiconductor industry remains to be evaluated, because it would undoubtedly require drastic revision of present production practices. Also, it is not clear that all the transistor types required for a planetary capsule could be made using the mesa or alloy technique which is most applicable for implementing this suggested approach.

The same considerations that apply to radiation damage of transistors will apply to radiation damage of solar cells. A reduction in minority carrier lifetime in the base region of irradiated solar cells reduces their power output. A fluence of about 10^{13} electrons/cm^2 (of 1 MeV energy) reduces typical solar cells power output on the order of 5%. Similar description of the effect of proton fluences, which predominate in free space, can not be given since it depends critically on the design of the solar cell array. With proper design, however, neither form of radiation prohibits the selection of solar cells for any conceivable mission.

Diodes and other semiconductor junction devices are generally less sensitive to radiation than are the above junction devices. The same forms of damage, however, are in evidence. The dominant effects are due to minority carrier lifetime decreases on either side of the junction. The dependence on minority carriers of pertinent properties of devices other than transistors and solar cells, however, is generally less significant so that about an order of magnitude greater exposure is necessary to develop serious effects.

NASA's program for developing radiation hardened semiconductors is being directed by a number of centers. Marshall is studying radiation resistant digital electronic circuit elements. Lewis is assessing radiation damage as related to nuclear-electric power systems. Development of hardened devices and materials is being sponsored principally by ERC. GSFC is directing its attention to radiation effects on advanced electronics and JPL is investigating

the development of hardened solar cells.

(2) Organic Materials. Radiation damage to organic polymers is principally due to ionization. The radiation breaks covalent bonds; the subsequent recombination of the free radicals is random and leads either to smaller molecules (scission) or to a union of adjacent molecules (cross-linking). When scission predominates, the degradation of the polymer is more pronounced. This occurs in polymers such as Teflon, Kel-F, and polymethyl methacrylate. Cross-linking does not affect the material properties so strongly; this occurs in polystyrene, polyethylene, mylar, silicone, epoxy and natural rubber. Cross-linking increases the viscosity of liquids, and the hardness and brittleness of solids. Scission, on the other hand, decreases viscosity and softens solids. Both of these modes of radiation damage can occur simultaneously in a given material, but one generally dominates. Hydrogen gas is also generated which may have deleterious effects.

The acceptability of a polymeric material after irradiation depends on a number of considerations. The use to which the material is put will determine the acceptable level of degeneration of a given property. The level of degeneration, for the given dose, is dependent to some extent on such factors as the temperature and atmospheric pressure, the inclusion of trace impurities such as antirads, the level of cure of a rubber, and the molecular size of the polymer. Without delving into these considerations, only broad ranges can be given for the radiation damage in individual polymeric materials.

Two such lists are reproduced here as Table 4-1. The materials are listed with the dose that will give approximately a 25% loss in a salient property. These lists are intended for survey use; they indicate that, most likely, some materials are unacceptable, and some are quite safe.

The extreme sensitivity of halogenated polymers is immediately apparent. Gaseous breakdown products, often corrosive, are liberated. Teflon and Kel-F, both fluorocarbon polymers useful as dielectric and insulating materials, lose resistivity at the levels quoted, embrittle, and generate volatile fluorocarbons. In the case of Teflon, it has been established that the presence of oxygen is partly responsible for its extreme sensitivity. When the irradiation

Table 4-1 Magnitude of a Dose in Megarads for Significant Damage

Base Oils (damage is usually to viscosity or acidity)	
5000	polyphenyls
1000	polyphenyl ethers, alkyl aromatics
100	polyglycols, mineral oils, methylphenyl silicones, aryl esters
50	silicates, disiloxanes, alkyl diesters
5	phosphates, alkyl silicones, olefins
Plastics (damage is usually to tensile strength)	
4000	polystyrene, phenol formaldehyde filler
400	polyester (mineral filler)
100	polyvinyl chloride, polyethylene
50	urea formaldehyde
20	monochlorotrifluoroethylene, cellulose acetate
10	phenol formaldehyde
1	methyl methacrylate, polyester (unfilled), teflon (in air)
Elastomers (damage is usually to tensile strength)	
90	polyethylene
25	polyisoprene (natural rubber)
10	styrene-butadiene
7	nitrile rubber
6	neoprene, silicone rubber
4	butyl rubber, fluoroelastomers
3	acrylate rubber
2	polysulfide

is carried out in a vacuum, the dose for significant damage to Teflon is about 10^6 rads. Lacking tabulations of thresholds for damage in vacuo or inert gas one may use the presented compilation to indicate conservative values of radiation sensitivity.

Fillers or inert additives such as carbon black, silica, glass fiber, cellulose fiber, talc, asbestos, and wood flour used to reinforce the polymer or merely as an economical extender, absorb part of the dose and thereby reduce the radiation damage.

The table indicates that the selection of elastomeric material is significant for control of radiation damage effects. Butyl rubber is quite sensitive, natural rubber is rather resistant, and nitrile rubber falls somewhere between. The molecular rearrangements that lead to these widely different sensitivities to radiation are not the same. In natural rubber, the polymer molecules tend to cross link under radiation exposure. In butyl rubber, on the other hand, the polymer molecules tend to undergo chain scission, and a sticky gum results. This latter effect is more critical to the elastomeric properties, hence the greater sensitivity of butyl rubber.

Nylon, also with a fairly low threshold, has a high ratio of chain scissions to cross linking when irradiated. This makes it more sensitive to radiation than is polyethylene, with respect to retention of strength and elongation.

Table 4-1 indicates that several highly radiation resistant materials are available; hence the development of additional materials for space missions which will encounter intense radiation environments does not appear warranted. Designers of such spacecraft must be made aware of the radiation susceptibility of insulating materials so that proper selections can be made from available polymers and oils.

4.4 ILLUMINATION

Solar illumination is of concern to planetary spacecraft which use solar cell arrays as their primary power source. Most inner planet missions and several Jupiter missions intend to employ solar cell systems. Design

considerations include the distance to the sun and the resultant mean level of illumination (see Table 4-2). The rapid decrease in solar constant for the outer planets essentially eliminates any possibility of the use of solar cell systems.

A secondary factor in solar power system design is planetary eclipse. For a mission orbiting or passing a planet, the duration of eclipse should be identified in order to size the energy storage requirement. For a planetary lander, the length of night is of importance.

Attenuation by planetary atmospheres affects the sunlight availability for photovoltaic power on the surface. On Earth, illumination drops about 30% due to atmospheric attenuation. On Venus, a greater drop can be expected; reflection alone removes 81% of the illumination, so that other power sources appear necessary for surface missions.

TABLE 4-2 SOLAR CONSTANT IN PLANETARY ORBITS

Planet	Radius	Mean Orbital Radius (AU)	Solar Constant (mw/cm^2)
Mercury	0.38	.387	920
Venus	.955	.724	270
Earth	1.00	1.000	137.4
Mars	.523	1.524	60
Jupiter	11.2	5.203	5
Saturn	9.48	9.54	1.5
Uranus	3.90	19.19	0.37
Neptune	4.16	30.07	0.15
Pluto	0.45?	39.46	.087

With a solar cell array, spacecraft thermal design is frequently concerned with conserving heat. Missions that approach closer than about 0.3 AU to the sun are an exception to this, of course, and will be

discussed separately. Missions to Venus, Mars, or the outer planets, when using solar arrays, can generate steady heat at a rate no greater than the spacecraft intercepts solar energy. If the array is in the form of a paddle with poor thermal coupling to the payload, only about 10% of the intercepted solar energy is available to the payload; the rest is re-radiated thermally by the paddle.

With an RTG, on the other hand, spacecraft thermal design is frequently concerned with reducing heat. Typical efficiencies of RTG units are in the range of 5%, so that large amounts of heat are produced for typical electrical requirements. On the basis of weight, it has been calculated that RTG's are superior to solar power beyond 3.5 to 4 AU from the sun*; cost considerations, however, may favor solar power as far as Jupiter.

Space RTG development activity is sponsored by the USAEC and its organizational elements working toward specifications established by NASA. Appendix A cites several on-going efforts.

4.5 METEOROID EFFECTS

Numerous theoretical and experimental studies have been conducted in an effort to evaluate the effects of meteoroid impacts on spacecraft. The decade of space flight experience in the vicinity of Earth has caused lessening of the concern about catastrophic or severely damaging impacts by meteoroids of cometary origin. The present models of asteroidal meteoroids contain estimates of integrated fluxes very similar to that for cometary meteoroids, thus the probability of sustaining impact is about the same as in the near Earth environment. However, it is incorrect to imply on this basis that the risk of damage from asteroidal debris impact would be comparable to that experienced in near Earth missions. There is actually substantial increase in the hazard because the asteroidal debris density is greater by a factor of nearly 10 (even though the average impact velocity may be slightly less), and because there is a probability of about .16 that the integrated flux of the upper limit asteroidal model is exceeded. Unless new data

*W.J. Dixon. Major System Design Problems for Deep Space Probes. J. Spacecraft & Rockets 4:9, Sept. 1967.

become available which reduce the model uncertainties by eliminating the upper limit model substantial spacecraft shielding or asteroid belt avoidance are indicated to reduce the risk of spacecraft damage to an acceptable level.

Specific spacecraft components requiring design attention from the standpoint of damage by interplanetary debris include optical and/or heat transfer surfaces, liquid-filled containers (radiators and fuel tanks), expandable structures, and vehicle hulls. Numerous theoretical and experimental studies have been conducted in an effort to evaluate the effects of meteoroid impacts on spacecraft. Much of this effort prior to 1965 has been summarized by Cosby and Lyle (ref. 30) and more recently (ref. 29) Lyle has reviewed the work related to degradation of spacecraft solar cells.

The effects of meteoroid impact can be divided into those resulting from the small dust particles (micrometeoroids) and those resulting from the more massive bodies (meteoroids). Momentum and/or energy considerations, which usually dominate hypervelocity impact problems, are essentially irrelevant when considering damage by micrometeoroids because the momentum imparted per unit impacted area is far too small to initiate a shock wave or to produce to any significant degree the damage mechanisms associated with deep craters. At escape velocities, it is most probable that evaporation processes obscure all other energy dissipative mechanisms for impacting micrometeoroids. Evaporation dissipates energy at a rate of 10^{34} ev/cm^2 sec so that long before any heat is conducted or radiated, the molecules and atoms of the micrometeoroid and of the local surface vaporize and dissociate, dissipating all the energy. The result is a shallow crater on the surface having the same area as the micrometeoroid and a depth dependent on micrometeoroid density of 5 to 50 percent of its width.

Bjork's hydrodynamic theory of impact penetration has been used to estimate that the rate of erosion of an aluminum plate in interplanetary space will be one angstrom per year. The erosion will be in the form of small hemispherical craters having diameters generally less than 10^{-3} cm if impacting particles have the density of solid stone. In brittle materials, such as glass and plastic, each crater will be surrounded by an area of cracks, or very shallow spall, several times the crater diameter.

Since the optical or thermal radiation characteristics of most spacecraft surfaces are controlled by a thin layer of material it is quite likely that these surfaces under continual bombardment by micrometeoroids were in time (three to ten years) degrade in their function. This is because the altering of optical properties requires surface erosion only to a depth of $\lambda/2$ (where λ is the radiation wavelength of interest, approximately 4000 angstroms), or less than 0.1 μ.

Studies of the reflectivity/emissivity changes produced by simulated micrometeoroid impacts on gold, aluminum, stainless steel (types 304 and 316), chromium plate on brass substrate, tungsten and silver indicate that the softer metals tend to sputter away more readily and to give a larger crater.

A small probability exists for a solar cell array to be catastrophically damaged or at least perforated by meteoroids, the more common hazard is due to micrometeoroid impingement resulting in erosion of the coverslide and reduced transmission of solar radiation to the cell. Studies of coverslide surface erosion on cell performance were reviewed (ref. 29) and it was found that simulated meteoroid erosion of coverslides causes short circuit current degradation. Damage to cell edges cause significant increases in leakage current with the resultant power degradation.

The uncertainties which persist concerning the meteoroid environment involve many orders of magnitude due to difficulties in defining the masses of particle debris and the flux-size distribution functions, as well as interpretations of observations and data from a variety of sensors employed in both ea earth-based and spacecraft studies. However, it is concluded that surface erosion, the most probable degradation of solar cells due to micrometeoroids, can be significantly retarded by the use of appropriately designed coverslides.

Impacts by the more massive meteoroids will be less frequent than those by micrometeoroids, but the larger bodies are capable of producing catastrophic damage due to their high kinetic energy; a typical 0.5 gm particle traveling at a speed of 30 km/sec possesses a kinetic energy of about 10^6 joules. The most damaging effects include cratering, perforation (puncture), and spallation.

Spall fragments from the inside surface of a vehicle hull may be ejected inward at a velocity sufficiently high to cause serious damage to components or personnel inside. Diameters of spalled fragments are usually several times the thickness of the impacted plate; thickness of spalled fragments may be from about 0.1 to 0.5 times the thickness of the impacted plate. In addition, impact of these more massive bodies on the surface of a vehicle will cause vibrations in the skin and/or other parts of the structure. The vibration amplitude may be sufficiently large to cause ceramic coatings to spall or flake off or even to crack welded joints in the structure (ref. 30).

Meteoroid impacts of liquid filled tanks will cause strong shock waves in the liquid leading to catastrophic damage. Cryogenic propellants would cause the tank walls more susceptible to brittle fracture. A secondary violent reaction may occur in cases where the fluid and tank materials combine to detonate and burn in the high energy environment caused by impact; such would be the case with liquid oxygen in a titanium alloy tank. Beryllium has been found to offer greater resistance to penetration per unit weight than either aluminum or steel. The high values of specific heat, melting point, and heat of fusion further contribute to the preference of beryllium over aluminum and steel for resistance to meteoroid damage.

Perhaps the most vulnerable component of a spacecraft containing a power system which must rid itself of waste heat is the radiator. One beneficial characteristic of a space radiator is that it lends itself to being segmented in such a manner that a penetrated segment can be isolated from the rest of the system without disastrous effects. However, preliminary analysis indicates that this component may require shielding or standby capacity involving a greater weight penalty than any other component of the spacecraft.

Spacecraft hulls present a problem to the designer from the standpoint that a large penetration could, as in the case of a radiator, be disastrous, particularly, in the case of a manned vehicle. For instance, if the hull of a vehicle were completely penetrated, both explosive decompression and penetrated fragments could cause serious damage to the contents of the vehicle. Also, the detachment of a spall from the inside of the hull, even without

complete penetration, constitutes a hazard. Obviously, the structural requirements to protect against such catastrophic impacts to spacecraft hulls should be considered in detail. To insure a high probability of survival for spacecraft of long duration missions this involves a large weight penalty, particularly in single-plate-thickness hull designs.

Protective Design Concepts — Two significant approaches in reducing the weight requirements of vulnerable areas are shields and/or self-sealing devices. The application of both techniques is complex as indicated by the many reports that have been published on this subject.

Meteoroid shield (bumper) The underlying concept of the shield is to provide a sacrificial element which would expend the energy associated with an impacting projectile. As has been discussed in the foregoing section of this report, when a plate is penetrated by a hypervelocity projectile an expanding bubble of fragments is produced. Not only are the fragments spread over a large area, but also, the velocity component, normal to the plate, of the many fragments is significantly reduced below the impact velocity of the original projectile. Both of these factors would reduce the effect of a projectile on a spacecraft component placed behind such a plate since much less momentum and energy per unit area would be applied than if the component were not shielded.

Various parameters such as shield material and thickness and distance from the target have been investigated to determine optimum conditions. Results have shown that considerable weight savings can be obtained without sacrificing safety; for the same probability of penetration, weight reductions of over 50 percent may be expected. The latter statement is, of course, predicated on the assumption that meteoroids can be shattered by shields to the same degree that simulated projectiles have been in the laboratory.

Suggested extensions of the bumper concept of spacecraft protection range from shields with multi-sheets to combinations of polymeric materials and composites with metallic structures in multiple-wall configurations. The emphasis recently given polymers results from the successful application of materials such as epoxy resin filament-wound Fiberglas composites in high-performance

pressure containers. Single wall configurations of such composites would still incur severe weight penalties. However, inasmuch as multidirectional orientations of the filaments would minimize crack propagation initiated by meteoroid impact, this characteristic combines with other advantages of filament-wound plastic composites to make them potentially promising materials for an inner wall of a multiple-wall structure.

Self-sealing structures The application of self-sealing structures to reduce the hazards of meteoroid perforation is a more recent approach, but considerable effort has been expended toward its realization. Design concepts may, in general, be classified as mechanical or chemical, depending on the mode of activating the sealing process. A variety of configurations, primarily variations of sandwich-honeycomb core structures, applying the concepts have been successfully tested in simulations of the meteoroid environment.

A highly effective mechanical approach has been to prestress the elastomeric sealant in compression. This technique, which utilizes the recovery of sealant material to achieve the closure, has been very successful for extremely localized damage. Materials for this application should have appropriate thermal and vacuum properties and low shear strength characteristics under dynamic conditions when simply confined. Another prestressing technique uses an elastomer and foaming reagent which causes an unconfined volume expansion of 200 to 300 percent upon curing. The sandwich-honeycomb core panel is filled with the uncured sealant compound to a volume fraction which would produce the desired prestress level; the sealant is then cured at the required temperature. Bonding of panel face plate should be accomplished with a material whose softening point is above the cure temperature of the sealant. This latter technique has shown successful sealing characteristics with a high degree of reliability. It is possible that under certain environmental conditions and with massive face sheet and sealant damage or tearout, macro-motion of sealant into the perforated zone will be required. For this reason, the elastomeric sphere concept was initiated. In this approach, the conventional sealant is replaced by elastomeric spheres to a predetermined packing density. Upon penetration, the pressure differential between the inside cabin and the vacuum of space forces

the spheres toward the hole and effects the sealing. Sphere size, packing density, and material will control the mobility of the spheres and the sealability. This concept has exhibited residual leakage rates comparable with the mechanical system employing sealant recovery as the mechanism of sealing.

Chemical concepts rely on the dynamic action of the penetrating particle to initiate a reaction which closes the hole. In one concept, an uncured polymer is separated from the catalyst by a thin, nonreactive membrane. Upon complete perforation, the pressure differential across the sandwich panel forces a mixture of polymer and catalyst through the hole. Extremely fast curing mixtures have been used with complete and repeatable sealing action. In another technique, small bags of catalyst are distributed in the sealant void to localize curing action to the area of penetration; catalyst bag size is an important factor in this method. For uniform distribution of the catalyst in the uncured elastomer, micro-encapsulation techniques could be adopted. In all chemical concepts where the sealant materials are initially fluid, careful attention must be given to the rheological or flow properties of the polymer. The viscosity of the material must be such as to permit an initial gradual flow through the hole without excessive loss. Cure rate must obviously be rapid enough to "set up" the material in the hole. Environmental stability must be carefully considered against mission time, as degradation can severely alter flow rates and, hence, sealability.

Typical self-sealing configurations consist of metallic or polymeric composite facings separated from an elastomer-reinforced back-up plate by a honeycomb core of polymeric and/or metallic material or various sections as necessary to combine multiple concepts. For example, a section of foamed elastomer may be used with a section containing elastomeric spheres or encapsulating bags. The honeycomb core functions to contain the sealant and provide damage confinement through the addition of bonding surfaces in the sealant volume. Required characteristics include: the sealing material should be elastomeric and have cohesive strength high enough to resist tearing but low enough for collapse into the puncture under the pressure differential, the honeycomb core should have a low shear modulus but a high tear strength. Unoriented fabric-reinforced elastomers seem best for the back-up sheets, and elastomeric adhesives appear best for bonding the sealing structure to the vehicle structure. Optimization in materials selection has not been reached, however.

4.6 EROSION AND CORROSION

A. Erosion Problems

The principal efforts in the studies of erosion in planetary environments have been directed toward Mars. For the most part these have compared the Martian environment to that of a terrestrial desert with very low atmospheric pressure, but high wind velocities.

In 1966, the development of a Martian Environmental Simulation Facility was announced by McDonnell Aircraft Corp. (ref. 58). The effects on spacecraft coatings (ref. 40) and surface transport phenomena for the simulation (ref. 93) have been done in this facility.

The parameters utilized within the system were as follows:

Gas Composition: CO_2, N_2, Ar

T : 198°K

P : 4 - 20 torr

Wind Velocity: 100 fps - 520 fps

Abrading Materials: silica flour 140 mesh (majority < 40 μ)
fine sand (105 - 210 μ)
coarse sand (297 - 420 μ)

It was reported that storms of 500 fps velocity produced severe abrasion in contrast to 300 fps effects. Weight profiles of particles indicate that one effect would be most severe on parts of the lander within several inches of the surface. Spacecraft coatings were particularly abraded; most coatings were completely removed in less than 30 min during 500 fps storms.

Results reported in these efforts are condensed in Table 4-3. As indicated, the main areas of interest include the coating loss due to abrasion and the change in the coatings' solar absorptance/thermal emittance ratio (α_s / ϵ_t).

Coatings	Exposure Time (Minutes)	Percent Increase Solar Absorptance	Percent Change Thermal Emittance (ε)	Percent Thickness Decrease	Percent Change α/ε
Silicone (Q92-009) Bonded Zinc Oxide (SP500)	15	340	-2.5	22.4	+268
	30	237	+2.5	20	
Silicate (K_2SiO_3)	15	184	-31	68	+312
Bonded Zinc Oxide	30	420	-60	100	+1207
Silicone (RTV602) Bonded Zinc Oxide (SP500)	15	156	-2.5	9.5	+172
	30	163	-6.5	14.3	
Epoxy Bonded Titanium Dioxide (R900)	15	48	0	8.3	+47.3
	30	50	+2.5	7.4	
White Porcelain Enamel	15	34	+3.8	34	+46.0
	30	58	-3.8	58	
Rokide A - Flame Sprayed Al_2O_3	15	87	-4.0	1.4	+84
	30	79	+2.7	0	
Silicone (DC-182) Bonded Lanpblack	15	0	+2.9	0	-1.7
	45	0.8	+1.9	0	
Silicone (DC-182) Bonded Titanium Dioxide (R900)	15	100	0	0	+101
	45	103	+1.9	0	
Silicone (DC-182) - Clear	15	1.1	0	0	+2.0
	45	1.1	-2.5	0	

TEST CONDITIONS: Abrading agent, 1-149μ Silica Dust; Wind Velocity, 220 FPS; Pressure, 5 Torr; Dust Concentration, 2.6×10^{-4} oz/ft^3; Coating Orientation, 45° with wind direction.

TABLE 4-3 ABRASIVE EFFECTS ON COATINGS

Abrasive Coating Loss Because dust adhered to or embedded in most coatings, thickness change was used, instead of weight change, to measure coating loss. Percent thickness decrease for each coating is shown in Table

All paint coatings showed an abrasive coating loss; however, only the silicate bonded zinc oxide coating was completely abraded. The most resistant paint coating, Rokide A—flame sprayed Al_2O_3, could possibly withstand up to 18 hr of continuous exposure. All silicone rubber coatings showed no measurable thickness change. A comparison between the two types of coatings indicates that a soft, resilient coating (silicone rubber), which can rebound particles without absorbing their total energies as do hard paint coatings, is much more abrasion resistant in the Martian surface environment. For longer Mars missions (over 48 hr), it appears that some type of abrasion-resistant, soft coating would be needed.

Radiative Property Changes All coatings, except black silicone rubber, showed increases in their α_s/ϵ_t ratio. In each case, the α_s/ϵ_t rise was due to a greatly increased α_s; the ϵ_t did not significantly change. An α_s/ϵ_t rise greatly reduces a surface coating's ability to radiate internal heat from equipment to its surroundings while absorbing little solar heat. An increased ratio could produce overheating of the spacecraft and cause equipment failure.

The increased α_s in each paint coating was caused by abrasion which changed the coating color from the initial white to varying shades of grey or tan. In most cases, this abrading action resulted in at least a 50% α_s/ϵ_t increase.

Since the silicone rubber coatings were not measurably abraded by storm exposure, their α_s/ϵ_t rise was not due to abrasion. In their case, the increased α_s/ϵ_t was caused by a heavy dust covering that could be removed to expose the original surface. With a method for decreasing the silicone rubber's affinity for dust, these soft coatings could become ideally suited for the storm environment expected on the surface of Mars.

The test results verify the following conclusions:

1. Particle transport and behavior in simulated Martian storms are quite similar to those of sand and dust occuring in earth deserts.

2. Even a short exposure to a typical Martian dust storm decreases the amount of coating and greatly increases the coating's α_s/ϵ_t ratio.

3. Soft, resilient surface coatings appear to resist the abrasive effects of Martian storms much better than hard paint coatings.

The investigations discussed are a start towards understanding the Martian surface environment and its effects.

No comparable work has been reported for Venus, although the high pressure, slow rotation and high sun-side temperatures should cause considerable thermal gradients with accompanying high winds. It is therefore necessary to conduct similar studies prior to planning Venus loading missions.

B. Corrosion Problems

High Temperature Corrosion It is likely that the most severe planetary environment with the Solar System with respect to probable corrosion is to be found on Venus. While Mercury is likely to be hotter, it lacks the dense atmosphere. Jupiter, while having the factors of high gravity and dense atmosphere is low in temperature. Venus with a high temperature, high pressure environment, with the probable presence of oxidizers presents a problem somewhat similar to the construction of suitable steam turbines.

In the construction of these turbines stainless steels predominate, and include type 316, 347, 321, 18 Cr - 8 Ni; Cr-W-Co steels such as stellite and others. High molybdenum steels tend to oxidize severely and require additional protection. Clad steels should also serve the purpose of minimizing corrosion. Inconel cladding is anaid, as are coatings composed of aluminum and silicon. The use of a noble metal such as gold would also provide a non-reactive material. In addition, the use of cermets and ceramics, designed for rocket engine nozzles, affixed with a suitable bonding medium to the surface, provide protection against the types of corrosion expected on Venus.

The use of gold and platinum in contacts, a feature well proven in terrestrial systems is mandatory not only on Venus, but on any of the other

planets as well. The well known resistivity of these metals to corrosive environments makes them obvious choices whenever environmental corrosion is expected.

In high temperature environments stress corrosion and intergranular attack with subsequent embrittlement are factors requiring consideration. The use of stabilizers such as Ti, Nb and Ta in steels minimize the latter factors, as does heat treatment for annealing and special quenching techniques for prevention of internal stresses leading to the former.

Stress Corrosion The prevention of stress corrosion is less understood than the others, and the selection of materials depends highly upon time-temperature and environmental attack conditions. Selection of materials requires stress-relief annealing to minimize this type of corrosion.

The best methods to date of preventing this type of attack have been the avoidance and/or relief of the internal stresses themselves and of cladding the materials to avoid the initial corrosion point. In the environment of Jupiter, copper-base alloys should be avoided as noted in Table

Nickel, Inconel and Monel are likely to be attacked on Venus, as are Aluminum and Magnesium, leaving the stainless steels and gold alloys as the most likely metals except for titanium and tantalum which are highly resistant to strongly corrosive materials such as those expected in the planetary environments under discussion. Zirconium is highly embrittled in the presence of H_2,O_2 and N_2 as well as with CO, CO_2 and SO_2 making its use on Venus and the other planets unlikely unless highly protected.

Other Factors The presence of hydrogen in many metals causes their embrittlement, a factor enhanced by low temperatures, as may be expected on the outer planets. Jupiter, particularly has high H_2 concentration coupled with the low temperature and selection of materials to avoid this problem is necessary.

Galvanic corrosion may be avoided by proper selection of materials with regard to their placement in the electromotive series, by cladding, and by proper insulation. It should not then cause a problem.

Table 4-4

Alloy Systems and Some Reported Stress-Corrosion Environments

Alloy System	Environments
Aluminum-base alloys.....	$NaCl-H_2O_2$ solutions NaCl solutions Sea water Air, water vapor
Copper-base alloys.....	Ammonia vapors and solutions Amines
Magnesium-base alloys.....	$NaCl-K_2CrO_4$ Rural and coastal atmospheres Distilled water
Mild steels.....	$NaOH-Na_2SiO_3$ solution (caustic embrittlement) Nitrate solutions (calcium, ammonium, and sodium nitrate) Aqueous solutions of HCN
Stainless steels.....	Acid chloride solutions $NaCl-H_2O_2$ solutions H_2S
Nickel.....	Caustic soda solutions
Monel.....	Fused caustic soda Hydrofluoric acid Hydrofluosilicic acid (H_2SiF_6) Steam
Inconel.....	Caustic soda solutions
Lead.....	Lead acetate solutions
Gold-copper-silver alloys.....	$FeCl_3$ solutions Acetic acid-salt solutions

4.7 STERILIZATION

The requirement to sterilize unmanned planetary spacecraft prior to launch also has technological implications. This requirement derives from an international agreement through the Committee On Space Research (COSPAR), under which the U.S. has established a policy to control outbound biological contaminants to ensure a probability of less than 0.001 of contaminating each planet of interest. This policy is currently implemented by means of heat sterilization prior to launch. Other techniques are, however, being investigated, e.g., radiation, noxious gases and combinations with and without heat and could be adapted within the 15 year time frame of this study.

Sterilization Procedures. Exposure of spacecraft hardware to a dry, inert gaseous environment at a temperature of at least 373°K (usually 398°K) is the only NASA approved sterilization process.* In 1968, the requirement for heat sterilization was set at a twenty-four hour soak at 398°K, with additional limits on the initial biological load. Present plans (such as for Viking '73) are to tailor the terminal sterilization cycle to specific mission hardware, so that the planetary quarantine requirement will be satisfied (ref. B). Exotech (ref. C) and others have developed mathematical models which take into account all the various factors of assembly, contamination, decontamination, cleaning, thermal characteristics, death mechanisms, integrated lethality, release probabilities, etc., to arrive at a sterilization specification for specific missions. These models permit the selection of various controllable parameters (including the duration and level of heat sterilization) to optimally fulfill quarantine requirements.

Current plans for Viking '73 call for a 60 hour exposure at + 398°K for all components in the flight acceptance cycle plus an additional terminal cycle of duration to be determined, based upon observed surface contamination encountered during final assembly. Total exposure including estimates for retests could exceed 100 hours. The implications of exposure

---

*NASA-NHB 8020.12 Planetary Quarantine Provisions for Unmanned Planetary Missions

of this degree are discussed in the following section.

It has been shown that unmanned planetary landing capsules can be sterilized by high energy X-rays or gamma rays with a dose of 5 megarads. A 5 megarad dosage is sufficient to give a probability of one viable micro-organism surviving the irradiation comparable to that obtained by a dry heat treatment of 53 hours at 398°K. X-rays from a 3 to 10MeV electron accelerator are preferred for a large (2500 lb) capsule, because of penetration requirements, but Cobalt-60 gamma rays can be used on small capsules .

Heat Sterilization Effects on Component Reliability. Earlier studies have assessed the ability of spacecraft materials and components to survive dry heat sterilization cycles as prescribed by current policy. Two years ago, fourteen items of hardware commonly used in planetary spacecraft were identified* for which sterilization-related reliability problems were expected. Research has reduced that list to at most two items - magnetic tape recorders and the solid rocket motors - and it is expected that current efforts will totally eliminate these susceptibilities.

Components, materials and systems being developed to better withstand sterilization temperatures without reliability degradation include:

- Batteries
- Guidance and control systems
- Actuators and inertial devices
- Tape recorders
- Digital electronics
- Solid rockets
- Liquid rockets
- Polymers
- Spacecraft structures

Current R&D efforts directed to this goal are summarized in Appendix A. Progress in this program has been encouraging and there is little doubt that continued efforts will be fruitful in providing for Viking '73 and later programs high reliability heat sterilizable conponents and systems.

Of particular note in this regard is the CSAD program at JPL which has demonstrated that a typical planetary lander capsule can be built within the planetary quarantine sterilization constraints and function properly following sterilization.

Radiation Sterilization Effects on Component Reliability. The most critical radiation-sensitive components are silicon transistors and certai organic polymers. Transistors are subject to damage by surface effects and permanent degradation of current gain.

The selection of 1 to 10 MeV photons as the most suitable radiation for this application makes the evaluation of radiation effects on components difficult because most test data have been obtained under irradiation by neutrons, electrons, or protons, rather than high-energy X-rays. Although very limited data are available for gamma ray damage alone, studies show that a dose ratio of less than 2 : 1 can be achieved within a 2500 pound capsule by using 10 MeV linear accelerator (linac) bremsstrahlung. These levels can keep transistor gain loss to $\leq .10$. Certain polymers, notably teflon, polyesters, methyl methacrylate, and polysulfide rubber have unacceptable sensitivities, but satisfactory substitutes are available. The use of other types of radiation sources such as a proton accelerator or combined gamma rays and neutrons from a nuclear reactor has disadvantages - in particular the production of induced radioactivity and the generation of excessive radiation damage. The direct irradiation of a capsule by electrons leads to a large dose variation with depth which would cause excessive radiation damage near the surface.

Current studies at Sandia Laboratories indicate that combinations of radiation and heat have a synergistic effect; the presence of each factor tends to enhance the lethality to microorganisms by the other. Since the degradation mechanisms of radiation and heat are different, such a combination should have less deleterious effect on equipment reliability than the use of either, singly, to produce the same sterilization. Thus, although present planetary quarantine plans are based on heat alone, the combined use of heat, radiation, and possibly other agents should be further investigated.

4.8 LONG FLIGHT TIMES

Where today's space programs are geared to lifetimes of 1 to 3 years, the J-S-P '77 mission, for example, will be exposed to space environments for about a decade before its final objective, Pluto, is reached. Such reliability requirements have far reaching effects on the design, manufacture, and testing of future space hardware.

Redundancy. One design approach to long life reliability is increased redundancy. In the past the penalty for this alternative was severe in terms of weight, size and cost, so that it was employed only when failure of a part, or a device was likely. With integrated digital circuitry electronics, however, redundancy can now be obtained without a severe weight penalty. The rising technology of Large Scale Integration (LSI) suggests that redundancy to enhance reliability of logic circuits is a subject worthy of intensive review. JPL is addressing this question under work units 125 and 186. The STAR (Self-Test and Repair) activity under project TOPS (Thermoelectric Outer Planet Spacecraft) is an example of an attempt to achieve long time reliability through redundancy.

Testing for Reliability. As indicated by the above discussion, quantitative knowledge of the reliability of components and devices is necessary to permit design of a system with an acceptable chance of success. This knowledge is based on test results.

After an initial burn-in period, during which device specimens fail at a high rate, it is usually observed that the rate of failure is proportional to the number of specimens. This observation leads to an exponential law for reliability, whereby the probability P that a device has not failed decreases with time t according to

$$\bar{P} = \exp(-t/T)$$

where T is the mean lifetime of the parts surviving the initial burn-in. Thus, if 990 of 1000 parts survive a test operation for 10,000 hours, the reliability would be 0.99 for a 14 month operation, but only about 0.93 for an eight year extended operation.

Although testing procedures have been developed to an advanced state, this example points to difficulties that are inherent in all testing. To

begin with, large numbers of specimens must be tested simultaneously so that one obtains confidence in the measurement. This is often not feasible; the specimen may be a prototype or an expensive, not easily-duplicated device. A second difficulty is the requirement of a long test time. In the above example only 1% of the specimens failed a fourteen month test, and this suggested that this part alone might contribute a 7% probability of failure of a mission to outer planets.

Test time raises the requirements that a design for a planetary mission be frozen far in advance of the launch date. Components which have been improved so that their newer forms offer some advantage in a spacecraft soon to be launched are, nevertheless, subject to rejection because of their unknown long life reliability. This is an especially severe hardship in the microelectronics category, where technology is advancing so rapidly.

Another difficulty is that of duplicating the environment during the test. The hard vacuum of space is not reached in testing chambers, and parameters such as temperature, meteoroids, and radiation present problems of definition. As a result, even when the duplication of environment is almost achieved, it is necessary to extrapolate test results as functions of pressure, radiation balance, etc. This extrapolation could in theory be done on the basis of a series of tests, at different pressures, and so forth. In practice, such a series of lengthy tests is often not feasible.

Recognizing the difficulties in simulation testing for reliability, some have advocated evaluations based upon physics of failure analyses. A side benefit of understanding the physics of failure is the possibility of speeding up tests. Frequently, the temperature is deliberately increased for a test. This has the effect of compressing the time between failures, and shortening the test time. For spacecraft to be used in long flight missions, there is an obvious desire to employ accelerated life testing techniques. An accurate extrapolation of data, however, requires a sound understanding of the phonomena involved.

Another reason exists for an investigation into the theoretical aspects of failure. In many reliability tests, there is observed a rapid

increase in failure rate after a long time. The exponential form of P no longer applies, instead the failure modes observed appear now to be due to a wearing out of the tested units. As a result, extrapolations of test data to long time periods (such as the examples above) can be misleading.

Failure Analysis. If testing is important to extimate reliability, the analysis of those units which fail a test is equally worth while. This is recognized by the NASA Reliability Program Provisions (NPC 250-1, Sec. 3.7), where analysis of failures and malfunctions is emphasized. This is not only important to identify failure modes due to poor design or workmanship; it is also important to identify basic failure modes. These basic failure modes frequently fall into two categories. Instability is one, such as the migration of atomic species in a material or at a connection: the "cold welding" of relays in space is an example. The second is wear out, whereby an essential property or constituent is depleted through use of the unit. Metal fatigue falls in this category.

Knowledge of the mechanisms by which a part may fail will lead to more precise evaluations of its reliability. In some situations, a dependence on time that is not exponential may be indicated.

Significant effort in NASA's SRT program is being devoted to the problem of long life reliability. Some of the more significant projects are summarized in Appendix A.

5.0 CONCLUSIONS AND RECOMMENDATIONS

Technology implications of many suggested space missions are severe and will require significant advances in the ability of equipment to perform:

- at temperature extremes
- in high radiation environments
- at low illumination levels
- in erosive and corrosive atmospheres
- during transit through the asteroid belt
- for long flight durations

Many SRT projects are being directed toward promoting these technological advances.

Temperature

Temperature appears to be the environmental factor providing the most severe strain on all planetary missions. The performance of conventional electronic circuits, under extremes of heat or cold, deserves a closer analytic study to determine what margins exist and how circuits may be "hardened" to endure extremes of heat or cold. Although there are work units for the development of heat sterilizable batteries, consideration should be given to the development of energy storage devices for operation at temperatures above 398°K

Venus probes, Jupiter probes and Venus landers could benefit from further effort in the development of high temperature plastics and electronic components. Research toward high temperature semiconductor devices should continue since this effort can also lead to higher reliability. Programs to develop unconventional electronics, such as III-V compounds for solid state devices, have potential for high temperature missions. These should be supported and expanded.

Radiation

All planetary missions should be planned with the effects of radiation considered, both during interplanetary flight and near a planet. Other factors being equal, components which are more resistant to radiation should be selected, such as n-p solar cells, n-p-n transistors, and plastics such as nylon. Parts standardization, systematic parts selection and assembly QC will become increasingly important as mission lifetimes increase and prelaunch testing becomes more lengthy and elaborate. Current standards programs and specifications

are generally not compatible with the needs of 6-10 year missions. Further work is suggested in determining the radiation susceptibility of commonly-used plastics. Such work can assist designers in selecting materials for missions with high radiation exposure. Radiation levels attendant with nuclear power sources and rocket engines should be more thoroughly studied.

A more current analysis than is available and necessary to evaluate the relative merits of RTG power and solar cell power for inner planet and Jupiter missions. This analysis should include cost, weight, reliability, and thermal requirements for each power source and should be in terms of the current state of the arts. Since solar cell systems are not feasible for outer planet missions, RTG development should be continued and objectives (performance and schedule) should be more concisely specified.

Meteoroids

Asteroidal debris fluxes calculated from the latest numerical model of the meteorid environment, and integrated over sample trajectories through the asteroid belt demonstrate that present knowledge of the environment is so uncertain that the shielding required to protect an outer-planet-bound spacecraft is significant if a low probability of impact-caused failure is required. In order to assess the environment more accurately and possibly to eliminate the upper limit model which predicts undesirably high fluxes it would be worthwhile to make an early attempt to detect 10^{-2} grams and smaller particles in the asteroid belt. Calculations have been performed for two trajectories in the ecliptic plane, one a transfer to Jupiter and the other a mission to 3.4 AU and return (ref. 39). The latter passes twice through the most densely populated portion of the asteroid belt. The conclusions from the two trajectory integrations are very similar and indicate that for a one square meter surface the probability of impact of a 3.5 g/cm^3 asteroidal debris particle at 12 km/sec is about 20 percent for a 10^{-6} gram particle and 1 percent for a 10^{-2} gram particle. For a probability of puncture as low as 1 percent the surface must resist penetration by the 10^{-2} gram particle, requiring a single wall thickness of at least one cm of aluminum. A lighter, but more complex solution would be to use a bumper shield for protection. In view of these results, work on meteoroid protection through lightweight

design concepts should be continued.

Although little can be done to prevent micrometeorid damage to optical surfaces, high velocity impact testing of materials such as low density oxides coated non-metallic sandwich panels, and solar cell coverslides are recommended to determine their actual behavior and to permit reliable estimates of lifetimes to be made.

The design philosophies from which evolved the micrometeoroid defense of the Outer Planetary Explorer, appear to be soundly based. Data necessary to significantly refine the shielding design criteria appear to be obtainable now only by in situ measurements. Results of micrometeoroid experiments on Pioneer F and G plus the first OPE missions should provide sufficient definition of the environment for nearly optimum design, but an analysis of how the results will affect overall design tradeoffs of future spacecraft (particularly the OPE), is recommended. A carefully pre-designed set of procedures anticipating an appropriately wide range of experimental results is felt to be a better approach than an ad hoc type of decision making at a later date.

Erosion

The erosion of surfaces of payloads landed on either Mars or Venus is presently estimated to be a significant problem. Work should be continued to identify and apply screening tests under simulated conditions to protective surface coatings and hardening treatments. The need is particularly great for protection treatments applicable to surfaces which must retain good optical or radiative heat transfer characteristics.

Design approaches for erosion and soil contamination effects could best be proven out only under environmental simulation. Total simulation would be prohibitively expensive and not necessary, since effects of airborne contamination would not be dependent upon many atmospheric parameters. Much of the technology and reliability testing procedures for desert operation of terrestrial equipment is probably quite valid. A study is recommended into present reliability testing for air-borne dust and dirt to determine existing applicabilities of criteria and changes necessary to make valid extensions to Martian operation.

Corrosion

The expected corrosive atmospheres and surface conditions of Venus, and possibly Mars, indicates the need for study to identify the possible corrosive mechanisms, and subsequently the transfer of materials protective technology developed for dealing with severe industrial environments. More definitive results concerning chemical constituents of the planetary environment are needed to permit estimation of the rates applicable to the various corrosive mechanisms.

Reliability

Further studies are recommended of reliability through redundancy for digital electronics (IC's and LSI's). Programs such as JPL's project STAR should be further supported. Consideration should be given to additional effort in physics of failure studies and accelerated life testing techniques as possible aids to the solution of long life reliability requirements. Accelerated life testing which provides requisite assurances of performance reliability and circumvents the problems of long lead times in parts selection, procurement and pre-flight testing should be investigated to support long duration missions.

Outer planetary probes will also share a common engineering problem of a magnitude not previously encountered in spacecraft design. Missions are necessarily of long duration, with certain proposed trajectories requiring up to 12 years. Reliability estimates for state-of-the-art hardware, most notably electronic devices, are widely considered inconclusive or speculative. In many cases, necessary information is unavailable or unknown. In deep space probes, concern is shifted from infant mortality to end-of-life in the reliability characterization of components. Burn in techniques to eliminate early failures, for example, are simply not adequate to cope with the requirements imposed by long mission durations. Accelerated life testing as a reliability criteria becomes immediately suspect when we consider that normal end-of-life of state-of-art components can not be reached and compared to prediction--except in retrospect. Nearly everyone connected with reliability engineering interviewed in the course of this study has cited a need for new criteria to reference in making decisions, but at that point, consensus ended. No specific

tasks could be responsibly offered due to the limited time to explore this problem. Fresh ideas in this area should be encouraged, however,

Hardware design is influenced not only by data available from representative planetary environmental models, but also by the relatively large amount of uncertainty remaining in those vectors significantly affecting system reliability or feasibility. For this reason, a somewhat greater than usual amount of over-design must be accepted as a necessary characteristic of early planetary missions. In view of the dearness of payload weight, sacrifices necessitated by conservative design are acutely felt. A primary goal of these first missions, then, is to attack the problem of defining accurately the gross environmental factors of greatest engineering concern in order to allow efficient design of advanced platforms carrying more sophisticated and subtle experiments. Selection of mission objectives, profiles, and on-board experiments should reflect this priority.

APPENDIX A

COMPONENTS	PROJECT TYPE	SPONSOR	CONTRACTOR	PRINCIPAL INVESTIGATOR	INFORMATION NUMBER	PERFORMANCE ENVIRONMENT	END USE
Advanced Space Vehicle Subsystems	1. Parachute & deployment mortar jettison mechanism; 2. entry mass spectrometer sampling system; 3. thermoelectric outer planet spacecraft deployable antenna	JPL			186-68-13-08	Entry heat	Venus probes
Alternator (573°K)	Design data to fabricate	AF Air Prop. Lab.	Westinghouse	Shillings	3145	High temperature High altitude	Aeronautics
Battery	Develop a Cd Ago battery having a hermetically sealed const.	U.S. Army Elec.Comm.	Gulton	Charlp	1C6-22001-A-02-13	Pressure	-
Battery	Evaluate secondary spacecraft batteries	GSFC	USNAD	Mains	120-34-01-22	Reliability	-
Battery	Low temperature secondary battery	GSFC			120-34-01-81	Low temperature	-
Battery	Identify failure modes in nickel-cadmium batteries	GSFC	USNAD Crane	Mains 812-854-1236	120-34-01-01	Long life	Power space
Battery	Evaluation for electrochemical cells developed on NASA/GSFC contracts	GSFC	USNAD	Mains 812-854-1236	120-34-01-96	General Reliability	-
Battery	Relate cell life and various cell operations parameters in sealed nickel-cadmium cells	GSFC	Internal		120-34-01-08	General Reliability	-
Battery	Design and develop 2 kw long life nickel-cadmium battery for sync. orbit appl.	USAF	TRW	Scott	3145-22-018	Long life	Earth orbit
Battery	Long life thermal battery	LRC			120-34-01-19	Long Life	-

COMPONENTS	PROJECT SCOPE	SPONSOR	CONTRACTOR	PRINCIPAL INVESTIGATOR	IDENTIFICATION NUMBER	SEVERE ENVIRONMENT	END USE
Battery	Development of heat sterilizable remotely activated Argo-zinc battery	JPL	Eagle Picher Ind.	Brill	NAS-7-100	Heat Sterilization	Planetary Landers and probes
Battery	Heat sterilizable batteries	JPL	TI		120-34-01-03	Heat Sterilization	Planetary Landers and probes
Battery, Ni-Cd Cell	Heat sterilization study, design, develop fabricate and testing	JPL	Texas Instr.	Jost	120-34-01-10	Heat Sterilization	Planetary Landers and probes
Battery, advanced systems	Develop batteries for complex and long duration missions	JPL	Internal		120-34-01-15	Long Life	Long Space Flight
Battery, zinc electrodes	Develop electric composition, method of fabrication and physical char.	LRC	McDonnell	Himy	120-34-01-22	Long Life Cycle	Space
Capacitors	High temperature ferroelectrics for capacitor applications	ERC			125-25-01-47	High Temperature	Venus Lander
Capacitor, Film	Tolerate relatively high ambient temperature and higher energy storage capability	ERC	North Star	Schwarz	120-33-08-05	High Temperature	-
Capacitors	High temperature devices and materials	ERC			120-33-08-05	High Temperature	Space
Capsule and lander actuator	Develop an actuator for future planetary exploration programs	JPL			186-68-02-35	Heat Sterilization	Planetary Landers and probes
Coatings	Erosion of satellite coatings	LRC			124-09-18-05	Erosion	Mars Lander

COMPONENTS	PROJECT SCOPE	SPONSOR	CONTRACTOR	PRINCIPAL INVESTIGATOR	IDENTIFICATION NUMBER	SEVERE ENVIRONMENT	END USE
Coatings	Development of thermal control coatings	MSFC			124-09-18-05	Temperature	Space
Coatings	Development of super-insulating coatings	LRC			124-09-18-08	High Temperature	Space
Computers and sequencers	Development of advanced circuit techniques and computer technology for flight applications	JPL			186-68-02-05	Heat Sterilization	Space
Connectors, electrical	Determine optimum metals for reliable low energy electrical contacts	ERC					
Control Systems for future missions	Develop control systems for future planetary exploration programs that will increase reliability	JPL			186-68-02-39	Heat Sterilization	Planetary Landers and Probes
Dielectric materials	Evaluation of sputtering as a technique for deposition	ERC			125-25-02-32	High temperature	Planetary Landers
Dopants	Study of radiation resistance	JPL			320-35201-2-3420	Radiation	Space
Elastomers	To relate changes in mechanical properties of heat sterilized urethene elastomers to chemical changes which occur during long time storage and assess the effect of planetary environment on properties	JPL			186-68-13-03	Long Life and Heat Sterilization	Planetary Landers and Probes

COMPONENTS	PROJECT SCOPE	LOCATIONS	CONTRACT	PRINCIPAL INVESTIGATOR	IDENTIFICATION NUMBER	SEVERE ENVIRONMENT	END USE
Electrical Components	Radiation damage to nuclear electric power system	LRC			120-27-04-35	Radiation	Long Space Flights
Electronic Compcnents	In flight failure rates of spacecraft electronic parts	JPL			125-25-04-03	Long life	Long Flights
Electronic Components	Examine the behavior pattern of electronic parts during life test and investigate methods of prediction	JPL	Boeing		186-70-01-05	Long life and stress	Long Space Flights
Electronic Equipment	Reliable circuit design techniques	LRC			120-25-04-02	Long life	Long Flights
Electronic Equipment	Radiation effects on advance electronics	GSFC	In House		125-25-02-01	Radiation	Van Allen Belts
Electronic Materials	Theoretical modeling effort related to radiation kinetics and formation of defects	JPL	Univ. of Utah	A.Sosia 801-322-7012	320-35401-3420	Radiation	Space
Electrical Systems, Nuclear	Develop technology required for design of electrical switch gear	LRC	GE	Powell	120-27-04-65	High temperature and vacuum	Space
Energy Conversion Devices	Reports for use in design and eng. of electric power systems	LRC	Internal		120-27-09-18	High temperature	Space
Flexible Array	Develop hardened flexible array submodule components	Air Force WPAFB	TRW Systems	Luft (213-679-8711)	314519	Radiation	Hardened Power
Fuel Cell Syst.	Develop long life fuel cell systems	MSFC	Allis-Chalmers	Platner 414-774-3600	120-34-02-01	Long life	Long Flights

COMPONENTS	PROJECT SCOPE	CONSOLE	CONTACT	PRINCIPAL INVESTIGATOR	IDENTIFICATION NUMBER	ENVIRONMENT	BRAND
GaAs Transistors	Develop a 673°K microelectronic circuit module	ERC	Texas Instruments	Strack	125-25-02-03	High temperature	Venus Lander
Guidance and Control System Integration	Develop and maintain capability for functional analysis and design or guidance and control subsystems	JPL			186-68-02-21	Heat sterilization	Planetary Lander and Probes
Guidance Approach Subsystem	Realization of technology for spacecraft based optical measurements	JPL			186-68-02-23	Heat sterilization	Planetary Lander and Probes
Heat Shield	Performance analysis for Venus entry	JPL			186-68-1?-08	Entry heat	Venus Probes
Inertial Sensors, Miniature and subminiature	Develop a group of such elements that are capable of surviving the sterilization temperature	JPL	Honeywell and General Precision	H-Bremer GP-Brophy	186-58-02-03	Heat sterilization	Planetary Lander and Probes
Instrumentation Infra-red	Develp and modify existing equipment for shorter response time	ERC			125-25-04-88	High temperature	Planetary Lander
Liquid Propulsion System, Sterilizable	Develop technology for the use of sealed, ethylene oxide-compatible, heat sterilizable liquid propulsion systems	JPL	Martin Denver	Lubens	186-58-08-02	Heat sterilization	Planetary Lander and Probes
Magnetic Components	Improve performance of static inverters and converters	ERC	Magnetic Metals	Brown	120-33-08-02	High temperature	Space
Materials	Attachment method for spacecraft thermal control; Materials designed for high temp.	AMES			188-68-11-05	High temperature	--

COMPONENTS	PROJECT SCOPE	SPONSOR	CONTRACTOR	PRINCIPAL INVESTIGATOR	IDENTIFICATION NUMBER	SEVERE ENVIRONMENT	END USE
Materials, Various	Interaction of radiation with S/C materials	LRC			124-09-11-04	Radiation	Space
Metals Refractory Alloys	Determination of weldability and long time elevated temperature stability	LRC	Westinghouse	Lessman	120-27-02-16	High temperature	Space
Methanol-Oxygen System	Develop fully fueled no maintenance methanol-oxygen battery	USA Electronics Comm.	Internal		IT6627054053-04-000-C8	Long life	Military
Modular electronic Packaging	Advanced development utilizing environmental discrete electronic components	JPL			186-68-10-09	Long life and severe environment	--
Piece Parts, Heat Sterilized	Study temperature-time relationship, effects of different number of temperature cycles, effects of different rates of temperature change and the effects of different storage period at high temperatures	JPL			186-58-13-08	Heat sterilization	Planetary Landers and Probes
Pivot Joints for Testing Pad Gas Bearings	Selection of material and testing	LRC	Mechanical tech.	Peterson	120-27-03-14	High temperature and argon envir.	
Polymers, Sterilizable	Establish a comprehensive list of polymeric products suitable for use in future entry lander/probe missions	JPL			186-58-13-02	Heat sterilization	Planetary Landers and Probes
Pressure Measuring Systems	Systems are being developed that will be capable of measuring small pressure fluctuations.	LRC	Consolidated Control Corp	Engdahl	120-27-04-39	Small Pressure fluctuations, overload	--

CLASSIFICATION	PROJECT SCOPE	SPONSOR	CONTRACTOR	PRINCIPAL INVESTIGATOR	AGENT IDENTIFICATION NUMBER	SEVERE ENVIRONMENT	END USE
Radiation Shield	Shielding for nuclear electric vehicles	LRC			120-27-06-07	Radiation shielding	Nuclear-electric S/C
Radiation Shield	Environment shielding study for nuclear electric power space-craft	GSFC			120-27-06-95	RTG radiation shielding	Nuclear-electric S/C
Rectifiers	Technology to be developed - is intended to be suitable for use as a basis for further design	NASA	GE	Coolidge	120-27-04-64	High temperature	Space
Rotary Actuation Technique	Provide technology for the integration of hyd/mech interfaces so that rotary actuators may be utilized for flight control surface actuation	USAF	Bendix	Verge	314530	Long life and fast response	Aeronautics
Semiconductors	High temperature devices for a nuclear electric power	LRC			120-27-01-25	High temperature	Long Space Flights
Semiconductors	Surface effects related to failure mechanisms	ERC			125-25-02-15	Long life	Long Space Flights
Semiconductors	Prepare device-quality crystals of AlP	ERC	Battelle	Reid	125-25-01-01	High temperature and radiation	Space
Semiconductor FET	Silicon carbide field effect transistor	ERC			125-25-02-50	High temperature	Venus Lander
Semiconductor, Junctions	Investigate feasibility of using transient IR radiation from S.C. junctions as non-destructive test method for performance and life expectancy	ERC	Raytheon		125-25-04-53	High temperature	Planetary lander

COMPONENT	PROJECT SCOPE	SPONSOR	CONTRACTOR	PRINCIPAL INVESTIGATOR	IDENTIFICATION NUMBER	SEVERE ENVIRONMENT	END USE
Semiconductors, SiC	Ion implantation of dopants	ERC	Hughes	Marsh	125-25-01-05	High temperature and radiation	Venus Lander
Semiconductors, SiC	High temperature radiation tolerant microelectronics	ERC			125-25-02-07	High temperature and radiation	Venus Lander and Close Solar Probe
Semiconductors SiC	Develop non-erosion S/C				125-25-02-07	Martian erosion	Mars Lander
Semiconductor, Various	Study of semiconductor materials for application in high temperature devices	ERC			125-25-01-39	High temperature	Venus Lander
Solar Cells	Provide eng'r data for radiation resistance	JPL	JPL		320-32301-2-3420	Radiation	Space
Solar Cells	Study and analysis of the action of lithium in silicon and silicon solar cells	JPL	Gulf	Naber	120-33-01-20	Radiation	Space
Solar Cells	Determination of radiation characteristics of photovoltaic devices	JPL	Internal		320-34001-2-3420	Radiation	Space
Solar Cells	Analysis of solar cell performance in space	JPL	Exotech	Barrett	952548	Radiation, temperature	Space
Solar Cells	Develop technology for fabricating hardened multilayer cells	AFAPL	Westinghouse	Johnson	314519-022	Radiation (neutrons)	Military
Solar Cell Panel	R&D of solar cell panel which can be heated in order to anneal radiation damage	GSFC	Boeing	Clarke	123	Temperature and radiation	Space
Solar Cells Si	Study relationship between recover and stability of recover of lithium solar cells and the effect of sodium impurities and germanium alloys on radiation damages	NASA	TRW	Carter	123-33-01-04	Temperature and Radiation	Space

COMPONENTS	PROJECT SCOPE	SPONSOR	CONTRACTOR	PRINCIPAL INVESTIGATOR	IDENTIFICATION NUMBER	SEVERE ENVIRONMENT	END USE
Solid Rockets, Sterilizable	Demonstrate feasibility and solve eng. problems involved in sterilizable solid propellant motors	JPL			186-58-08-01	Heat sterilization	Planetary Landers and Probes
Sterilizable Science Data Buffer	Gain understanding of design and manufacture of sterilizable memory	JPL	General Precision		186-58-03-02	Heat sterilization	Planetary Landers and Probes
Structures	Thermal Design of planetary probes	LRC			124-08-03-16	Extreme temperatures	Space
Structures	Structural design for meteoroid protection	MSFC			124-08-01-09	Meteoroids	Outer Planet Missions
Structures	Meteoroid protection design	LRC			124-08-01-32	Meteoroids	Outer Planet Missions
Structures, Planetary Entry and Landing	Study and develop systems and means of application of materials with high energy dissapating capabilities for the protection of spacecraft from impact loads during terminal landing	JPL	GE		186-68-01-01	High temperature and pressure	Planetary Landers
Tape Recorder	To conduct R/D relevant to large capacity data storage subsystems for advanced spacecraft	JPL			186-68-03-01	Heat sterilization	Planetary Landers and Probes
Thermionic Generators	Design and fabricate engineering evaluation models and design multi-converter thermionic generator	JPL	Thermo Electron Corp.	Brosens	NASA 7-100		
Thermoelectric Outer Planet Spacecraft Advanced System	Demonstrate the capability to perform missions to the outer planets and develop understanding of	JPL			186-68-09-09	Long life and and severe envir.	TOPS

COMPONENT	PROJECT TITLE	SPONSOR/CONTRACTOR	PRINCIPAL INVESTIGATOR	IDENTIFICATION NUMBER	ENVIRONMENT	USE
Thin Film Devices	High speed, high temperature active thin film devices	ERC		125-25-02-35	High temperature	Venus Lander
Valve, High Temperature	Develop component for nuclear electric power system	LRC		120-27-02-34	High temperature	Long Space Flight

APPENDIX B

STATUS OF SILICON CARBIDE HIGH TEMPERATURE SPACE COMPONENTS

1. INTRODUCTION

Semiconductors were launched into prominence with the discovery of the transistor in 1948. The original semiconductor material, germanium, was soon joined by its higher temperature equivalent, silicon. Developments over the next several years in the manufacture of these elemental semiconductor materials resulted in the ability to produce crystals with purities of the order of 0.1 part per billion. Experimental studies provided the detailed structure of the electron energy bands, the effective masses of the electrical carriers, their transport and scatter characteristics, their interaction with impurity atoms or structural defects and their response to electric and magnetic fields.

Technology then caught up with basic understanding with the development of planar diffusion processes which provided sharper p-n junctions and devices with improved reproducibility, speed and versatility. This was followed by the development of highly controlled vapor-solid reactions (epiaxial and evaporation techniques) which led to the integrated circuit.

2. HIGH TEMPERATURE MATERIALS

The search for semiconductor materials capable of operating in high temperature environments (such as exists in the surface of Venus) has been underway for more than a decade. Various compounds of elements have been and are being investigated for this application. The compound semiconductors consist of elements positioned symmetrically about group IV in the periodic table of the elements; Gallium arsenide (a group III-V compound), zinc sulfide (a group II-VI compound), and silicon carbide (a group IV-IV compound) are typical semiconductor compounds. As a class they represent phenomena and applications with higher frequencies, high speeds, higher power, and higher temperatures than those

of elemental silicon and germanium. They are also the potential key to electro optics where interaction of light and semiconductivity are involved and where electronic signals are coupled with light energy rather than with electrical charge or magnetic flux.

Progress with semiconductor compounds has been very slow, the main reason being that preparation of these materials with high chemical and structural perfection has not been achieved in a reproducible way.

Of all semiconductor compounds, gallium arsenide and indium antimonide, belonging to the group III-V class, have received the greatest overall attention. Some remarkable advances have been made. Gallium arsenide varactor diodes having cutoff frequencies up to 300 gigacycles have been realized. Equally remarkable are the microwave oscillators of gallium arsenide which are capable of generating at least 25 milliwatts of continuous power, or 350 watts of pulsed power at the amazing frequencies of 10 gigahertz. This type of application implies revolutionary developments in radar technology.

Texas Instruments, under contract to ERC, developed a high temperature logic circuit of diffused GaAs capable of performing up to 573°K. At temperatures above 573°K, leakage currents became excessive and performance deteriorated.

Under a recent contract, RCA will develop GaAs-P diodes using vapor deposition.

Autonetics is investigating epitaxially grown GaAs and chemical deposition in the development of semiconductor devices. The temperature limit for GaAs is probably 573°K. To perform at 650-750°K will require coolers (such as Peltier Effect devices). There is a trade off decision to be considered: use of GaAs and coolers vs. development of a SiC line.

Pertinent characteristics of some semiconductor compounds are listed below:

	GaAs	GaP	SiC
Band Gap (eV)	1.4	2.2	2.3/2.9
Melting Point (°K)	1513	1738	3073
Electronegativity Difference	~ .4	~ .5	~ .7
Debye Temperature (°K)	~ 400°	~ 450°	~ 1300°

Silicon carbide has also been extensively studied, principally for its potential as an extremely high temperature operating material with high resistance to ambient radiation fluxes. Almost ten years ago the AFCRL sponsored the first conference to present results in the research and development of silicon carbide semiconductor devices.

Silicon carbide (SiC) has favorable basic properties of:

- high band gap (2.3 ev for α, 2.9 ev for β)
- high mobility (500 to 1000 cm^2/volt-sec.)
- chemical stability
- thermal stability (Debye temperatures of 1200-1430°K)

These factors permit high junction temperatures which favor:

- performance in high temperature environments
- performance at high power in normal environments
- performance at high current densities

SiC devices potentially include:

- optical diodes
- high temperature diodes
- majority carrier devices
- Shottky barrier diodes
- cold cathode devices
- severe environment devices

Although operating SiC junction devices have been made there exist several problems inhibiting further development. These include:

- crystal growth
- fabrication techniques (such as device encapsulation) lead attachment, and materials of construction)

3. CRYSTAL GROWTH

Unfortunately, the very properties that make silicon carbide technically attractive also make it very difficult to grow as reproducible single crystals of acceptable size and purity. Moreover, silicon carbide exists

in many crystallographic polytypes. There is only one cubic form (β) but there are many closely related hexagonal and rhombohedral polytypes (α). These various forms of SiC exhibit the largest energy gaps found in common semiconductor materials, ranging from 2.39 ev (β) to 3.33 ev (α-2H). The most abundant polytypes are the 6H and 15R structures, from which most devices are fabricated.

Most of the usual methods of crystal growth have been successfully demonstrated for silicon carbide. From the vapor phase there are sublimation (or vapor transport), pyrolysis (or chemical vapor deposition), and a sublimation analogue to the liquid phase Czochralski technique. From the liquid phase, in most cases using a Si or Cr-Si solvent, crystals have been grown by melt cooling, by drawing and zone refining or traveling solvent.

Excellent crystals of both alpha and beta silicon carbide are presently produced in several laboratories by remarkably different techniques. Purity levels approaching the part per billion range have been mentioned, although the problem of avoiding nitrogen contamination is perhaps the most difficult.

Sublimation growth of SiC is the most successful method presently known for producing device grade single crystals. This method uses the vaporization of a SiC charge followed by condensation and crystal growth into a cooler cavity.

Doped crystals, or crystals containing p-n junctions are prepared by adding the proper dopants to the ambient during growth. The highest rated SiC power rectifiers are produced by this technique. To prepare grown junctions, p-type and n-type impurities are serially introduced into the growth cavity. Generally, the p-type dopant is added directly to the SiC charge (aluminum or boron) and after it has been depleted, the n-type dopant (nitrogen) is introduced. The grown junction crystals thus have a p-type shell.

Growth of high purity SiC crystals by the sublimation technique requires extensive outgassing and gettering at elevated temperatures.

Major impurities are nitrogen (n-type dopants). Highest purity crystals are n-type with a donor concentration of 10^{15} -10^{16} cm^{-3}, exhibiting electron mobilities of 300-600 cm^2 $volt^{-1}$ sec^{-1} (11), corresponding to diffusion lengths of about 10 microns. Compared to silicon, these are relatively short lifetimes and diffusion lengths and pose one of the problems in designing SiC devices. The SiC transistor studies, for example, have concentrated on majority carrier devices, because a minority carrier device would require a base widths of only 1-2 microns.

The problem in silicon carbide growth is not one of simply making crystals grow to sufficient size, but rather of controlling twinning, structure and preventing excess nucleation which leads to crystal interactions ("hexagonality" or "polytypism"). Since for each type there exists a different energy gap, successful production processes require that the type be predictable and controllable. Several theories have been advanced to explain how various polytypes form but none of these permit one to predict in advance which type will form.

4. FABRICATION TECHNIQUE

The techniques for mechanically shaping SiC crystals, such as lapping, abrasive cutting, ultrasonic cutting, etc., are all standard, but diamond or boron carbide must be used since these are the only materials harder than the SiC. Etching techniques are extensively used on SiC, but care must be taken since hexagonal SiC is a structurally polarized crystal, with a carbon face and a silicon face. Etching rates on the carbon face are usually very much faster than the same etch on the silicon face. Molten salt etching of SiC provides very rapid etch rates (1-2 microns per second). Lack of suitable etch masks make the molten salts unsuitable for most device work. SiC can be electrolytically etched using a dilute solution of HF in water and methyl alcohol. This etch is specific for p-type material and has been used to etch mesa structures on p-n junctions and to determine junction depth. A preferred technique is the use of gaseous etching with chlorine or chlorine-oxygen mixtures from 1023-1323°K. Etching rates of 0.25 ± 0.02 microns per minute are obtainable.

The etching rate on the silicon face is several orders of magnitude slower than the above rate which was determined on the carbon face.

Oxidation of SiC is a fundamental step in device preparation and fabrication. Silicon dioxide can be grown on SiC with steam oxidation techniques similar to those used for silicon crystals. Oxidation takes place at 900-1200°C in a carrier gas saturated with water vapor. As before, the oxide attack rate is approximately ten times faster on the carbon face than on the silicon face, but even the carbon face oxidizes much slower than silicon crystals.

Of additional technical importance is the fact that the oxide grows at a different rate on p-type and n-type regions of a single crystal containing a p-n junction. This leads to a different coloration of these regions due to thin film interference effects. This difference in oxidation is thus used in the delineation of junctions, after edge polishing a crystal, to determine the junction depth.

The self-masking diffusion and etching process is of paramount technological importance for the precision fabrication of SiC planar devices. Aluminum or boron diffusion in SiC requires temperatures from 2073 to 2373°K. At these temperatures SiO_2 can no longer be used as a diffusion mask. Various refractory materials have been investigated but only SiC itself has proved effective and practical to date. On the other hand, SiO_2 is very effective as a mask for chlorine etching at 1270°K. By using the photoresist technique, a precision configuration of openings can be etched into the SiO_2 mask and in turn a corresponding configuration of SiC can be formed on SiC by the chlorine etching.

Construction, heating, control of thermal gradients and mechanical manipulation becomes more difficult with SiC than with lower temperature materials. Instead of the quartz or platinum crucibles used to grow II-VI crystals, garnets and spinels, there are only a few materials not molten at SiC growth temperatures. Most of these, the refractory metals, carbides and silicides, are not compatible chemically with silicon carbide at these temperatures. Metal-silicon-carbon binary, and ternary eutectics and low

melting compounds, rule out practically everything but graphite for the crystal growing zone. Graphite porosity, adsorption and permeability to a wide variety of impurities at the use temperatures require the use of a totally clean system to prevent contamination.

Two solutions suggest themselves. First, a carbon-graphite system of maximum simplicity and purity can be used. The second alternative, and one that has received less attention, is to "make things happen" under less severe conditions.

A number of silicon carbide preparations have been made below 1270°K. Crystals have been grown by sublimation well below 2270°K in quite short periods of time. However, as in so many other cases, the tendency has been to continue to beat on the high temperature systems that are known to work and try for successive though slight improvements. What really is needed are fresh ideas and a new, "completely different" approach rather than to learn to live with crystal growth at 2500°C and find suitable materials.

John Schier of ERC feels that the GaAs contact problem has been "provisionally" solved with the use of thermal bonding techniques. For SiC, however, temperatures in the range of 1470 - 1670°K are necessary to achieve the bond. He is currently investigating tantalum doped gold as a contact material.

Encapsulation design is as important to the successful operation of the device as is the SiC itself. The basic requirements of the encapsulation are to provide protection of the package components from the operating environment. The main concern is the tungsten which is generally used as a base plate to the SiC crystal, which must be protected from oxidation. Also, since the device may be used from 200°K - 770°K, the encapsulation must provide for the differing thermal expansions of the device components. The realization of these requirements is a study in compromises.

The Russians, through intensive work over a number of years, overcame many of the obstacles associated with silicon carbide, with the

result that electroluminescent diodes made of silicon carbide are widely used in the Soviet Union and monolithic alpha-numeric devices are being mass produced.

However, the silicon carbide technology needed for transistors and integrated circuits is not likely to be developed in the next five years. During that period the sales volume of high temperature and high power semiconductor devices ($5 to $15 million per year in the United States) may not be sufficient to encourage the required development work on silicon carbide. It is more likely that it will be another 10 years before the many potential applications of silicon carbide are realized, unless there is a government crash program.

5. COMPONENT TYPES

Reliable diodes of gallium arsenide will very shortly become more widely available for microwave or other specialized applications. Similarly, an increased number of devices of indium antimonide and indium arsenide will find application in infrared-detection and other high-speed devices. Compound semiconductors will complement germanium in radiation detection and radiation analysis in the near future. Silicon carbide could be used in this field also, if the need for high-temperature detection becomes compelling.

On the other side of the spectrum, diodes for handling high levels of electrical power will continue to be of great importance. In this category belong the high-power rectifiers and the Thyristor switches whose bistable action is based on a p-n-p-n type structure. Semiconductor devices of this type are being used in the automobile industry (solid-state alternators) and in some electric appliances. For high power control SiC in grown junction form is the most suitable material. The time and rate of introduction of nitrogen into the growth cavity determines, to a great extent, the final electrical properties of the junction. By using the nitrogen introduction rate to control the width of the intrinsic region and the degree of compensation, the forward voltage drop and reverse voltage capability of the junction can be controlled. SiC rectifiers

prepared from the grown junction crystals operate at temperatures of 773°K and some exceptional units have been run at 873°K. The forward voltages of these devices decrease with increasing temperature, but even at 773°K are always larger than two volts.

Thus far, rectifiers operating up to 50 amps (peak) have been prepared and specially processed units have exhibited a reverse capability of 600 PIV. The reverse characteristics of SiC rectifiers generally show a "soft" breakover, rather than the avalanche breakdown sometimes noted in silicon rectifiers. This is generally attributed to the carrier generation mechanism at the junction and to local areas breaking down at different voltages so that the total effect is one of gradually increasing reverse current. The following table lists the properties of some SiC diodes which have been produced.

Table B-1

Electrical Properties of Typical SiC Rectifiers

Unit Type	Forward Voltage (V) half wave av.		Forward Current (A) half wave av.		Reverse Voltage (V) peak		Reverse Current (MA) peak	
	303°K	773°K	303°K	773°K	303°K	773°K	303°K	773°K
Power Rectifier	4.2	2.8	1.5	1.5	200	150	0.01	0.40
Low Current Instrument Device	5.0	2.5	0.5	0.5	500	300	0.001	0.008
High Voltage (stacked unit)	31	20	0.01	0.01	2000	1500	0.001	0.005
Low Voltage Blocking Diode	5.1	4.3	15.0	15.0	120	100	0.8	1.6

The operation of a semiconductor p-n junction as a detector of photons or nuclear particles depends on the formation and collection of electron-hole pairs produced by the passage of the photon or particle through the detector. These electron-hole pairs are separated in the junction region, collected and give rise to a charge or voltage. SiC devices are being made for charged particle, neutron or photon detection.

SiC diode structures have been prepared which are capable of detecting alpha particles up to , and with the addition of a conversion layer, thermal neutrons have been counted.

SiC, with a band gap near 3.0 eV, has an absorption coefficient several orders of magnitude less than that of SiC at 4000 Å, and therefore surface effects at 4000 Å or less would not be so important. Detectors have been prepared from Si C which show a maximum spectral response in the ultraviolet region which could be shifted by varying the junction depth.

Both broad band detectors, with a relatively uniform response from 2000 Å to 4000 Å and peaked response detectors with about a 100 Å bandwidth, can be prepared from diffused SiC crystals.

Measurements of quantum efficiency show that at room temperatures these devices exhibit a quantum efficiency of 0.1 to 10 percent which increases with temperature to about 15 to 50 percent at 773°K. The peak response wavelength can be readily varied by oxidation-chlorination chemical milling of the detector surface.

In the last 10 years considerable work has been carried out on electro-luminescent diodes, where electronic excitation leading to emission of light is brought about across a p-n junction. Here again there are the usual materials limitation. In order for the emitted light to be visible, the energy gap of the semiconductor must be greater than 2 electron volts. Germanium and silicon, with energy gaps of 0.6 and 1.1 electron volts, respectively, are disqualified completely. Gallium arsenide diodes can be made to electroluminesce with high efficiencies (greater than 20 percent at room temperature), but their light is in the

infrared region (1.45 electron volts). The choice of available materials that have appropriate energy gaps and that can be prepared as n- and p-type is limited indeed: galium phosphide (2.24 electron volts), aluminum phosphide (3.1 electron volts) and silicon carbide (2.7 electron volts).

Essentially all of the work on electroluminescence has been concentrated on these three materials, and working electroluminescent diodes have been obtained in all cases. All three semiconductors have indirect energy band gaps, which are less favorable than direct band gaps for achieving high efficiencies. For this reason, extensive work has been done in alloying the gallium phosphide or aluminum phosphide with the direct-gap material gallium arsenide. In this process direct band gaps can be achieved that are somewhere between that of gallium phosphide (or aliminum phosphide) and that of gallium arsenide. The external quantum efficiencies attained with such alloys (the light quantum emitted per injected carrier) are greater by about two orders of magnitude than those attained with the pure compounds (1 percent as opposed to 0.01 percent). But this increase in efficiency is achieved at the expense of shifting the light in the red part of the spectrum, where the eye is more than an order of magnitude less sensitive.

Silicon carbide has also been intensively studied, with impressive results. A silicon carbide diode with a remarkably narrow line light source, well suited for recording voice or other types of information on photographic films, has been developed and marketed.

REFERENCES

1. Alexander, J. K.: Decameter Wavelength Observations of Jupiter, October, 1966 – March, 1967. NASA TM X-55996, 1967.

2. Alexander, W. M.; McCracken, C. W.; Secretan, L.; and Berg, O. E.: Review of Direct Measurements of Interplanetary Dust from Satellites and Probes. NASA TM X-54570, 1964.

3. ASTM Committee E-10: Space Radiation Effects on Materials. Special Tech. Pub. No. 330, Am. Soc. Testing & Materials, Oct. 1962.

4. Anon.: Advanced Mariner Probe Missions. Presentation 761902P, AVCO/Northrop corps., Dec. 1966.

5. Anon.: The Interplanetary Meteoroid Environment – 1969. NASA Space Vehicle Design Criteria Monograph (Review Copy), April 1969.

6. Anon.: IRE Third Annual Seminar: Reliability of Space Vehicles. Conference, Inst. Radio Engrs., Oct. 1962.

7. Anon.: Mariner-Mars 1964. Final Project Report. NASA SP-139, 1967.

8. Anon.: Meteoroid Environment Model - 1969 (Near-Earth to Lunar Surface). NASA SP-8013, 1969.

9. Anon.: Models of Mars Atmosphere [1967]. NASA SP-8010, May 1968.

10. Anon.: Models of Venus Atmosphere [1968]. NASA SP-8011, Dec. 1968.

11. Anon.: Multiple Outer Planet Mission. Grand Tour, Astro-Sci. Center, IIT Res. Inst., May 1968.

12. Anon.: Planetary Quarantine Provisions for Unmanned Planetary Missions. NASA Handbook NHB 8020.12, 1969.

13. Arnoldy, R. L.; Kane, S. R.; and Winckler, J. R.: The Observation of 10 - 50 KEV Solar Flare X-Rays by the OGO Satellites and Their Correlation with Solar Radio and Energetic Particle Emission. NASA CR-91510, 1967.

14. Avduyevskiy, V. S.; and Marov, M. Ya.: Model Atmosphere of Planet Venus According to the Results of Measurements on the Soviet Automatic Interplanetary Station Venera-r. NASA CR-94109, 1968.

15. Baicker, J. A.; and Rappaport, P.: Radiation Damage to Solar Cells. Report TID-7652, Atomic Energy Com., Nov. 1962. (pp. 118-135)

16. Barrett, A. H.: Passive Radio Observations of Mercury, Venus, Mars, Saturn, and Uranus. Radio Sci, vol. 69D, Dec. 1965.

17. Baruch, P.: Radiation Damage in Semiconductors. (DDC document no. AD-621 049), July 1965.

18. Bates, F. C.: Subsolar-Meridian Mean-Annual Distributions for Martian Troposphere Below 50 Kilometers. NASA CR-1043, 1968.

19. Bauer, P.: Batteries for Space Power Systems. NASA SP-172, 1968.

20. Behrndt, K. H.; and Khan, I. H.: High Temperature Materials for Thin Film Circuits. Government Microcircuit Applications Conf., Vol. 1, pp. 228-230, Oct. 1968.

21. Bigg, E. K.: Influence of the Satellite Io on Jupiter's Decametric Emission. Nature, vol. 203, no.

22. Binder, A. B.; and Cruikshank, D. P.: Evidence for an Atmosphere on Io. Icarus, vol. 3, no. 4, Nov. 1964.

23. Staff of the Boeing Co.: Integrated Manned Interplanetary Spacecraft Concept Definition. Volume 2: System Assessment and Sensitivities. Final Report D2-113544-2, vol. 2, Aerospace Group, Boeing Co., Jan. 1968. (Also available as NASA CR-66559)

24. Bolt, R. O.; and Carroll, J. G., eds.: Radiation Effects on Organic Materials. Academic Press, 1963.

25. Brereton, R. G.; et al: Venus/Mercury Swingby with Venus Capsule. Preliminary Science Objectives and Experiments for Use in Advanced Mission Studies. Tech. Memo. 33-332, Jet Propulsion Lab., Calif. Inst. Tech., May 1, 1967.

26. Brereton, R. G., et al: Venus: Preliminary Science Objectives and Experiments for Use in Advanced Mission Studies. Rev. no. 1. Tech. Memo. 33-282, Jet Propulsion Lab., Calif. Inst. Tech., Aug. 1, 1966.

27. Campbell, R. B.; and Berman, H. S.: Electrical Properties of SiC Devices. Paper presented at 1968 Silicon Carbide Symposium, 1968. (pp. S 211-S 222)

28. Compton, D. M. J.: Radiation Effects on Lasers. Final Report, 1 July 1965 - Oct. 1967. NASA CR-86068, Nov. 1967.

29. Cooley, W. C.; and Barrett, M. J.: Handbook of Space Environmental Effects on Solar Cell Power Systems. Tech. Report TR-025, Eng. Systems Div., Exotech Inc., Jan. 1968.

30. Cosby, W. A.; and Lyle, R. G.: The Meteoroid Environment and Its Effects on Materials and Equipment. NASA SP-78, 1965.

31. Craven, C. W.; and Wolfson, R. P.: Planetary Quarantine: Techniques for the Prevention of Contamination of the Planets by Unsterile Spaceflight Hardware. NASA CR-91343.

32. Cruikshank, D. P.; and Binder, A. B.: Minor Constituents in the Atmosphere of Jupiter. Astrophys. & Space Sci., vol. 3, March 1969, pp. 347-356.

33. Davydov, V. D.: New View of Venus. Sci. & Tech., No. 73, Jan. 1968.

34. Deerwester, J. M.: Jupiter Swingby Missions to Nonspecific Locations in Interplanetary Space. NASA TN D-5271, 1969.

35. DeGraff, E.; and Cooley, W. C.: Evaluation of Current Technology in Attaining Planetary Quarantine Requirements for Spacecraft Sterilization. Vol. I. Tech. Report TR-018, Eng. Systems Div., Exotech Inc., April 1967.

36. DeGraff, E.: Status Review of Technology Developments for Spacecraft Sterilization. Vol. I. Tech. Report TRSR-032, Systems Res. Div., Exotech Inc., May 1968.

37. Dessler, A. J.: Penetrating Radiation. Satellite Environment Handbook, F. C. Johnson, ed., Dec. 1960.

38. De Vaucouleurs, G.: Physics of the Planet Mars. An Introduction to Aerophysics, Faber & Faber (London), 1964.

39. Devine, Neil: Asteroidal Debris Distribution, Hazard and Detection. JPL Summary 37-56, Vol. III, Jet Propulsion Lab., Calif. Inst. Tech., April 30, 1969.

40. Dyhouse, G. R.: Simulated Martian Sand and Dust Storms and Effects on Spacecraft Coatings. J. Spacecraft & Rockets, vol. 5, no. 4, April 1968, pp. 473-475.

41. Staff of Electronic Components Research: Semi-Annual Review of Research and Development, July 1, 1967 to Dec. 31, 1967. PM-44, NASA/ERC, (Cambridge, Mass.), April 1968.

42. Ellis, G. R. A.: The Decametric Radio Emissions of Jupiter. Radio Sci., vol. 69D, Dec. 1965.

43. Evans, D. E.; Pitts, D. E.; and Kraus, G. L.: Venus and Mars Nominal Natural Environment for Advanced Manned Planetary Mission Programs. NASA SP-3016, 1967.

44. Fjeidbo, G.; and Eshleman, Von R.: The Atmosphere of Mars Analyzed by Integral Inversion of the Mariner 6 Occultation Data. NASA CR-92718, 1967.

45. Foreman, K. M.; Nowatzki, E.; and Pomilla, F. R.: A Review of the Environments of Mercury, Venus, and Mars. GRD Memo. RM-420, (DDC document AD 838 016), Res. Dept., Grumman Aircraft Engr. Corp. (Bethpage, N. Y.), July 1968.

46. Frank, M.; and Larin, F.: Effect of Operating Conditions and Transistor Parameters in Gain Degradation. IEEE Trans., Nuclear Sci., vol. NS-12, no. 5, Oct. 1965, pp. 126-133.

47. Gault, D. E.; Shoemaker, E. M.; and Moore, H. J.: Spray Ejected from the Lunar Surface by Meteoroid Impact. NASA TN D-1767, 1963.

48. Staff of General Electric Co. (Philadelphia), Missile & Space Div.: Mars Atmosphere Definition. Final Report: Voyager Spacecraft. NASA CR-61185, 1968.

49. Georgiev, S.: A Feasibility Study of an Experiment for Determining the Properties of the Mars Atmosphere. Vol. I - Summary. NASA CR-530, 1967.

50. Gledhill, J. A.: The Structure of Jupiter's Magnetosphere and the Effect of Io on Its Decametric Radio Emission. NASA TM X-55980, 1967.

51. Staff of Goddard Space Flight Center: Data Book for Environmental Testing and Spacecraft Evaluation. Vol. 2, Sections IV-VI. The Space Environment; the Launch Environment and the Pre-Launch Environment. NASA TM X-59349, n. d.

52. Staff of Goddard Space Flight Center: Planetary Explorer Summary Description. Goddard Preprint X-724-69-10, Planetary Explorer Study Staff, NASA/GSFC, Jan. 1969.

53. Staff of Goddard Space Flight Center: A Venus Multiple-Entry-Probe Direct-Impact Mission. Scientific Objectives and Technical Description. Jan. 1969.

54. Goldberg, M. F.; and Vaccaro, J.: Physics of Failure in Electronics. ARF Series, Spartan Books (Baltimore), 1963.

55. Hanst, P. L.: Temperatures in the Upper Atmosphere of Venus as Indicated by the Infrared CO_2 Bands. NASA TM X-57346, 1963.

56. Head, V. P.: Correlation of Meteoroid Environments in the Solar System. AIAA J., vol. 5, no. 11, Nov. 1967, pp. 1976-1984.

57. Heller, G.B., ed.: Thermophysics of Spacecraft and Planetary Bodies. Radiation Properties of Solids and the Electromagnetic Radiation Environment in Space. Academic Press, 1967.

58. Hertzler, R.G.; Wang, E.S.J.; and Wilbers, O.J.: Development of a Martian Environmental Simulation Facility. Paper presented at the 3rd Annual IES/AIAA/ASTM Space Simulation Conference (Seattle, Wash.), Sept. 1968.

59. Hymowitz, E.W., Study Mgr.: Galactic Jupiter Probe. Phase A Report, Volume I. Goddard Preprint X-701-67-566, Advanced Proj. Office, NASA/Goddard, Nov. 1967.

60. Hymowitz, E.W., Study Mgr.: Galactic Jupiter Probe. Phase A Report, Volume II. Goddard Preprint X-701-67-566 (Sections 9-16), Advanced Proj. Office. NASA/Goddard, Nov. 1967.

61. Hymowitz, E.W., Study Mgr.: Space Programs Summary 37-47, Volume 1. Flight Projects. NASA CR-90544, Sept. 1967.

62. Staff of Jet Propulsion Lab.: Preliminary Status Report of Multi-Planet Mission Study to NASA/OSSA. Prelim. Status Report, Advanced Planetary Studies Grp., JPL, Calif. Inst. of Tech., June 1968.

63. Jones, M.F.: Trajectories to the Outer Planets Via Jupiter Swingby. NASA CR-61186, Jan. 1968.

64. Kellermann, K.I.: The Thermal Radio Emission From Mercury, Venus, Mars, Saturn, and Uranus. Icarus, vol. 5, Sept. 1966, pp. 478-490.

65. Kiess, C.C.; Karrer, S.; and Kiess, H.K.: Astron. Soc. Pacific, vol. 72, 1960, pp. 256.

66. King-Hele, D.G., ed. (J.W.T. Palmer, trans.): The Flight of the Spacecraft Venus 4, and Its Descent to the Surface of the Planet Venus. Library Trans. No. 1264, Min. of Tech., Gt. Britain Royal Aircraft Estab. (Farnborough Hants, England), Nov. 1967.

67. Koval', I.K., ed.: Problems in Astrophysics. Investigation of the Atmospheres of Venus and Mars. NASA TT F-394, 1965.

68. Lehr, S.N.; Martire, L.J.; and Tronolone, V.J.: Equipment Design Considerations for Space Environment. Report TRW 9990-6032-RU 000 (ASTIA No. AD 288 341), TRW Space Tech. Labs., Feb. 1962.

69. Lehr, S.N.; and Tronolone, V.J.: The Space Environment and Its Effect on Materials and Component Parts. IRE Trans. Reliability & Quality Control, vol. RQC-10, no. 2, Aug. 1961, pp. 24-37.

70. Libby, W. F.: Ice Caps on Venus? NASA CR-93741, [1967].

71. Lindgren, S. T.: The Solar Particle Events of May 23 and May 28, 1967. Report, Space Sci. Lab., Calif. Univ. (Berkeley), Feb. 1968.

72. Lockyear, W. H.: Electronic Parts and Long Duration Space Missions. Paper presented at the Symposium on Long Life Reliability, NASA/MSFC (Huntsville, Ala.), March 1969.

73. Long, W. G.: Testing Electrical Components for the Snap Environment. Paper presented at the 1965 Annual Tech. Meeting of the Inst. of Environmental Sciences, 1965.

74. Marcus, A. H.: Number Density of Martian Craters. NASA CR-93407, 1968.

75. Staff of Martin Marietta Corp. (Denver): Technology Feasibility Spacecraft. Final Report. Volume II. Vehicle Design and Fabrication. Res. Report R-68-2(Vol. II), TFS Program, Martin Marietta Corp., Feb. 1968.

76. Melrose, D. B.: Rotational Effects on the Distribution of Thermal Plasma in the Magnetosphere of Jupiter. Planetary & Space Sci., vol. 15, Feb. 1967, pp. 2.

77. Mercey, K. R.: Environmental Test Contribution to Spacecraft Reliability. NASA TN D-4181, 1967.

78. Michaux, C. M., et al: Handbook of the Physical Properties of the Planet Jupiter. NASA SP-3031, 1967.

79. Michael, W. H., Jr.; Wood, G. P.; and Young, A. T.: NASA Viking Project. Mars Engineering Model. Report M73-106-0, Viking Proj. Office, Langley Res. Center, 1969.

80. Moroz, V. I.: Physics of Planets. NASA TT F-515, 1967.

81. Morris, D.; and Berge, G. L.: Measurements of the Polarization and Angular Extent of the Decimeter Radiation from Jupiter. Astrophys. J., vol 136, 1962, pp. 276-289.

82. Narin, F., compiler: A Survey of Missions to Saturn, Uranus, Neptune, and Pluto. NASA CR-80846, 1966.

83. O'Connor, J. R.; and Smiltens, J., eds.: Silicon Carbide - A High Temperature Semiconductor. Pergamon Press (London), 1960.

84. Ogilvie, K. W.: Plasma Measurements in Interplanetary Space. Tech. Note BN-447, Inst. Fluid Dynamics & Appl. Math., Maryland Univ., May 1966.

85. O'Leary, B. T.: Visible and Near Infrared Studies and the Composition of the Surface. NASA CR-90495, Nov. 1967.

86. Olesen, H. L.: Radiation Effects on Electronic Systems. Plenum Press, 1966.

87. Owen, T. C.: [Spectroscopic Observations of Mars]. NASA CR-93481, Feb. 1968.

88. Pallmann, A. J.: Radiative Heating and Cooling Functions for the Lower Martian Atmosphere Under the Condition of Local Thermodynamic Equilibrium (LTE). NASA CR-1044, 1968.

89. Palmer, J. W., trans.: The Flight of Venus 2 and 3. (Extracts from Pravda, Jan. 1, 2 and 6 March 1966). Library Press Trans. No. 97, Min. of Tech., Gt. Britain Royal Aircraft Estab. (Farnborough Hants, Engl.), n. d.

90. Pearson, G. L.: Fundamental Studies of the Metallurgical Phosphide. NASA CR-95950, June 1968.

91. Piddington, J. H.: Jupiter's Magnetosphere. NASA CR-92559, Sept. 1967.

92. Ragsdale, G. C.; and Mesnard, D. C.: Mariner Venus 67 Spacecraft Environmental Test Results. Tech. Report 32-1249, Jet Propulsion Lab., Calif. Inst. Tech., June 1968.

93. Robinson, G. P.; and Wang, E. S. J.: Martian Surface Transport Phenomena Under Simulated Environments. Paper presented at 3rd Annual IES/AIAA/ASTM Space Simulation Conf. (Seattle, Wash.), Sept. 1968.

94. Rittenhouse, J. B.; and Singletary, J. B.: Space Materials Handbook, 2nd ed., Suppl. 1. Space Materials Experience. NASA SP-3025, 1966.

95. Roberts, J. A.; and Komesaroff, M. M.: Observations on Jupiter's Radio Spectrum and Polarization in the Range from 6 cm to 100 cm. Icarus, vol. 4, 1965, pp. 127-156.

96. Ryan, C. E.: Perspectives on Silicon Carbide. Paper presented at 1968 International Conference on Silicon Carbide, 1968. (pp. S1 - S13)

97. Sagan, C.; and Pollack, J. B.: A Windblown Dust Model of Martian Surface Features and Seasonal Changes. Special Report 255, Smithsonian Astrophys. Observatory, Nov. 1967.

98. Steg, S. E.; and Cornell, R. G.: A Martian Quarantine Risk Model. NASA CR-93695, March 1968.

99. Steiner, S. A.: Degradation of GaAs Injection Diodes. PhD Thesis, Syracuse Univ., 1967. (Paper no. 68-5493)

100. Strack, H.; Doerbeck, F; Harp, E.; and Mehal, E.: Development of a Micro-Electronic Module. NASA CR-86097, June 1968.

101. Staff of TRW Systems Group: Study of Pioneer Missions to Jupiter. Final Oral Briefing. Report no. 11339-6002-RO-00, Oct. 1968.

102. Thorne, K. S.: Dependence of Jupiter's Decimeter Radiation on the Electron Distribution in Its Van Allen Belts. Radio Sci., vol. 69D, Dec. 1965.

103. Trainor, J. H.: Outer Planets Explorer Position Papers. 7 Position Papers, NASA/Goddard Space Flight Center, March 1969.

104. Van Allen, J. A.: Absence of Martian Radiation Belts and Implications Thereof. Report 65-30, Iowa Univ., Aug. 1965.

105. Vaughan, O. H., Jr.: Model Atmospheres of Mercury. NASA TM X-53693, Jan. 1968.

106. Waddel, R. C.: ATS-1 Solar Cell Radiation Damage Experiment, First 120 Days. NASA TM X-55772, 1967.

107. Warwick, J. J.: Mechanisms of Decameter Radiation. Report AFCRL-64-774, Air Force Cambridge Res. Labs (Bedford, Mass.), Sept. 1964.

108. Weidner, D. K., ed.: A Collection of Papers Related to Planetary Meteorology. NASA TM X-53693, Jan. 1968.

109. Weidner, D. K.; and Hasseltine, C. L., eds.: Natural Environment Design Criteria Guidelines for MSFC Voyager Spacecraft for Mars 1973 Mission. NASA TM X-53616, June 1967.

110. Wilcox, J. M.: The Interplanetary Magnetic Field: Solar Origin and Terrestrial Effects. NASA CR-93369, Jan. 1968. (Available from DDC no. AD 664 509)

111. Young, R. E.: The Two-Planet Flyby Problem. Rev. of NASA Sponsored Res. (Experimental Astronomy Lab.), Jan. 1967, pp. 65-70.